Molecular analysis of translation initiation machinery involved in the recognition of UUG start codon in *Saccharomyces cerevisiae*

By

CHARLESANTONY.A

LIFE11201004009

National Institute of Science Education and Research (NISER),

Bhubaneshwar

A thesis submitted to the
Board of Studies in Life Sciences
In partial fulfillment of requirements
for the Degree of
DOCTOR OF PHILOSOPHY
of

HOMI BHABHA NATIONAL INSTITUTE

April, 2018

Homi Bhabha National Institute[1]

## Recommendations of the Viva Voce Committee

As members of the Viva Voce Committee, we certify that we have read the dissertation prepared by **CHARLESANTONY.A** entitled "**Molecular analysis of translation initiation machinery involved in the recognition of UUG start codon in *Saccharomyces cerevisiae***" and recommend that it may be accepted as fulfilling the thesis requirement for the award of Degree of Doctor of Philosophy.

Chairman – Prof.A.Srinivasan,NISER   **Date:** 13.04.'18

Guide / Convener – Dr.Pankaj V.Alone, Reader-F, NISER   **Date:** 13/04/2018
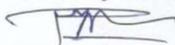
Co-guide - <Name> (if any)   **Date:**

Member 1 – Dr. Majusha Dixit, Reader-F, NISER   **Date:** 13/04/2018
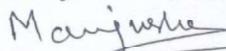
Member 2- Dr. Praful Singru, Associate professor, NISER   **Date:** 13.4.2018
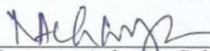
Member 3 - Dr. Narottam Acharya, Scientisr-E, ILS   **Date:** 13.4.18

External examiner - Prof.Umesh Varshney, IISc   **Date:** 13/4/2018
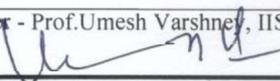
Final approval and acceptance of this thesis is contingent upon the candidate's submission of the final copies of the thesis to HBNI.

I/We hereby certify that I/we have read this thesis prepared under my/our direction and recommend that it may be accepted as fulfilling the thesis requirement.

Date: 13.04.2018

Place: Bhubaneswar   <Signature>   <Signature>   13/4/2018

                  Co-guide (if applicable)   Guide

---

[1] This page is to be included only for final submission after successful completion of viva voce.

STATEMENT BY AUTHOR

This dissertation has been submitted in partial fulfillment of requirements for an advanced degree at Homi Bhabha National Institute (HBNI) and is deposited in the Library to be made available to borrowers under rules of the HBNI.

Brief quotations from this dissertation are allowable without special permission, provided that accurate acknowledgement of source is made. Requests for permission for extended quotation from or reproduction of this manuscript in whole or in part may be granted by the Competent Authority of HBNI when in his or her judgment the proposed use of the material is in the interests of scholarship. In all other instances, however, permission must be obtained from the author.
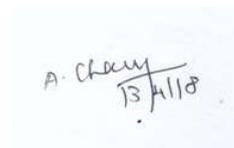
CHARLESANTONY.A

DECLARATION

I, hereby declare that the investigation presented in the thesis has been carried out by me. The work is original and has not been submitted earlier as a whole or in part for a degree / diploma at this or any other Institution / University.
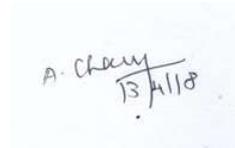
CHARLESANTONY.A

# List of Publications arising from the thesis

JOURNAL

1. "Defect in the GTPase activating protein (GAP) function of eIF5 causes repression of *GCN4* translation", **Charles Antony A**, Pankaj V. Alone, *Biochemical and Biophysical Research Communications*, **2017**, 486, 1110-1115.

2. "Fidelity of *HIS4* start codon selection influences 3-Amino-1,2,4-Triazole (3AT) sensitivity in GTPase Activating Protein (GAP) function defective eIF5", **Charles Antony A**, Pankaj V. Alone, *Journal of genetics* (Article in press).

3. "Ribosomal mutation in helix 32 of 18S rRNA alters fidelity of eukaryotic translation start site selection" **Charles Antony A**, Pankaj V. Alone (Article under revision).

CHAPTERS IN BOOKS AND LECTURES NOTES

None

CONFERENCES

1. "Molecular analysis of ribosomal residues involved in the recognition of UUG as a start codon in *Saccharomyces cerevisiae*", **Charles Antony A**, Pankaj V. Alone. Seventh meeting of RNA group meeting organized by Indian Institute of Chemical Biology, Kolkata, India, 2014.

2. "Hyper UUG codon recognition by eIF5^{G31R} mutant causes repression of the *GCN4* and *HIS4* translation and hyper sensitivity to starvation", **Charles Antony A**, Pankaj V. Alone. Fifteenth conference on Translational Control, Cold Spring Harbor Laboratory, New York, USA,2016.
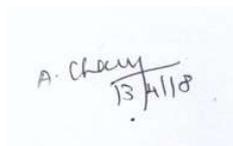
A. Chary
13/4/18

CHARLESANTONY.A

DEDICATIONS

With great respect and love, I dedicate this thesis to my

parents and teachers who have been the source of inspiration to

serve the society in the form of scientific discoveries.

ACKNOWLEDGEMENTS

CONTENTS

CHAPTER 1: Review of literature

CHAPTER 2: Materials and methods

CHAPTER 3: Defect in the GTPase activating protein function of eIF5 causes repression of *GCN4* translation

CHAPTER 4: Fidelity of *HIS4* start codon selection influences 3AT sensitivity in GTPase defective eIF5 mutant

CHAPTER 5: C1209U suppressor mutation in 18S rRNA restores start codon selection fidelity of GTPase defective eIF5 and eIF2β mutant

SYNOPSIS

ABSTRACT

In eukaryotes, the selection of open reading frame (ORF) on mRNA is the key fundamental step carried out by the 40S ribosome along with Met-tRNA$_i^{Met}$ and several translation initiation factors. The factor eIF5 plays a critical role in maintaining the fidelity of AUG start codon selection by providing GTPase activating protein (GAP) function through its N-terminal domain (NTD) to hydrolyse the GTP into GDP and P$_i$ by the eIF2 ternary complex. The eIF5 C-terminal domain (CTD is reported to take part in the 48S assembly/post-assembly process and mutations in this region confer both Gcn⁻ (general control non-derepressed) and Gcd⁻ (general control derepressed) phenotype in a temperature-sensitive manner. However, none of the mutations in the eIF5-NTD is known to associate with either Gcn⁻ or Gcd⁻ phenotype, and this domain is only implicated in GAP function, suggesting a predominantly catalytic function to this region. The eIF5^{G31R} mutant at the NTD was originally isolated as a dominant Sui⁻ (Suppressor of initiation codon) mutant and observed to be recessive lethal. It has been proposed that the Sui⁻ phenotype is the result of premature GTPase activity conferred by eIF5^{G31R} mutant that causes premature release of P$_i$ from the 48S complex, leaving Met-tRNA$_i^{Met}$ at the P-site of the 40S with a mismatch at the UUG codon. Our investigation of the eIF5^{G31R} mutant in this study reveals, downregulation of *GCN4* expression (Gcn⁻ phenotype) due to a novel mechanism that is linked with upUUG initiation codon recognition present at the 5′ regulatory region between uORF1 and the main *GCN4* ORF. An extragenic suppressor screening of eIF^{G31R} mutant in the 18S rRNA revealed C1209U substitution mutant could suppress Sui⁻ phenotype of both GTPase-defective eIF5^{G31R} and eIF2β^{S264Y} mutant.

CHAPTER 1: Introduction

All the living organisms synthesize proteins by decoding genetic code on the mRNA with the help of ribosomes, tRNAs, and specialized translation factors. However, selection of open reading frame (ORF) by locating AUG start codon is the key fundamental step in the translation initiation step. In *Saccharomyces cerevisiae*, more than twelve translation initiation factors are known to be involved in this process. The factors eIF1, eIF1A, eIF3, and eIF5 binds to the 40S ribosome and recruit eIF2-GTP-Met-tRNA$_i^{Met}$ Ternary complex (TC) to the P-site of the 40S ribosome to form 43S preinitiation complex (Hinnebusch 2014). The mRNA binds to the cap binding protein in the eIF4F complex and it is recruited to the 43S complex to form a 48S complex. The resultant 48S complex is proposed to be in 'Open/P_{OUT}' conformation capable of scanning mRNA from 5′ to 3′ direction in the search for AUG start codon (Hinnebusch 2011). The factor eIF5 plays critical role in maintaining the fidelity of AUG start codon selection by providing GTPase activating protein (GAP) function through its N-terminal domain (NTD) to hydrolyze the GTP into GDP and P_i by the eIF2 ternary complex, while the factor eIF1 present at the P-site of the ribosome monitors codon-anticodon interaction and prevents non-AUG codon selection (Huang *et al.* 1997). The base pairing of AUG codon and CAU anticodon at the P-site causes a conformational change in the 48S complex resulting in the 'Closed/P_{IN}' state with the release of eIF1 and P_i (Martin-Marcos *et al.* 2014).

Yeast genetics has played an important role in the identification and characterization of genes involved in the translation initiation process. One of the important genetic assays which is employed to study the translation initiation process is the expression of a GCN4 protein under amino acid starvation conditions that cross pathway regulates expression of genes involved in amino acid metabolism. The *GCN4* expression is regulated at the translational initiation level by trans-acting factors (products of Gcd and Gcn genes) as well as cis-acting elements, consist of four upstream short open reading frames (uORFs) present at the 5′ regulatory region of *GCN4* mRNA and represents an in-vivo barometer of initiation factor activity and integrity (Hinnebusch 2005). Any mutation that affects the integrity of the translation initiation complex and down-regulates the de-repression of *GCN4* expression under the starvation condition is termed as Gcn⁻

(general control non-de-repressed) phenotype and the genes were historically identified as 'Gcn'. On the other hand, a mutation that constitutively de-repressed the *GCN4* expression in the absence of GCN2 kinase is termed as Gcd¯ (general control de-repressed) phenotype and the genes were historically identified as 'Gcd' (Dever *et al.* 2016). Suppressor of initiation codon (Sui¯) phenotype is another genetics assay that is used to study the fidelity of AUG codon selection. Mutations in the translation initiation factors that causes translation initiation at the third UUG codon of *HIS4* transcript (*HIS4-303*) when the first AUG codon was mutated to AUU codon were historically identified as Sui¯ mutants (Donahue and Cigan 1988).

The G31R substitution mutation at the N-terminal GAP region of eIF5 causes hyper GTPase activity and shows dominant Sui¯ phenotype while it is lethal under recessive condition. It has been observed that eIF5^{G31R} mutation has a strong penchant for UUG codon recognition than the Sui¯ mutations in other translation initiation factors which also utilizes GUG and CUG initiation codons (Huang *et al.* 1997). Extensive study of eIF5 protein suggests a novel role of GDI function (Guanine nucleotide dissociation inhibitor) to its middle region while the C-terminal domain (CTD) is reported to be involved in 48S assembly/post-assembly process and mutations in this region confer both Gcn¯ and Gcd¯ phenotype in a temperature-sensitive manner (Singh *et al.* 2005; Jennings and Pavitt 2010a). However, the eIF5-NTD is only implicated in GAP function and none of the mutations in this region are known to be associated with Gcn¯ and Gcd¯ phenotype, suggesting a predominantly regulatory function to this region. We hypothesize that the strong Sui¯ phenotype of eIF5^{G31R} mutant in the GAP region might affect *GCN4* expression.

18S rRNA provides a scaffold for the interaction of different translation initiation factors during the selection of AUG start codon. Many critical 18S rRNA residues are shown to participate in the stabilization of the AUG start codon and CAU anti-codon at the P-site (Nemoto *et al.* 2010). It is possible that the hyper GTPase activity of eIF5^{G31R} mutant may be prematurely changing the conformation of 48S initiation scanning complex in 'Closed/P$_{IN}$' state and exposing other residues in the P-site of 18S rRNA that can stabilize the UUG codon and CAU anti-codon interactions. A genetic suppressor screening can be

employed to identify critical residues in the 18S rRNA that are involved in the recognition of UUG start codon in the eIF5^{G31R} mutant.

Following aims and objectives are undertaken in this study.

1) Genetic characterization of eIF5^{G31R} mutant on the expression of *GCN4*.

2) Screening for extragenic suppressor of Sui$^-$ (Ssu$^-$) mutant of eIF5^{G31R} mutant in the 18S rRNA.

3) Genetic characterization of 18S rRNA suppressor mutation.

CHAPTER 2: Materials and methods

Gene deletion in yeast was performed using homologous gene deletion method (Gueldener *et al.* 2002). Transformation of plasmids to yeast is performed by lithium acetate method (Gietz and Woods 2006).

β-galactosidase assay

Yeast cells were transformed with appropriate reporter plasmids using a standard protocol. Three colonies from each transformation were grown overnight at 30°C with shaking at 220 rpm in Synthetic-Complete Dextrose (SCD) medium containing required amino acids along with histidine. The cells were harvested and washed twice with SCD medium with no histidine followed by sub culture in 35 ml of SCD media with histidine (un-induced) and without histidine (induced) with initial O.D$_{600}$ ~ 0.1. The cells were grown at 30°C for 2 h, followed by induction with 25 mM 3AT for 8 h (the cells that are growing in SCD minus histidine media). Both induced and un-induced cultures were harvested after 8 h. The cells were re-suspended in LacZ buffer (60 mM Na$_2$HPO$_4$, 40 mM NaH$_2$PO$_4$, 10 mM KCl, and 1 mM MgSO$_4$, pH-7.0) and lysed using acid washed glass beads (200-300 micron from Sigma) in Fast prep-24® (MP biomedicals) for 20 Sec at 4 m/s followed by 1 min incubation on ice and repeated thrice. Cell extracts were spun down twice at 13000 xg for 5 min to remove glass beads and cell debris. Clarified extract (~30 μg) was mixed with LacZ buffer (to make up to 20 μl), followed by addition of 180 μl of ONPG (4 mg/ml in lacZ buffer).

After 30 min of incubation, absorbance was measured using 420 nm wavelength filter (Bio-Rad iMark plate reader). Protein estimation was done using Bradford assay and the β-galactosidase activity per min per mg of total cell extract was calculated using following formula.

$$\text{Specific activity} = \frac{\text{O. D.}_{420} \times \text{Assay volume (ml)}}{\text{molar extinction coefficient of ONPG} \times \text{Time (min)} / \text{protein used (mg)}}$$

Growth assay

Yeast cells were inoculated in the SCD media containing essential nutrients and grown to mid log phase at 30°C at 220 rpm overnight. 5 μl of serially diluted cultures (with optical densities O.D.$_{600}$-0.5, 0.05, 0.005, 0.0005, and 0.00005) were spotted on corresponding plates and incubated at 30°C for the stipulated time.

CHAPTER 3: Defect in the GTPase activating protein (GAP) function of eIF5 causes repression of *GCN4* translation

The eIF5^{G31R} mutation in the GAP region of eIF5-NTD is by far one of the strongest dominant Sui^{-} mutant known so far. However, the eIF5^{G31S} mutation was earlier reported to be recessive Sui^{-} and Gcn^{+}. It is possible that G31S substitution may have a weak effect on eIF5 function that could not have affected *GCN4* expression. It is hypothesized that the strong Sui^{-} phenotype of eIF5^{G31R} mutant might affect *GCN4* expression. In order to test this hypothesis, we first compared the Sui^{-} phenotype of eIF5^{G31R} and eIF5^{G31S} mutant by transforming *HIS4^{AUG}-LacZ* or *HIS4^{UUG}-LacZ* reporter constructs. The eIF5^{G31R} mutant has significantly high UUG/AUG ratio in comparison to vector control. However, no significant difference was observed with eIF5^{G31S} mutant suggesting that G31S substitution has a weak effect on eIF5 function and probably is weak Sui^{-} in dominant condition. To test whether G31R substitution causes Gcn^{-} phenotype, we used *GCN2^{+}* yeast strain and transformed with either single copy empty vector or single copy vector carrying derivatives of *TIF5* gene; eIF5^{WT}, eIF5^{G31S} and eIF5^{G31R} and spotted on SCD or SCD +3AT (3-

Amino-1,2,4-triazole) media. The 3AT is a competitive inhibitor of the *HIS3* enzyme and induces histidine starvation (Hilton *et al.* 1965). While the wild-type (WT) cells can overcome histidine starvation by de-repressing *GCN4* expression and grow on 3AT media, the Gcn⁻ mutants cannot grow on 3AT media and show 3AT sensitivity. Consistently, the eIF5[G31R] mutant could not grow on 3AT media in comparison to eIF5[G31S] mutant and vector control, suggesting that eIF5[G31R] mutant confers Gcn⁻ phenotype while eIF5[G31S] mutant remains Gcn⁺ possibly due to the weak effect of G31S substitution. Next, we tested the levels of *GCN4* expression of these mutants by using *GCN4-LacZ* reporter construct, as the Gcn⁻ mutants down-regulate the *GCN4* expression. Consistent with its 3AT sensitivity, the eIF5[G31R] mutant causes significant down-regulation of *GCN4* expression, while the eIF5[G31S] mutant showed no significant difference in *GCN4* level in comparison to the vector control. The data confirmed that eIF5[G31R] mutant shows Gcn⁻ phenotype. The lower level of *GCN4* expression in Gcn⁻ phenotype can be attributed to various defects such as slow scanning of uORFs, premature release of the 40S subunit post uORF1 translation, or leaky scanning of uORF1 by the 48S complex. In order to decipher the molecular mechanism behind the Gcn⁻ phenotype shown by the eIF5[G31R] mutant, modified derivatives of *GCN4-LacZ* reporter constructs were used that can test leaky scanning or slow scanning defects. The results indicate, there are no leaky or slow scanning defects rather premature dissociation defects probably due to the utilization of ten upUUG codons present in the 5′ UTR region of the *GCN4* transcript between uORF1 and the main *GCN4* ORF. Elimination of upUUG-ORF1-10 along with uORF1-4 significantly increase the *GCN4* expression in the eIF5[G31R] mutant. The data suggest that eIF5[G31R] mutant causes premature dissociation of 40S ribosome possibly due to the utilization of upUUG-ORF from the 5′ UTR region of the *GCN4* transcript leading to the repression of *GCN4* expression.

CHAPTER 4: Fidelity of *HIS4* start codon selection influences 3AT sensitivity in GTPase defective eIF5 mutant.

Another important observation with respect to the eIF5^{G31R} mutant was that the 3AT sensitivity could be rescued in the presence of *HIS4^{UUG}* allele. It is possible that the eIF5^{G31R} mutant may have downregulated AUG codon recognition while UUG codon recognition of *HIS4* transcript may have up-regulated under 3AT starvation conditions. In order to test this, the UUG/AUG ratio of *HIS4-lacZ* expression was compared under normal and 3AT conditions. Consistently, there was a 2.4-fold increase in UUG/AUG ratio under 3AT starvation conditions. eIF1 has an important gate-keeper function at the P-site of the 40S ribosome that monitors the codon:anti-codon interaction. The increased utilization of UUG codon caused by the premature release of eIF1 from the P-site is suppressed by the overexpression of eIF1. Consequently, the overexpression of eIF1 should increase the stringency of AUG codon utilization while concomitantly weakening UUG codon recognition by the Sui¯ mutant. Consistently, with the overexpression of eIF1, we observed slow growth in the strain that was expressing the eIF5^{G31R} mutant along with the *HIS4^{UUG}* allele and restores 3AT sensitivity, suggesting the 3AT sensitivity is contributed by the defective start codon selection of *HIS4* transcript. However, a major question remains: how can the *HIS4^{UUG}* allele contribute to overcome the 3AT induced inhibition of the HIS3p? Important is the fact that there are no known reports that 3AT inhibits the HIS4 enzyme. The *HIS4* gene encodes a multifunctional enzyme (histidinol dehydrogenase/phosphoribosyl-AMP cyclohydrolase/phosphoribosyl-ATP pyrophosphatase) that catalyzes the biochemical steps 2, 3, 9 and 10 of the histidine biosynthesis pathway (Alifano *et al.* 1996). Thus, poor expression of the *HIS4^{AUG}* allele by the eIF5^{G31R} mutant under 3AT starvation conditions may block the biochemical steps prior to HIS3p and can cause very limited availability of the substrate (D-erythro-imidazole-glycerol-phosphate) for the HIS3p, making it more sensitive to 3AT inhibition. However, the presence of *HIS4^{UUG}* allele triggers additional GCN4 expression which further stimulates all the enzymes in the histidine synthesis pathway (including *HIS3*). This causes *eIF5^{G31R}*/*HIS4^{UUG}* cells to grow on 3AT media.

CHAPTER 5: C1209U suppressor mutation in 18S rRNA restores start codon selection fidelity of GTPase defective eIF5 and eIF2β mutant

In order to identify the critical residues in the 18S rRNA that are involved in the recognition of UUG start codon in the eIF5^{G31R} mutant, a genetic suppressor screening was employed with the yeast strain having chromosomal *RDN* gene deletion. The growth of this strain is sustained by the high copy plasmid borne *RDN* gene under *GAL7* promoter. The eIF5^{G31R} mutant utilizes *HIS4^{UUG}* allele and could support growth on a medium lacking amino acid histidine. The aim was to identify suppressor mutations in the 18S rRNA that prevents UUG codon recognition of *HIS4^{UUG}* allele by the eIF5^{G31R} mutant and can be selected by growth assay on media lacking histidine. A mutation C1209U was identified in the head region of the *18S* rRNA that prevents the growth of eIF5^{G31R} mutant in the presence of *HIS4^{UUG}* allele. Genetic characterization of *18S* rRNA-C1209U mutation reveals the strong suppression of UUG codon recognition of *HIS4^{UUG}* allele, thus it is a Suppressor of Sui$^-$ (Ssu$^-$) mutant. Interestingly the 18S rRNA-C1209U also suppresses the Sui$^-$ and Gcd$^-$ phenotype of another intrinsic GTPase-defective eIF2β^{S264Y} mutant. As the 18S rRNA-C1209U mutation is located in the head region and it is away from the P-site, eIF2, and eIF5 binding site, it may not have directly affected the GTPase activity of the eIF2 complex. It has been proposed that the Sui$^-$ phenotype caused by the hype GTPase activity of the eIF5^{G31R} mutant is due to premature P$_{IN}$ conformation of the 48S scanning complex (Saini *et al.* 2014). It is likely that the 18S rRNA-C1209U mutation perturbs the premature head rotation and prevents P$_{IN}$ conformation at the UUG codons and hence suppresses the Sui$^-$ phenotype of eIF5^{G31R} and eIF2β^{S264Y} mutant.

CHAPTER 6: Summary

- eIF5^{G31R} mutation causes Gcn^{-} phenotype.

- The Gcn^{-} phenotype is due to the utilization of upUUG codons in the 5′ UTR of *GCN4* transcript.

- eIF5^{G31R} mutation also confers 3AT sensitivity that can be rescued by over expression of *HIS4* gene.

- The 3AT sensitivity of eIF5^{G31R} mutation is due to defect in start codon recognition fidelity of *HIS4* transcript.

- UUG codon recognition (Sui^{-} phenotype) of eIF5^{G31R} is suppressed by C1209U substitution mutation in 18S rRNA.

- The 18S rRNA-C1209U mutation also suppresses both Sui^{-} and Gcd^{-} phenotype of eIF2β^{S264Y} mutant.

LIST OF FIGURES

CHAPTER 1: Review of literature

CHAPTER 3: Defect in the GTPase activating protein function of eIF5 causes repression of *GCN4* translation

CHAPTER 4: Fidelity of *HIS4* start codon selection influences 3AT sensitivity in GTPase defective eIF5 mutant

CHAPTER 5: C1209U suppressor mutation in 18S rRNA restores start codon selection fidelity of GTPase defective eIF5 and eIF2β mutant

LIST OF TABLES

Chapter 1
Review of literature

1.1 Introduction: Overview of translation initiation

All physiological and metabolic functions of any organism are largely performed by proteins. These are the polymers of amino acids and synthesized using ribosomes by decoding the series of codons present in the messenger RNA, a process known as 'Translation'. Nearly three decades of genetic studies from yeast revealed the basic steps involved in this vital process, that is initiation, elongation, and termination (Walsh and Mohr 2011). Among these steps, initiation is highly evolved and regulated by a series of initiation factors to recognize AUG as start codon and to set an open reading frame (ORF) to decode genetic code into an amino acid sequence (Jackson *et al.* 2010; Dubitzky *et al.* 2013).

The key initiation factors involved in the translation initiation process are the heterotrimeric GTPase eIF2•GTP•Met-tRNA$_i$^Met Ternary Complex (TC), eIF1, eIF1A, eIF5 and eIF3 that are assembled on the 40S ribosomal subunit (Hinnebusch 2011, 2014). The cooperative interaction of these factors along with mRNA and eIF4F complex results in the formation of the 48S complex. (Asano *et al.* 2001a; Valasek *et al.* 2003; Jivotovskaya *et al.* 2006; Passmore *et al.* 2007; Hinnebusch and Lorsch 2012). Proper assembly of 48S complex leads to GTP hydrolysis by the TC with the help of the GTPase activating protein (GAP) eIF5 leading to GDP + P_i formation; however, the P_i remains bound to the complex (Lomakin *et al.* 2003; Maag *et al.* 2005; Alone and Dever 2006; Passmore *et al.* 2007). The 48S complex is proposed to be in a scanning competent "Open" conformation and the Met-tRNA$_i$^Met is considered to be in the P_{OUT} state as it is yet to engage with the mRNA in the P-site (Passmore *et al.* 2007; Yu *et al.* 2009; Saini *et al.* 2010). At this stage, the 48S complex scans the mRNA in the 3′ direction in search of an AUG codon. Base-pairing between the anticodon and an AUG codon causes a conformational change in the Met-tRNA$_i$^Met resulting in the P_{IN} state and repositioning of eIF1 away from the P-site, thus

converting the scanning competent 48S complex from an "Open" state to a "Closed" non-scanning state (figure 1.1). This is coupled with the release of eIF1 and concomitant release of P_i from eIF2•GDP, leading to the selection and delivery of Met-tRNA$_i^{Met}$ to the AUG codon (Pestova *et al.* 1998; Maag *et al.* 2005; Passmore *et al.* 2007). It is proposed that eIF1 antagonizes the premature GTPase by eIF5 in the absence of AUG codon, and thus stringently controls AUG codon selection (Valasek *et al.* 2004a; Maag *et al.* 2005).

1. 2 Cryo-EM studies of Initiation complex

Recent advance in refining the cryo-EM structure of 40S ribosome bound to translation initiation factors, tRNA and mRNA have provided new insights into the understanding of the assembly and scanning function of the translation initiation complex (Valasek *et al.* 2003; Passmore *et al.* 2007; Dubitzky *et al.* 2013; Fernández *et al.* 2013; Hussain *et al.* 2014). It has been observed that the mRNA entry channel latch is formed by the non-covalent interaction between helix h18 from body and helix h34 from the head region of 18S rRNA, which prevents mRNA to accommodate in the mRNA channel in the absence of initiation factors (Passmore *et al.* 2007). The 4.0 Å cryo-EM structure of the partial yeast 48S initiation complex (py48S) showed detail densities for eIF1, eIF1A, mRNA, tRNA$_i^{Met}$ and eIF2α subunit on the 40S ribosomal subunit (Hussain *et al.* 2014). It confirms the binding of eIF1 and eIF1A to the P-site and the A-site of the 40S subunit respectively with eIF1A-NTT (N-terminal tail) making contact with the codon: anticodon interaction, while the tRNA$_i^{Met}$ was oriented in P_{IN} state causing insertion of anticodon stem loop (ASL) deep inside into the P-site. The eIF2α mimic the E-site tRNA and the eIF2α-DI (domain I) interact with mRNA at the -2, -3 nucleotides through Arg[55] and Arg[57] residue probably monitoring sequence context as proposed by Kozak (Kozak 1986, 1987; Hussain *et al.* 2014). This structure also explained the conformational changes needed to occur in eIF1 in order to

accommodate Met-tRNA$_i^{Met}$ in P$_{IN}$ conformation. Subsequent 6.0 Å cryo-EM structure of py48S complex solved in the presence mRNA consists of either AUG codon or near cognate AUC codon revealed two conformations. The former showed mRNA entry channel constricted, latch closed and the tRNA$_i^{Met}$ is locked into the P$_{IN}$ state, dubbed as "py48S-Closed", while the latter shows tRNA$_i^{Met}$ not fully engaged in the P-site and showed open scanning competent state dubbed as "py48S-Open" (Llácer *et al.* 2015). In this structure, the densities of eIF3 subunit and all three subunits of the eIF2 complex were visible. eIF3 appeared to span the entire solvent exposed side and connect the entry and exit channels. The eIF3b-CTD/eIF3i/eIF3g-NTD module appeared to interact with TC and eIF1 close to the P-site. A model proposed by Llacer et al., suggests that the mRNA entry latch is closed in the 40S subunit, binding of eIF1 and eIF1A leads to the 8° rotation of the head which likely facilitated binding of TC in the P$_{OUT}$ state to form the 43S complex. A further 5°-6° head rotation allows recruitment of mRNA bound eIF4F complex to form py48S-Open scanning competent complex in which the mRNA is held loosely in the channel, tRNA$_i^{Met}$ is not fully engaged with the P-site and the eIF1A-NTT is disordered. The recognition of the start codon results in the downward movement of the head causing constriction of mRNA channel, latch closing and changing the orientation of tRNA$_i^{Met}$ to P$_{IN}$ state (Llácer *et al.* 2015).
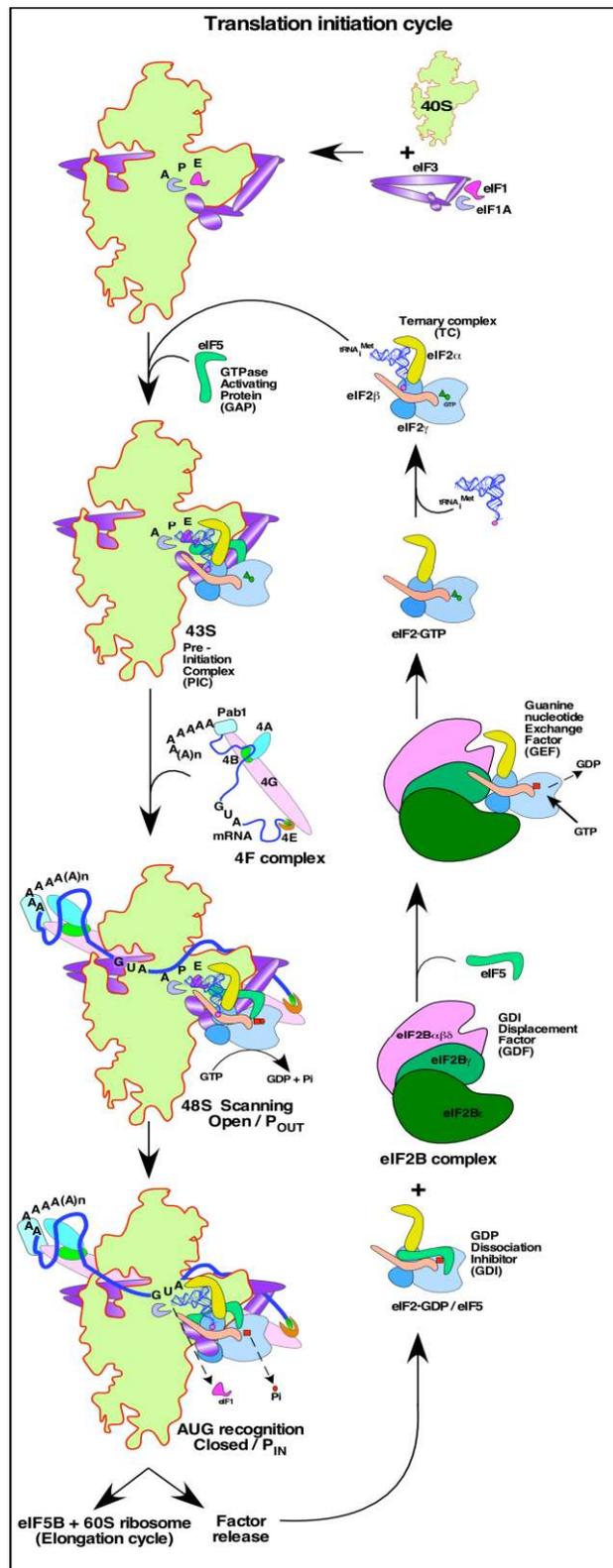
Figure 1.1. Steps involved in eukaryotic translation initiation (please refer section 1.1 and 1.2 for details)

1.3 General amino acid control and its relationship with regulation for translation initiation

It was observed earlier that, in response to starvation of any of several amino acids caused cross pathway increase expression of more than 30 genes involved in amino acid biosynthesis. The synergistic increase in the expression of these genes was identified to be controlled by the the b-Zip family of transcription factor *GCN4* and referred as general amino acid control (GAAC) (Hinnebusch and Natarajan 2002; Hinnebusch 2005). Interestingly, the regulation of *GCN4* expression is controlled at translation level by the presence of four upstream short open reading frame (uORFs 1-4) in its 591 nucleotides 5′ leader sequence. Under non-starved condition, the uORF1 is translated, and approximately 50% of the 40S ribosomes stay bound to the mRNA and have ability to translate uORF2-4 by re-acquiring the abundantly available TC. After translating the inhibitory uORF4, the 40S ribosome dissociates and seldom translates the main *GCN4* ORF (figure 1.2A). However, under the starvation condition, the GCN2 kinase phosphorylates eIF2α. The eIF2α-P complex binds to the GEF (Guanine Nucleotide Exchange Factor) eIF2B and becomes a competitive inhibitor of GDP to GTP exchange, thus lowering the level of TC. The ribosomes that are translating the uORFs of the *GCN4* mRNA are not able to re-acquire the low abundant TC after uORF1 translation and bypasses the uORF2-4 and re-acquire TC at main *GCN4* ORF (figure 1.2B). The level of GCN4 protein increases and up-regulates transcription of amino acid metabolizing enzymes and thus overcomes starvation.

GCN4 regulation

A)

Normal Conditions

GCN2 (Inactive)

↓

Ternary Complex (TC) (high)

1 2 3 4 GCN4

GCN4p ↓↓

B)

Starvation Conditions

GCN2-P (active)

↓

eIF2α-P

↓

Ternary Complex (TC) (low)

1 2 3 4 GCN4

GCN4p ↑↑

C)

Starvation Conditions

GCN2-P (active)

↓

eIF2α-P

↓

Ternary Complex (TC) (low)

Gcn⁻ Phenotype

1 2 3 4 GCN4

Slow scanning

Premature fall off

GCN4p ↓↓

D)

Starvation Conditions

Δgcn2

✗

↓

eIF2α

↓

Ternary Complex (TC)

Gcd⁻ Phenotype

1 2 3 4 GCN4

GCN4p ↑↑

Figure 1.2 Schematics of *GCN4-LacZ* reporter construct and mechanism of Gcn⁻ and Gcd⁻ phenotype.

GCN4 mRNA has four upstream open reading frame (uORF).

A) In normal conditions ribosome initiates translation at uORF1 and after termination, the 40S subunit keeps scanning downstream till it acquires ternary complex (TC). Once the uORF4 is translated the ribosome dissociates and it seldom translates *GCN4* main ORF.

B) Under starvation conditions *GCN2* kinase phosphorylates eIF2α, the Ternary complex (TC) level goes down, the ribosome reacquires TC after scanning uORF4 and translates *GCN4* main ORF and overcome starvation.

C) The Gcn⁻ mutant cannot translate *GCN4* main ORF even under starvation condition due to a defect in slow scanning, or leaky scanning, or reinitiation defect.

D) Gcd⁻ mutant is assessed under *gcn2* deletion conditions. Thus, despite the absence of eIF2α phosphorylation and high TC levels, Gcd⁻ mutants skips uORF4 and translate main *GCN4* ORF.

Any defect in the translation initiation pathways that down-regulates the de-repression of *GCN4* expression under the starvation condition is termed as Gcn¯ (general control non-de-repressed) phenotype (Hinnebusch 2005). Such defects were observed in the GCN2 kinase protein or mutation in the eIF2α subunit that abrogates phosphorylation at the Ser^{51} position (Krishnamoorthy *et al.* 2001). Gcn¯ mutations were also isolated in the steps that are downstream of TC formation which are independent of TC levels. These defects are related to slow scanning of uORFs, premature release of the 40S subunit post uORF1 translation, or leaky scanning of uORF1 by the 48S complex (figure 1.2C) (Hinnebusch 2005; Szamecz *et al.* 2008).

On the other hand, a mutation that constitutively de-repressed the *GCN4* expression in the absence of GCN2 kinase is termed as Gcd¯ (general control de-repressed) phenotype (Harashima and Hinnebusch 1986; Cuesta *et al.* 1998). The Gcd¯ mutant can overcome amino acid starvation even in the absence of GCN2 kinase. Mutations that lead to the lower abundance of TC and show the Gcd¯ phenotype were identified in the subunits of the eIF2 complex, Met-tRNA$_i^{Met}$ and also in the eIF2B complex that inhibits the GDP to GTP exchange (Harashima and Hinnebusch 1986; Donahue *et al.* 1988; Williams *et al.* 1989; Castilho-Valavicius *et al.* 1990; Dever *et al.* 1995; Yang and Hinnebusch 1996; Pavitt *et al.* 1997; Alone *et al.* 2008). Recently it has been reported that eIF5 acts as guanine nucleotide dissociation inhibitor (GDI) by binding tightly to the eIF2-GDP complex and prevented its access to eIF2B complex; thus overexpression of eIF5 leads to the Gcd¯ phenotype (Jennings and Pavitt 2010a; Jennings *et al.* 2013). A mutation that lowers the rate of TC loading on the 40S subunit or delivery of the TC in an altered conformation independent of TC abundance also showed Gcd¯ phenotype (figure 1.2D) (Alone *et al.* 2008).

1.4 Suppressor of Initiation codon (Sui⁻) Phenotype

The Suppressor of initiation codon (Sui⁻) phenotype, first identified in *Saccharomyces cerevisiae* by Donahue *et al.*, where certain mutants were able to utilize the in-frame third UUG codon of *HIS4* gene (*HIS4-303 or HIS4^UUG*) as a translation initiation codon when AUG was mutated to AUU codon, resulting in cell growth in a medium lacking histidine (Castilho-Valavicius *et al.* 1990). The Sui⁻ mutants were identified in all three subunits of eIF2, Met-tRNA$_i^{Met}$, subunits of the eIF3 complex, eIF5, eIF1 and eIF1A that compromises the fidelity of AUG codon selection (Cigan *et al.* 1988b; Castilho-Valavicius *et al.* 1990; Huang *et al.* 1997; Valasek *et al.* 2004a; Fekete *et al.* 2007; Nanda *et al.* 2009). However, mutants that suppress the recognition of UUG codon and restore the fidelity of AUG codon selection were termed as suppressor of Sui⁻ phenotype (Ssu⁻) (Luna *et al.* 2012).

1.5 Role of Initiator tRNA in the start codon selection

There are five genes (IMT) that encode initiator tRNA and are spread out on different chromosomes in yeast. Using elegant yeast molecular genetic technique Donahue and colleague showed that the anticodon of tRNA$_i^{Met}$ plays a critical role in the start codon selection. By mutating the anticodon sequence from 5′-CAU-3′ to 5′-CCU-3′ in one of the tRNA$_i^{Met}$ gene, the yeast cells were able to initiate translation of *HIS4* transcript where the AUG codon was mutated to the AGG codon, thus converting it from His⁻ to His⁺ phenotype (Cigan *et al.* 1988a). Interestingly, when an additional AGG codon was inserted out-of-frame with respect to the AGG codon in the upstream leader sequence, it blocked His4p production, suggesting that the anticodon region of the tRNA$_i^{Met}$ inspect mRNA in a base-by-base manner in the scanning translation initiation complex (Cigan *et al.* 1988a). The internal AUG codon present in the ORF is decoded by a distinct set of elongator tRNA (tRNA$_e$) which does not bind to the eIF2-GTP complex. The discriminating functional

differences between tRNA$_i$ and tRNA$_e$ are a) A1:U72 and C3:G70 base pairs in the acceptor arm; b) A54 and A60 in the T loop; c) Three G:C base pairs in the anticodon stem loop and d) O-ribosyl phosphate modification of A64 base (von Pawel-Rammingen *et al.* 1992; Aström, von Pawel-Rammingen 1993). Substitution mutation G1:C72 in the tRNA$_i$ caused defect in TC formation and binding to the 40S ribosome (Kapp *et al.* 2006). Disruption of C3:G70 base pair caused Sui$^-$ phenotype and reduced rate of TC binding to the 40S subunit, this defect was suppressed by a mutation in eIF1A that stabilizes the "Open/P$_{OUT}$" conformation (Dong *et al.* 2014). Substitution of conserved G31:C39 base pair with different base pair lead to Sui$^-$ phenotype, whereas eliminating this base pair makes it more accurate (Dong *et al.* 2014). Disruption of 2-O-ribosoyl phosphate modification at A64 residue due to lack of *RIT1* gene caused mistargeting of tRNA$_i$ to the elongation stage (Aström 1994).

1.6 eIF1 plays a key role in start codon selection

eIF1 is a 12.3 kDa protein encoded by *SUI1* gene. The hydroxyl radical probing data suggests that the eIF1 binds near to the P-site of 40S subunit and monitors codon:anticodon base pairing (Lomakin *et al.* 2003). It is well known that, analogous to this position of eIF1, IF3 in bacteria binds to P-site of the 30S and abort non-AUG codon selection by disturbing the codon:anticodon duplex formation (Sussman 1996). It is interesting to note that both IF3 and eIF1 can functionally replace in eukaryotic and prokaryotic cell-free translation system respectively (Lomakin *et al.* 2006). The importance of eIF1 on start codon selection can be much understood by the fact that similar to IF3 (having non-AUG as start codon), eIF1 also downregulates its own expression due to the poor sequence context around its translation start site (Ivanov *et al.* 2010) (Martin-Marcos *et al.* 2011). Extensive genetic studies proved that eIF1 has a major role in determining the fidelity of AUG start codon selection in translation (Nanda *et al.* 2009). Mutational

and structural studies suggest that the positively charged (K52, K53, K56, K59, K60) lysine residues of eIF1 play critical role in the interaction with the negatively charged 18S rRNA. The eIF1^{K60E} mutation reduces the affinity of eIF1 on the 40S ribosome and preferentially recognize UUG as a start codon and showed Sui⁻ phenotype (Martin-Marcos *et al.* 2014). Interestingly this Sui⁻ phenotype was suppressed by an intragenic eIF1^{D61G} mutation which reduces the overall negative charge in the K60E mutant and allowed tighter binding of eIF1 to 40S. This clearly suggests the binding of eIF1 is very much important for the selection of AUG start codon (Martin-Marcos *et al.* 2014). The in-vitro 48S assembly data suggests that the eIF1 dissociates faster in the presence of AUG mRNA compared to mRNA carrying UUG start codon. This clearly indicates that eIF1 is retained on 40S subunit until the AUG start codon enters into the P-site of 40S ribosome and establish codon:anticodon with the Met-tRNA$_i^{Met}$ (Maag *et al.* 2005; Cheung *et al.* 2007).

1.7 eIF1A promotes scanning of 48S complex and control AUG codon selection

eIF1A is an OB-fold containing protein encoded by *TIF11* gene and it binds to the A-site of the 40S ribosome and along with eIF1 subunit it likely involved in preventing the accommodation of tRNA$_i^{Met}$ in the A-site during translation initiation (Yu *et al.* 2009). The eIF1A has ~25 amino acid residues unstructured N-terminal tail (NTT) and ~34 amino acid residues C-Terminal tail (CTT). The deletion of CTT diminishes the ability of eIF1A to bind to eIF5 and eIF3 and showed a defect in recruiting TC resulting in Gcd⁻ phenotype. It is also observed that the ribosome cease scanning and form either an aberrant complex near the 5′ cap region or forms an initiation complex at GUG codon (Sui⁻ phenotype) (Fekete *et al.* 2005). The 10 amino acid direct repeats in CTT were shown to stabilize the open scanning conformation of 48S complex that allows the scanning and hence dubbed as scanning enhancer 1 (SE$_1$; amino acid 121-127) and

scanning enhancer 2 (SE$_2$; amino acid 131-136) region respectively (Saini *et al.* 2010). Mutating the critical amino acids residue F121, F123 in SE$_1$ and F131, F133 in SE$_2$ shows strong Sui$^-$ phenotype that can be suppressed by eIF1 overexpression, while the Gcd$^-$ phenotype shown by these mutants could be suppressed by overexpression of the TC (Saini *et al.* 2010). Recent structural studies of 43S pre initiation complex (PIC) showed that eIF1A CTT traverse P-site and did not allow full accommodation of Met-tRNA$_i^{Met}$ in the P-site thus promoting scanning competent P$_{OUT}$ state (Hussain *et al.* 2014). It is proposed that the SE mutant destabilizes P$_{OUT}$ state and facilitate P$_{OUT}$ to P$_{IN}$ transition at UUG codon causing Sui$^-$ phenotype (Saini *et al.* 2010).

Remarkably, the mutation in eIF1A-NTT dubbed as scanning inhibitor (SI) region (NDSDG17 − 21AAAAA) suppresses the Sui$^-$ phenotype conferred by the eIF1A-CTT defective SE$_1$ and SE$_2$ elements. It is suggested that the premature closed scanning conformation caused by CTT mutant is reversed by the NTT (17-21) mutant (Saini *et al.* 2010). It implies that while CTT involved in scanning enhancement, the NTT tail has opposite effect of scanning inhibition on start codon selection. Thus, the Ssu$^-$ phenotype shown by the eIF1A-NTT (17-21) mutant lacks the scanning arrest elements could be able to skip the UUG codon and hence suppresses the Sui$^-$ phenotype of other known strong Sui$^-$ mutants such as eIF2β^{S264Y} and eIF5^{G31R} (Fekete *et al.* 2007; Saini *et al.* 2010).

1.8 eIF2 regulates tRNA delivery and GTP hydrolysis

The eIF2 is a heterotrimeric complex consist of core eIF2γ subunit (encoded by *GCD11*) to which binds eIF2α (encoded by *SUI2*) and eIF2β (encoded by *SUI3*) subunits. The core eIF2γ subunit has three distinct domains; G-domain has GTP binding site and classical switch region (SW-I and SW-II) involved in GTP hydrolysis, a characteristic of G-proteins (Hall *et al.* 2002).

The β-barrel Domain II and Domain III are packed against the G-domain (Schmitt *et al.* 2012; Hussain *et al.* 2014; Llácer *et al.* 2015).The heterotrimeric eIF2 complex binds to the GTP molecule and Met-tRNA$_i^{Met}$ to form TC (Levin *et al.* 1973). Based on the homology modeling with EF-Tu-Phe RNA complex, the eIF2γ showed that tRNA binds in between G domain and domain II. To support this model, mutating a residue (Y142H) in that binding pocket conferred slow growth (Slg⁻) phenotype, which is rescued by overexpression of tRNA$_i^{Met}$ (Erickson and Hannig 1996; Roll-Mecak *et al.* 2004). Hydroxyl radical probing and cryo-EM of 48S PIC showed, unlike the tRNA binding pocket created by Domain II and Domain III in EF-Tu, the domain III of eIF2γ did not interact with tRNA$_i$ (Shin *et al.* 2011; Hussain *et al.* 2014). The T stem-loop of tRNA does not bind to domain III of eIF2γ as in EF-Tu, rather it hangs out and protrudes toward helix 44 of 18S RNA, a helix known to regulate start codon selection in the 40S (Shin *et al.* 2011). The eIF2γ^{N135D} SW-I mutation causes increased rate of Met-tRNA$_i^{Met}$ dissociation from TC and showed Gcd⁻ and Sui⁻ phenotype (Alone *et al.* 2008). Isolation and characterization of the intragenic suppressor mutant of the eIF2γ^{N135D} mutations in the SW-II region (A208V) revealed higher tRNA$_i$ binding affinity and rescued Gcd⁻ and Sui⁻ phenotype, suggesting lower tRNA$_i$ binding affinity may be the cause of Sui⁻ phenotype. Another suppressor mutation in Domain-II (A382V) restored the tRNA$_i$ binding affinity, however, did not suppress the Sui⁻ or Gcd⁻ phenotype, suggesting that mere tRNA$_i$ binding is not important rather the tRNA$_i$ should be delivered in the proper orientation. To support this notion, third suppressor mutation in G-domain (A219T) did not restore tRNA$_i$ binding affinity, however, it had the ability to suppress the Sui⁻ phenotype (Ssu⁻) phenotype. These results suggested that Sui⁻ phenotype is not caused by hyper tRNA$_i$ dissociation, rather the conformation of tRNA$_i$ bound to the 43S complex determines the

Sui⁻ phenotype, underlines the importance of the P_{IN} and P_{OUT} conformation during start codon selection. (Alone *et al.* 2008).

Post GTP hydrolysis the eIF2-GDP complex binds to GDP with higher affinity (Kd ~0.02 μM) as compared to GTP (Kd ~1.7 μM). Thus replenishing GDP with GTP to recycle TC, requires Guanine nucleotide exchange factor (GEF) eIF2B (Kapp and Lorsch 2004). One of the interesting eIF2γ^{K250R} mutation causes weak GDP or GTP binding thus causing slow growth phenotype, which can be suppressed by overexpression of tRNA$_i$ (Erickson and Hannig 1996). This mutant could survive in the absence of eIF2α subunit (Erickson *et al.* 2001). This suggested that the eIF2α subunit plays a role in stimulating the eIF2B-catalyzed guanine nucleotide exchange on eIF2.

The eIF2α subunit consists of three domains; N-terminal OB fold, central α-helical domain and C-terminal α/β domain. The eIF2α binds to the Domain II of eIF2γ via its C-terminal α/β domain (Dhaliwal and Hoffman 2003; Hussain *et al.* 2014; Llácer *et al.* 2015). The key role of eIF2α subunit is in the regulation of global translation initiation. Under stress or nutrient deprivation condition, the eIF2α kinase GCN2 phosphorylates eIF2α at Ser51 residue (Dever *et al.* 1992). The phosphorylated form of eIF2 complex interacts non-productively with eIF2B and blocks GDP to GTP exchange causing a decrease in TC levels (Krishnamoorthy *et al.* 2001; Nika *et al.* 2001). Apart from its role in regulating the levels of TC, the eIF2α has a role in improving the translation efficiency of AUG codon. Cross-linking experiment of thiolated mRNA revealed the interaction of eIF2α subunit to the -3 region when the AUG codon was occupying P-site (Pisarev *et al.* 2006). This is also strengthened by a recent py48S cryo-EM structure, where eIF2α occupies E-site of the 40S and mimic like an E-site tRNA in the initiation complex (Hussain *et al.* 2014). eIF2 complex lacking eIF2α shown to have a reduced tendency of AUG recognition along

with the diminished capacity to recognize good sequence context preceding the AUG codon (Pisarev *et al.* 2006).

The eIF2β subunit consists of three elements; the N-terminal unstructured region consists of three clusters of lysine repeats [K-boxes], central helix-turn-helix, and the C-terminal Zinc binding domain (ZDB). K-boxes consists of seven Lysine residues and one Serine or Threonine residue. Truncation studies revealed that at least one K-box is required for cell viability and positive charge amino acid in that position is required for its function (Laurino *et al.* 1999). The K-boxes are shown to interact with the negatively charged C-terminal AA boxes (acidic and aromatic amino acids) of eIF5 or eIF2Bε (Asano *et al.* 1999). Mutational studies in C-terminal Zinc binding domain revealed a defect in the mRNA binding (Laurino *et al.* 1999). Mutation in the ZBD (S264Y and L254P) leads to the intrinsic GTPase activity of eIF2 complex (Huang *et al.* 1997). The eIF2β^{S264Y} mutant is functionally suppressed by the deletion of K-box I and II, which causes the impaired contact of mRNA and eIF2β and hence reduce GTPase activity on 48S PIC (Laurino *et al.* 1999). Alternatively, it could have worked by affecting the interaction of GTPase activating protein (eIF5) to eIF2β and reduces the GTPase activity in the 48S complex.

1.9 eIF3 recruit initiation factors and regulates AUG codon selection

eIF3 is a multi-subunit protein complex consists of six subunits in yeast (Tif32/a, Prt1/b, Nip1/c, Tif34/i, Tif35/g and Hcr1/j). The eIF3b is considered to form the primary scaffold to which eIF3j subunit and eIF3a binds. The central part of eIF3b interacts with eIF3c while the eIF3i and eIF3g bind to the C-terminal end of eIF3b (Kouba, Rutkai, Karaskova, & Valasek, 2012). The N-terminal region of the eIF3c interacts with eIF1 and eIF5 along with the TC (Valasek *et al.* 2004a). Mutation in the NTD of eIF3c (Alanine substitutions in box12) confers Sui⁻ phenotype in a manner that can be either suppressed by overexpression of eIF1 or exacerbated by overexpression of eIF5.

This proved that both eIF1 and eIF5 has opposite function in start codon selection by increasing and decreasing the stringency for AUG codon respectively (Valasek *et al.* 2004b). A recent study involving detailed analysis of this phenotype gave much extensive insight into the mechanism of eIF3c in regulating the start codon selection. eIF3c NTD itself has 3 distinct regions namely, 3c0, 3c1, and 3c2. Among them, 3c0 is involved in interaction with eIF5, while 3c1 and 3c2 have interaction with eIF1 (Obayashi et al. 2017). This also showed that impaired interaction between eIF3c and eIF1 in 43S PIC reduces the eIF1 ability to inhibit eIF5-GAP activity at non-AUG codons. In contrast mutating box2 (Alanine substitutions) and box6 (Arginine substitutions) in NTD of eIF3c confer Ssu⁻ phenotype. Because this mutation impaired binding of eIF3c-CTD to eIF5 and hence reduced GAP function and in turn suppress Sui⁻ phenotype conferred by $eIF1^{D83G}$, $eIF2\beta^{S264Y}$, and $eIF5^{G31R}$ (Valášek 2004).

The Cryo-EM structure reveals that eIF3 complex binding area spans from mRNA entry to exit channel on the solvent accessible side of the 40S subunit. This binding is facilitated by eIF3a which interacts with helix h16 to helix h18 in 18S rRNA, Rps2e, and Rps3e at the entry channel, and NTD of eIF3c subunit which interacts with Rps13 at the exit channel respectively (Chiu *et al.* 2010) (Valasek *et al.* 2003). Mutations that disturb the binding of eIF3a (KERR motif and box6) affect the interaction between mRNA and 43S PIC and lead to defect in the mRNA loading (Chiu *et al.* 2010). In addition, the functional interaction between CTD of eIF3a and 40S components (h16 and Rps3e) is believed to contribute to the formation of open scanning conformation of the mRNA entry channel (Khoshnevis *et al.* 2014).

1.10 eIF4F allows scanning through structured 5′ UTR

The eIF4F complex consists of core eIF4G to which binds eIF4A and through eIF4E subunit this complex interacts with the 5′ Cap of mRNA. Although 43S complex is capable of

scanning the mRNA for AUG codon, it is proved that the mRNA with stem loop structure (-30 kcal/mol) from 12 nucleotide from the cap region blocks the binding of 43S complex to mRNA, and stem loop structure (>-60 kcal/mol) from 72 nucleotide from the cap ceases the scanning of 43S PIC complex (Kozak 1989). These stem loop structures are removed by ATP dependent DEAD box RNA helicases. They include Dhx29, and Ded1/Ddx3 (involved scanning) and eIF4A (involved in both binding and scanning). The ATPase and helicase activity of eIF4A is activated by its interaction with HEAT domain of eIF4G and proceeds to unwind the secondary structure (Dominguez *et al.* 1999). Recent structural studies have shown that the eIF4A-4G complex is binding in a half open conformation which favors the release of mRNA after its unwinding followed by an exchange of ADP with ATP to make active form of eIF4A for the next cycle (Meng *et al.* 2014). Biochemical studies have shown that the strand separation by eIF4A in the presence of non-hydrolysable nucleotides (ADP-BeFx), which suggests that the ATP hydrolysis is not required for this reaction *per se*, rather it causes the release of helicase from mRNA and recycles helicases for many cycles of reactions (Kozak 1989). The ssRNA binding activity of eIF4B prevents the reannealing of unwound stem loop of mRNA (Dominguez *et al.* 1999; Asano 2014).

1.11 eIF5 regulates GTP hydrolysis and Pi release

Yeast eIF5 is encoded by *TIF5* gene, it is an essential monomeric protein with the molecular weight of 46 kDa and contains three functional domains; the N-terminal domain (NTD), middle domain and the C-terminal domain (CTD). It functions as a GTPase activating protein (GAP) for eIF2γ by interacting with the eIF2γ-G domain and trigger the GTP hydrolysis during the assembly of 48S PIC (Das *et al.* 2001; Majumdar and Maitra 2005; Alone and Dever 2006). Structural studies revealed, that eIF5 N-terminal domain (NTD) possesses a conventional characteristic functional arginine finger motif [13]FYRYKM[18] (Genbank Accession no: P38431).

Genetic studies revealed that the eIF5^{R15M} mutation completely abolished its GAP function and shown to be recessive lethal (Das *et al.* 2001). Apart from Arg^{15}, two conserved Lys^{33} and Lys^{K55} residues are also shown to be important for its GAP function (Das *et al.* 2001). eIF5 activated GTP hydrolysis of eIF2 is a fast reaction followed by the release of eIF1 from PIC is a slow reaction; hence reduce the rate of Pi release. It has been proposed that eIF1 negatively regulated GAP activity of eIF5 (Valášek et al. 2004). Initial finding involves that addition of eIF5 promotes rapid release of eIF1 from the AUU mRNA compared to AUG mRNA. Also, the addition of eIF5 stimulates the dissociation of a variant of eIF1^{G107K}, which otherwise retained on the 40S for a longer time. Thus, eIF5 plays a critical role in promoting the release of eIF1 besides its GAP function. Interestingly, the eIF5-NTD has structural resemblance with eIF1 which can bring competition between them to bind to 40S P-site. Though eIF5 NTD is closer to eIF2γ to provide GAP function, it is hypothesized that after GTP hydrolysis the NTD switch the place towards eIF1 whose binding is already weakened by deeper insertion of tRNA$_i^{Met}$ (Nanda *et al.* 2013).

The eIF5^{G31R} mutation in the GAP region causes the recognition UUG as a start codon (Sui^{-} phenotype) possesses hyper GTPase activity and observed to be recessive lethal (Huang *et al.* 1997; Saini *et al.* 2014). It has been shown that the eIF5^{G31R} causes premature release of both eIF1 and P$_i$ to deliver the Met-tRNA$_i^{Met}$ at the UUG codon (Saini *et al.* 2014). However, the Sui^{-} phenotype is suppressed by NTT variant of eIF1A (eIF1A$^{17-21}$) which is proposed to block premature P$_{IN}$ conformation at UUG codon and promote P$_{OUT}$ conformation to favor the scanning down to search AUG codon. Similar suppression effect was also observed in another eIFβ^{S264Y} Sui^{-} mutant (Fekete *et al.* 2007).

Apart from the GAP function, the eIF5 performs an equally important role in the formation of the multifactor complex (MFC) through its C-terminal domain (CTD). It possesses the ability

37

to coordinate with other initiation factors in the complex including eIF1, eIF1A, eIF2β, eIF3C, and eIF4G (Bandyopadhyay and Maitra 1999; Asano *et al.* 2000, 2001b; Majumdar and Maitra 2005; Yamamoto *et al.* 2005). Recently, Pavitt and colleagues found a novel role of eIF5 in regulating the TC recycling. It is well known that after the delivery of tRNA$_i$ to AUG codon in P-site, the dissociated eIF2-GDP complex from the 40S subunit needs to exchange GDP to GTP in order to bind new Met-tRNA$_i^{Met}$ with the help of eIF2B. It was observed that the eIF5 stay bound with eIF2-GDP complex and through its middle domain DWEAR motif inhibited GDP dissociation. This function of eIF5 was labeled as GDP dissociation inhibitor (GDI) (Jennings and Pavitt 2010b; Jennings *et al.* 2013).

1.12 18S rRNA modulates tRNA delivery and eIF1 binding

Eukaryotic ribosomes possess two subunits namely 40S (composed of 32 proteins and 18S rRNA), and 60S (47 proteins, and three rRNAs [5S, 5.8S, and 25S]) (Woolford and Baserga 2013). The ribosome biogenesis starts in nucleolus where the rRNAs are robustly transcribed from 150 tandem copies of *35SRDN* gene under constitutive *POLI* promoter. The initial transcript contains 18S, 5.8S, and 25S together with two external and two internal spacer sequences. Upon splicing and modifications by various enzymes, it is cleaved and processed into mature 18S, 5.8S and 25S rRNA particles (Woolford and Baserga 2013). Yeast strain, where all copies of *35SRDN* genes were deleted and supplemented with a high copy plasmid borne *RDN* construct paved the way to understand the role of rRNA in the translation process of yeast (Wai *et al.* 2000).

In 40S ribosomal subunit, the 18S rRNA serves as a platform for various ribosomal proteins and initiation factors binding. The secondary structure of 18S rRNA is largely divided into 4 major domains. They are i) 5′ domain, ii) central domain, iii) 3′ major domain, and iv) 3′ minor domain (Nemoto *et al.* 2010). However, based on its three-dimensional folding pattern and structure it

possesses following distinct functional structures such as head, platform, body, beak, shoulder, left foot, and right foot (Klinge *et al.* 2011). The region of the 18S rRNA where amino acylated tRNA binds is called A-site, peptidyl-tRNA binds is P-site and the unacylated tRNA binding region is called E-site.

The 5′ major and central domain of 18S rRNA together constitutes the major portion of platform and body of the 40S subunit. The 3′ major domain forms head and the 3′ minor domain consists of helix h44 extends from the P-site towards the foot of the 40S subunit. The mature 40S subunit is synthesized by series of modifications of both rRNA and ribosomal protein (Woolford and Baserga 2013). Mutagenic studies of 18S rRNA showed that residues present in both 3′ major and 3′ minor region affects TC binding to 40S and lead to constitutive *GCN4* expression. Mutating G1575 and G1576 residues eliminated the A-minor contact with the anticodon stem loop (ASL) of tRNA$_i$ and conferred Gcd$^-$ phenotype and leaky scanning (Dong *et al.* 2008). Analysis of eIF1A hydroxyl radical probing of the 40S subunit in the presence of either AUG codon containing mRNA or non-AUG codon (AUC) containing mRNA showed that residues G1575, A1576, A1577, U1578 in helix 29 are in close proximity to ASL helix of tRNA during scanning (Zhang *et al.* 2015).

Upon encountering the AUG codon, the ribosome undergoes a critical conformational change that involves the clockwise rotation of 40S head by 5 Å. This structural change is associated with the downward movement of head which helps in reforming the interaction between helix h18 and helix h34 causing narrowing of mRNA entry channel and arresting the scanning process. The "Closed" conformational change in the 40S ribosome is majorly driven by residues in helix h22, h28, h31 and h34 of the head region (Zhang *et al.* 2015; Llácer *et al.* 2015). The scanning arrest brings tRNA$_i$ much deeper into the P-site by 7 Å referred as P$_{IN}$ state which helps in recognizing

39

the start codon (AUG) present in the P-site, during this state the 18S residues G1575-A1576 interact with the three consecutive G:C base pairs of ASL to stabilize this binding (Zhang *et al.* 2015). The steric clash between tRNA$_i$ ASL and β-hairpin loop of eIF1 resulted due to P$_{IN}$ conformation weaken the binding of eIF1 with the 40S subunit (Martin-Marcos *et al.* 2013). Thus, it favors the release of both eIF1 from P-site and P$_i$ from eIF2-GDP complex which otherwise antagonized by eIF1 (Hinnebusch and Lorsch 2012). The role of 18S rRNA is further enlightened by the study of helix h28 of 18S rRNA which contacts the first base of the start codon ('A' in 'AUG' codon). Also, mutation in the helix h31 residue (A1139U) present below the codon-anticodon formation increases the leaky scanning and suppresses the Sui⁻ phenotype of eIF2β^{S264Y} mutant (Nemoto *et al.* 2010). It is also found that in addition to the AUG codon, purines at −3 and +4 positions probably affect the initiation codon selection by stabilizing conformational changes that occur upon codon–anticodon base pairing, by interacting with the nucleotides A1818–A1819 in helix h44 of 18S rRNA, which forms part of the A-site (Pisarev *et al.* 2006).

1.13 eIF5B helps in subunit joining

The factor eIF5B is encoded by *FUN12* gene which is an ortholog of bacterial IF2 and helps in 60S subunit joining with the 40S subunit. The cryo-EM structure suggested that the domain IV of eIF5B interact with Met-tRNA$_i$^{Met} in the P-site (Fernández *et al.* 2013; Kuhle and Ficner 2014). The domain IV of eIF5B interacts with the last five residues of eIF1A C-terminal tail and mutation in the C-terminus region affects subunit joining (Olsen *et al.* 2003; Acker *et al.* 2006; Fringer *et al.* 2007). The GTPase activity of eIF5B is necessary to release eIF1A, but it did not affect 60S subunit joining (Fringer *et al.* 2007; Acker *et al.* 2009). It has been proposed that the eIF5B stabilizes the Met-tRNA$_i$^{Met} in the 80S complex post eIF1A release. In the absence of

eIF5B, the 48S PIC cannot stably anchor the initiator tRNA in the P site and either dissociate or resume scanning towards downstream AUG codon (Leaky scanning) (Lee *et al.* 2002).
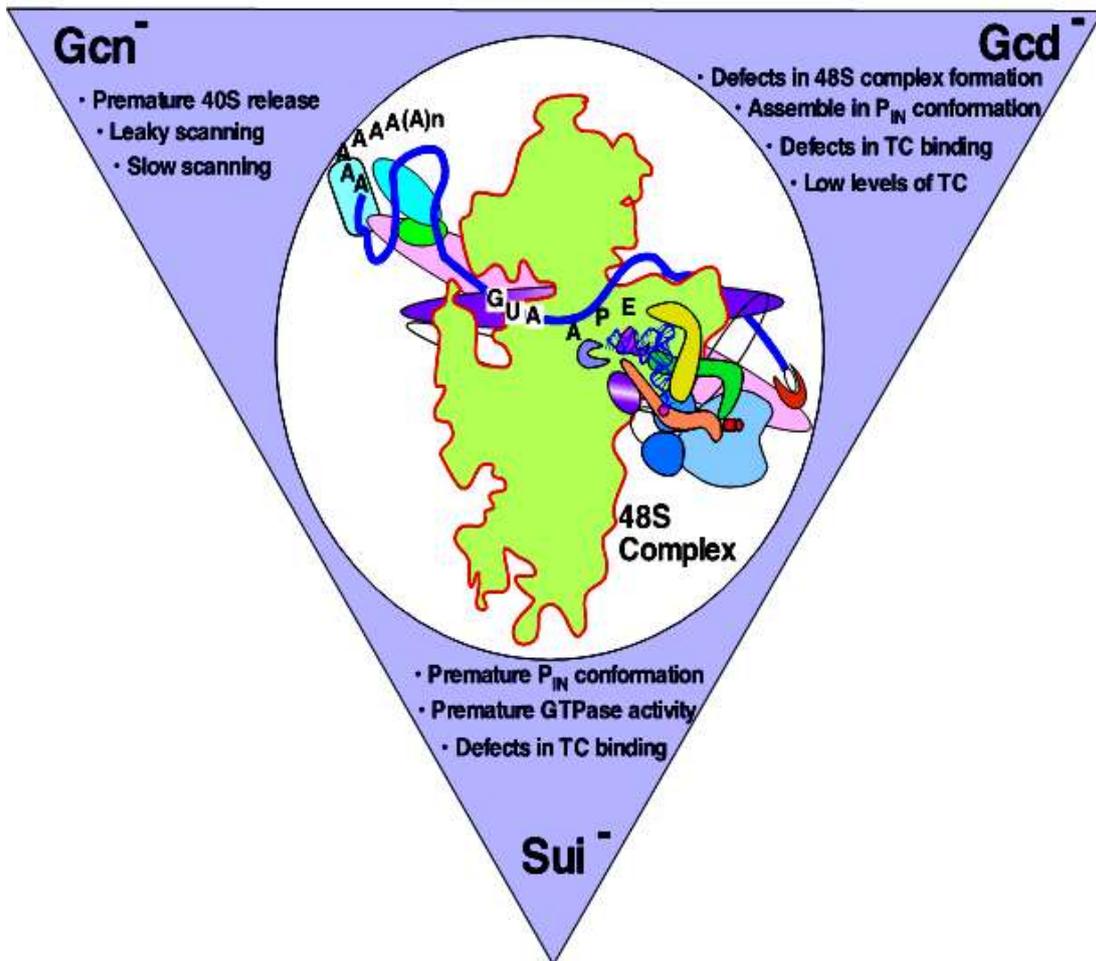
Figure 1.3: Model depicting the possible relationship between different phenotypes of translation initiation defective mutants.

Mutation in translation initiation factors can have a defect in either 48S PIC assembly or post 48S assembly to cause Gcn¯ or Gcd¯ phenotype respectively. Also, some mutants can alter the fidelity of start codon selection from AUG to non-AUG codons (UUG). Remarkably, all Sui¯ mutations are associated with the defect in forming 48S PIC assembly and hence causes Gcd¯ phenotype.

1.14 Aim of the study

Current understanding of molecular events in translation initiation is largely understood by the conventional genetic approaches in yeast. Extensive studies from different groups have isolated various mutants that affect translation initiation. These mutants affect either the scanning of mRNA or fidelity of start codon selection or both. The scanning defect can be studied using *GCN4* mRNA as a model system, whose gene expression mechanisms were well understood. A defect in having non derepression of *GCN4* in starvation causes decrease in *GCN4* expression and confer Gcn⁻ phenotype while constitutive derepression of *GCN4* expression causes Gcd⁻ phenotype. However, the defect associated with start codon selection (Sui⁻ mutants) can be studied using *HIS4* mRNA possessing AUG or UUG as a start codon. Hence, translation initiation mutants confer Sui⁻, or Gcn⁻, or Gcd⁻ phenotype (figure 1.3). In this study, we have explored one of the strongest Sui⁻ mutants that possess high efficiency towards non-AUG (UUG) codon as start codon and characterized its effect on general amino acid control (GAAC) in yeast using *GCN4* as a model system. Also, we tried to understand the role of 18S rRNA of the 40S subunit in controlling the UUG codon selection in this hyper GTPase defective eIF5^{G31R} mutant. Based on these goals we proposed following objectives for this study.

1. Genetic characterization of eIF5^{G31R}
   a. Sui⁻ phenotype (*HIS4-lacZ* reporter)
   b. Gcn⁻/Gcd⁻ phenotype (*GCN4-lacZ* reporter)
2. Mutagenesis and screening of 18S rRNA for the suppressors of Sui⁻ (Ssu⁻) for eIF5^{G31R}
3. *In vivo* genetic characterization of Ssu⁻ phenotype.
   a. Ssu⁻ phenotype (*HIS4-lacZ* reporter)
   b. Gcn⁻/Gcd⁻ phenotype (*GCN4-lacZ* reporter)

Chapter 2
Materials and methods

2.1 Nutrient supplements

S.No	Nutrient	Stock	Solvent	Working concentration	Storage
1	Leucine	100 mM	Water	2 mM	RT
2	Uracil	20 mM	Water	0.2 mM	RT
3	Tryptophan	40 mM	Water	0.4 mM	4°C
4	Histidine	100 mM	Water	0.3 mM	RT
5	Isoleucine/valine	50 mM	Water	0.5 mM	RT
6	Adenine	10 mM	Water	0.15 mM	RT

2.2 Antibiotics and drugs

S.No	Name	Stock	Solvent	Working Concentration	Storage
1	Ampicillin	100 mg/ml	Water	100 µg/ml	-20°C
2	Kanamycin	30 mg/ml	Water	30 µg/ml	-20°C
3	G418	300 mg/ml	Water	300 ug/ml	-20°C
4	Phleomycin	10 mg/ml	Water	10 µg/ml	-20°C
5	3-Amino1,2,4 triazole	1M	Water	50 mM	-20°C
6	X-gal	20 mg/ml	DMSO	40 µg/ml	-20°C

2.3 Dropout media preparation

S.No	Components	Weight (g)
1	Adenine	0.5
2	Alanine	2
3	Arginine	2
4	Asparagine	2
5	Aspartic acid	2
6	Cysteine	2
7	Glutamine	2
8	Glutamic acid	2
9	Glycine	2
10	Inositol	2
11	Isoleucine	2
12	Lysine	2
13	Methionine	2
14	Para-Amino benzoic acid	0.2
15	Phenylalanine	2
16	Proline	2
17	Serine	2
18	Threonine	2
19	Tyrosine	2
20	Valine	2

The above nutrient's powders were homogeneously mixed and stored in RT.

2.4 Media preparation

LB medium: Mix 1% peptone, 1% sodium chloride, and 0.5% yeast extract in double distilled water (ddH$_2$O) and sterilized by autoclaving.

YPD medium: Mix 2% peptone, and 1% yeast extract in ddH$_2$O and sterilized by autoclaving. After cooling to RT, 2% of filter sterilized dextrose was added.

YPGal medium: Mix 2% peptone, and 1% yeast extract in ddH$_2$O and sterilized by autoclaving. After cooling to RT, 2% of filter sterilized galactose was added.

Synthetic Complete Dextrose (SCD) medium (250 ml): Mix 0.17% YNB without ammonium sulfate and 0.5 % ammonium sulfate in 200 ml of ddH$_2$O, sterilized by autoclaving add filter sterilized mixture of 0.2% Amino acid dropout supplemented with appropriate amino acids along with 2% dextrose. To prepare agar plates, 2% agar was added before autoclaving.

G418 plate preparation: Same as SCD plate except add 0.5% monosodium glutamate as nitrogen source instead of ammonium sulfate. Add 300 μg/ml of G418 just prior to plating.

3-Amino-1,2,4-Triazole (3AT) plate preparation: Same as SCD plate preparation, different concentration of filter sterilized 3AT was added as desired, just before plating.

5-Fluoroorotic Acid (5-FOA) plate preparation: 125 ml of 2x SCD medium mixed with 5 ml of 20 mM uracil and 0.25g 5-FOA were heated at 50°C and filter sterilized followed by mixing with 125 ml of autoclaved 2% agar before plating.

2.5 Strains and plasmids

The yeast strains, plasmids, and oligonucleotides used in this study are listed in Table 1, Table 2 and Table 3 respectively.

2.6 Deletion of the *HIS4* gene

The yeast strain YP823 having a genotype of *Matα, Ura3-52, Leu2-3,112, trpΔ63, GAL2⁺* was used to delete *HIS4* gene as follows. Plasmid construct pFA6a-*KanMx6* (pA559) carrying *KanMx6* gene disruption cassette (1.6 kb) (Wach *et al.* 1997), was PCR amplified using oligonucleotide flanking 40 nucleotides of 5′ and 3′ end of *HIS4* ORF (using oligos oPA164 and oPA165 respectively). Approximately 3 μg of PCR amplified product was gel purified and transformed into the yeast using standard protocol (Gietz and Woods 2006). The transformants were screened based on their resistance on modified SCD plate (0.17% yeast nitrogen base, 0.5 % monosodium glutamate) containing G418 (300 μg/ml) antibiotic. The resistant colonies were further confirmed by PCR (using oligonucleotides oPA162 and oPA254) for the authenticity of the *HIS4* gene deletion. The resultant strain is labeled as YP824.

2.7 Deletion of the *GCN2* gene

To delete *GCN2* gene in the strain YP824, a disruption cassette *LoxP-URA3-LoxP* was PCR amplified using oligonucleotide oPA781 and oPA782 having 40 bp flanking region of *GCN2* ORF (Gueldener *et al.* 2002). Approximately 3 μg of PCR amplified deletion cassette (1.7 kb) was transformed into yeast strain YP824 and plated on SD-Ura drop out medium. Successful recombinant cells were screened for stable *URA3* incorporation into *GCN2* locus by checking the sensitivity to 3AT inhibition followed by the eviction of *URA3* gene using recombination at *LoxP* site in the presence of 5-Fluoroorotic acid (5-FOA). The deletion of *GCN2* ORF was further

confirmed by PCR using oligonucleotide oPA772 and oPA790. The resultant strain is labeled as YP865.

2.8 Manipulation of yeast strain lacking 35S*RDN* gene

The Yeast strain YP807 (*rdn*ΔΔ) carries high copy plasmid borne *RDN* genes pNOY353 [P_{GAL7}-35S*RDN*^{WT}/*TRP1*] under Galactose promoter was transformed with pNOY130 [P_{GAL7}-35S*RDN*^{WT}/*URA3*] and the plasmid pNOY353 was evicted out by growing on YPGal medium. *HIS4* gene was deleted using homologous recombination approach as mentioned in section 2.6. the resultant strain was labeled as YP844. The strain NOY892 (*MATa ade2-1 ura3-1 trp1-1 leu2-3,112 his3-11 can1-100 rdn*ΔΔ::*HIS3 gcn2Δ::KanMx4* carrying pNOY130) also subjected to *HIS4* gene deletion as mentioned above except the disruption cassette (1.3 kb) is PCR amplified from pUG66 (p4032) and the transformants were selected on YPGal containing phleomycin antibiotic (10 μg/ml). The resultant strain was labeled as YP851.

2.9 Cloning of *18SRDN* gene and generation of mutant library

To generate a random pool of mutant library the intermediate gateway vector (pA688) was generated as follows. A stuffer DNA was PCR amplified from yeast (YP823) genomic DNA using oligos oPA543 and oPA708 and the resultant PCR product was cloned under NdeI and DraIII site in pA687 plasmid to replace ~ 2 kb *18SRDN* segment.

The C1209U substitution mutation was introduced in the *18SRDN* plasmid DNA (pA687) by multi-site directed mutagenesis kit (Stratagene) using oligonucleotide oPA677 to generate the plasmid P_{POLI}-*18SRDN*^{C1209U} (pA761).

2.10 Cloning of eIF5 variants in yeast shuttle vector

The eIF5^{G31R} encoding DNA (2.1 kb) was derived from the plasmid pRS313-*eIF5*^{G31R} (C3097) [provided by Thomas E. Dever] was digested with EcoRI-SalI restriction endonuclease and sub cloned into pYCplac22 (pA823), pYCplac33 (pA309), and pYCplac111 (pA308) vector to generate pYCplac22-*eIF5*^{G31R} (pA860), pYCplac33-*eIF5*^{G31R} (pA703), and pYCplac111-*eIF5*^{G31R} (pA681). Another eIF5 variant (eIF5^{G31S}) was created by fusion PCR using oligonucleotides oPA854, oPA985, oPA986, and oPA855 and plasmid pA860 as a PCR template, and cloned into pYCplac22 vector at EcoRI-SalI site to generate pYCplac22-*eIF5*^{G31S} (pA1034). Wild type *eIF5* gene was generated by quick change multi-site mutagenesis kit (Stratagene) using oligonucleotide oPA834 and plasmid template pA860 to generate pYCplac22-*eIF5*^{WT} (pA870). All recombinant positive clones were identified using appropriate restriction digestion and further confirmed by DNA sequencing.

2.11 Cloning of eIF2β^{S264Y} in yeast shuttle vector

The *eIF2β*^{S264Y} cassette (1.9 kb) was derived from the plasmid pRS313-*eIF2β*^{S264Y} (C3096) [provided by Thomas E. Dever] by BamHI-SalI digestion and sub cloned into pYCplac22 (pA823) to generate pYCplac22- *eIF2β*^{S264Y} (pA890).

2.12 Cloning of *HIS4* alleles in yeast shuttle vector

The 3.1 kb *HIS4*^{AUG} DNA was PCR amplified from yeast (YP823) genome using oligonucleotides oPA162 and oPA163 and cloned into pYCplac22 (pA823), pYCplac33 (pA309), pRS314 (p701), pRS424 (p1377), pYCplac22-*eIF5*^{G31R} (pA860), and pYCplac22-*eIF2β*^{S264Y} (pA890) plasmid at BamHI site to generate pYCplac22-*HIS4*^{AUG} (pA858), pYCplac33-*HIS4*^{AUG}

(pA839), pRS314-$HIS4^{AUG}$ (pA616), pRS424-$HIS4^{AUG}$ (pA780), pYCplac22-$eIF5^{G31R}/HIS4^{AUG}$ (pA861), and pYCplac22-$eIF2\beta^{S264Y}/HIS4^{AUG}$ (pA952).

The $HIS4^{UUG}$ allele was generated by mutating AUG into AUU. The plasmid pYCplac22-$eIF5^{G31R}/HIS4^{AUG}$ (pA861) was subjected to site directed mutagenesis using oligonucleotide oPA154 using quick change multi-site mutagenesis kit (Stratagene) to generate pYCplac22-$eIF5^{G31R}/HIS4^{UUG}$ (pA862) plasmid. Further this $HIS4^{UUG}$ allele is derived using BamHI digestion and sub cloned into pYCplac22 (pA823), pYCplac33 (pA309), pRS314 (p701), pRS424 (p1377), and pYCplac22-$eIF2\beta^{S264Y}$ (pA890) to generate pYCplac22-$HIS4^{UUG}$ (pA859), pYCplac33-HIS^{UUG} (pA840), pRS314-$HIS4^{UUG}$ (pA792), pRS424-$HIS4^{UUG}$ (pA781), and pYCplac22-$eIF2\beta^{S264Y}/HIS4^{UUG}$ (pA953).

The 6xHA-tag was introduced at the C-terminal end of $HIS4$ alleles by fusion PCR using oligonucleotides oPA166, oPA904, oPA905, and oPA163 using construct pA858. The PCR amplified product was digested with BamHI and cloned into pA823 or pA860 plasmid at BamHI site to generate pYCplac22-$HIS4^{AUG}$-6xHAtag (pA974) and pYCplac22-$eIF5^{G31R}/HIS4^{AUG}$-6xHAtag (pA975) respectively. The pYCplac22-$HIS4^{UUG}$-6xHAtag (pA978), and pYCplac22-$eIF5^{G31R}/HIS4^{UUG}$-6xHAtag (pA979) were generated as procedure outlined above except using construct pA859 as a PCR template.

2.13 Construction of P_{GAPDH}-HIS4-LacZ reporter plasmids

The $GAPDH$ (glyceraldehyde-3-phosphate dehydrogenase) promoter (687 bp) was PCR amplified from yeast genome (YP823) using oligonucleotide oPA987 and oPA1014. The $HIS4$ sequence containing 5′ UTR region and N-terminal 10 amino acids were PCR amplified using p3989 or p3990 plasmid template and fused with $GAPDH$ promoter using oligonucleotide

oPA1015 and oPA1016. The resultant PCR product was digested with HindIII-SalI restriction endonuclease and cloned into a plasmid containing *LacZ* ORF to generate P_{GAPDH}-*HIS4*^{AUG}-*LacZ* (pA1056) and P_{GAPDH}-*HIS4*^{UUG}-*LacZ* (pA1057) plasmids respectively.

2.14 Construction of uORF-less and UUG-less 5′ UTR in *GCN4-lacZ* plasmids

All the 10 UUG codons from the 5′ UTR of *GCN4* were removed by fusion PCR using oligonucleotides oPA848, oPA871, oPA852, oPA869, oPA868, oPA849, oPA866, oPA892, oPA891, and oPA851 and plasmid p227 as a PCR template. The resultant fusion PCR product (958 bp) was cloned at SalI-BamHI site in p227 by replacing the corresponding 5′ UTR region to generate pYCP50-*GCN4 lacZ*-uORF-less and upUUG-less (pA901).

2.15 Construction of *HIS3* plasmid

The 1.2 kb *HIS3* gene was PCR amplified from yeast genomic DNA using oligos oPA839 and oPA840 and cloned into pRS424 vector at BamHI site to generate pRS424-HIS3 (pA905) construct.

2.16 Construction of *HIS3-LacZ* reporter plasmid

The promoter along with DNA region encoding N-terminal 21 amino acids of *HIS3* gene was PCR amplified from yeast genome using oligos oPA1021 and oPA1022. The resultant PCR product was digested with SalI-BamHI and cloned into a plasmid containing *LacZ* ORF to generate pYCplac33-HIS3-lacZ (pA1062) vector.

Table 1. Yeast strains used in this study

S.No.	Stock No.	Genotype	Source or reference
1	YP823	**H1511:** *Mat α Ura3-52 Leu2-3,112 trpΔ63 GAL2⁺*	(Foiani *et al.* 1991)
2	YP824	*Mat α Ura3-52 Leu2-3,112 trpΔ63 GAL2⁺ his4::KanMx6*	This study
3	YP865	*Mat α Ura3-52 Leu2-3,112 trpΔ63 GAL2⁺ his4::KanMx6 gcn2::loxP*	This study
4	YP807	**NOY891:** *MATa ade2-1 ura3-1 trp1-1 leu2-3,112 his3-11 can1-100 rdnΔΔ::HIS3* carrying pNOY353	(Wai *et al.* 2000)
5	YP843	*MATa ade2-1 ura3-1 trp1-1 leu2-3,112 his3-11 can1-100 rdnΔΔ::HIS3* carrying pNOY130	This study
6	YP844	*MATa ade2-1 ura3-1 trp1-1 leu2-3,112 his3-11 can1-100 rdnΔΔ::HIS3 his4::KanMx6* carrying pNOY130	This study
7	YP851	*MATa ade2-1 ura3-1 trp1-1 leu2-3,112 his3-11 can1-100 rdnΔΔ::HIS3 gcn2Δ::KanMx4 his4::ble* carrying pNOY130	This study

Table 2. Plasmids used in this study

S. No	Plasmid number	Plasmid name	Copy (Yeast)	Source or Reference
1	p1377	pRS424	h.c	(Christianson et al. 1992a)
2	p180	pYCP50-WT *GCN4-LacZ*	s.c	(Hinnebusch 1985)
3	p227	pYCP50-*GCN4 LacZ* [uORFless]	s.c	(Miller & Hinnebusch 1989)
4	p3989	P_{HIS4}-$HIS4^{AUG}$-*LacZ*	s.c	(Donahue & Cigan 1988)
5	p3990	P_{HIS4}-$HIS4^{UUG}$-*LacZ*	s.c	(Donahue & Cigan 1988)
6	p4032	pUG66	Bacterial	(Gueldener *et al.* 2002)
7	p4033	pUG72	Bacterial	(Gueldener et al. 2002)
8	p701	pRS314 *TRP1* vector	l.c	(Sikorski & Hieter 1989)
9	pA1034	pYCplac22-*eIF5^{G31S}*	s.c	This study
10	pA1056	pYCplac33-P_{GAPDH}-$HIS4^{AUG}$-*LacZ*	s.c	This study
11	pA1057	pYCplac33-P_{GAPDH}-$HIS4^{UUG}$-*LacZ*	s.c	This study
12	pA308	pYCplac111 *LEU2* vector	s.c	(Gietz & Sugino 1988)
13	pA309	pYCplac33 *URA3* vector	s.c	(Gietz & Sugino 1988)
14	pA417	pYEplac181	h.c	(Gietz & Sugino 1988)
15	pA538	pNOY353	h.c	(Wai et al. 2000)
16	pA539	pNOY130	h.c	(Wai et al. 2000)

17	pA559	pFA6a-*KanMx6*	Bacterial	(Wach et al. 1997)
18	pA616	pRS314-*HIS4^{AUG}*	l.c	This study
19	pA681	pYCplac111-*eIF5^{G31R}*	s.c	This study
20	pA687	pNOY373 (pYEplac351-*P_{POLI}-18SRDN^{WT}*)	h.c	(Wai et al. 2000)
21	pA688	pYEplac351-Stuffer DNA	h.c	This study
22	pA761	pYEplac351-*P_{POLI}-18SRDN^{C1209T}*	h.c	This study
23	pA780	pRS424-*HIS4^{AUG}*	h.c	This study
24	pA810	pYEplac181-*eIF1*	h.c	This study
25	pA823	pYCplac22 *TRP1* vector	s.c	(Gietz & Sugino 1988)
26	pA839	pYCplac33-*HIS4^{AUG}*	s.c	This study
27	pA840	pYCplac33-*HIS4^{UUG}*	s.c	This study
28	pA858	pYCplac22-*HIS4^{AUG}*	s.c	This study
29	pA859	pYCplac22-*HIS4^{UUG}*	s.c	This study
30	pA860	pYCplac22-*eIF5^{G31R}*	s.c	This study
31	pA861	pYCplac22-*eIF5^{G31R}/HIS4^{AUG}*	s.c	This study
32	pA862	pYCplac22-*eIF5^{G31R}/HIS4^{UUG}*	s.c	This study
33	pA870	pYCplac22-*eIF5^{WT}*	s.c	This study

34	pA901	pYCp50-*GCN4-lacZ* [uORFless upUUG less (UUG 1 to 10)]	s.c	This study
35	pA952	pYCplac22-*eIF2β^{S264Y}/HIS4^{AUG}*	s.c	This study
36	pA953	pYCplac22-*eIF2β^{S264Y}/HIS4^{UUG}*	s.c	This study
37	pA974	pYCplac22-*HIS4^{AUG}*-6xHAtag	s.c	This study
38	pA975	pYCplac22-*eIF5^{G31R}/HIS4^{AUG}*-6xHAtag	s.c	This study
39	pA978	pYCplac22-*HIS4^{UUG}*-6xHAtag	s.c	This study
40	pA979	pYCplac22-*eIF5^{G31R}/HIS4^{UUG}*-6xHAtag	s.c	This study
41	pM199	pYCp50-*GCN4-lacZ* [uORF1 only with 140 nt 5′ UTR]	s.c	(Grant et al. 1994)
42	pM226	pYCp50-*GCN4-lacZ* [uORF1 extended]	s.c	(Grant et al. 1994)
43	pM231	pYCp50-*GCN4-lacZ* [uORF1 only with 50 nt 5′ UTR]	s.c	(Grant et al. 1994)

44	pA792	pRS314-*HIS4*[UUG]	l.c	This study
45	pA781	pRS424-*HIS4*[UUG]	h.c	This study
46	pA703	pYCplac33-*eIF5*[G31R]	s.c	This study
47	pA905	pRS424-*HIS3*	h.c	This study
48	pA1062	pYCplac33-*HIS3-lacZ*	s.c	This study

Table 3. Oligos used in this study

S. No	Oligo name	Sequence (5'-3')
1	oPA135	CCTGCCAGTAGTCATATGC
2	oPA142	TGAAAACTCCACAGTGTG
3	oPA154	CAAAATTTTTTTCTGAATAATTGTTTTGCCGATTCTACC
4	oPA156	GCCAATTTTCGACCCCCC
5	oPA157	ACGTACTTCACCAAGCAC
6	oPA162	CCAGGATCCGCCAATTTTCGACCCCCC
7	oPA163	CACGGATCCGCCCTAAATGCCTCTTGC

8	oPA164	ATAATGGTTTTGCCGATTCTACCGTTAATTGATGATCTGGC GGATCCCCGGGTTAATTAA
9	oPA165	AATCTACTGGAAATCCTTTGGGATCAACCCAAGCTTACTCG AATTCGAGCTCGTTTAAAC
10	oPA166	CACCGGATCCGCCAATTTTCGACCCCCC
11	oPA182	GAGATTCAAGATGCTGTCC
12	oPA254	CTGCAGCGAGGAGCCGTAAT
13	oPA255	TGATTTTGATGACGAGCGTAAT
14	oPA543	CACCCATATGTCTGCTCCAGAAGCT
15	oPA677	TCAACACGGGGAAACTCATCAGGTCCAGACACAATAAGG
16	oPA708	CCAGCACAGTGTGTTAGAATCTCTTCTTTTGAG
17	oPA772	GTTGGAAAGCCTCGTTGTC
18	oPA781	TCAATAATTTTCCGTTCCCCTTAACACATACTATGTATAAC AGCTGAAGCTTCGTACGC
19	oPA782	ACTGATGCGTTATAGCGCCGCACAGATCTTTAAAGGCGCA TAGGCCACTAGTGGATCTG
20	oPA790	TTGGTCTTCTTCTCTGTAGC

21	oPA834	AGGTGGAAGGTAGAGGTAACGGTATCAAGACTGCCGTTTT GAACG
22	oPA848	TAACGTCGACCCCGTCCTGTGGATCTTCG
23	oPA849	GGTAACGAAACGAATAACTCTTCGAAAAACTGACAGTTTT CGAAAAAGTAAAGGAC
24	oPA851	CACCGGATCCTCTTCAGTCTTGATG
25	oPA852	CTTGCTAAACCGATTATATTTCGTTTTTAAAGTAGATTATT ATTAG
26	oPA854	CACAGAATTCGAAAACGTAGTGATCAGAGAATCC
27	oPA855	CATAGTCGACAGGTCATACGGATATTAGC
28	oPA858	GACTACAAGGACGACGATGACAAATAGCTTAGGAGGGGG CAAAAG
29	oPA859	CTATTTGTCATCGTCGTCCTTGTAGTCTTCGTCGTCTTCTTC ATC
30	oPA866	CCAATCGCTATCAGGTACCCGTAGAATTTTATTC
31	oPA868	TTTATCGAAAGAGAAAATTTATTTTCCCTTATTA
32	oPA869	AATTTTCTCTTTCGATAAATTTAACACAG

33	oPA871	GAAATATAATCGGTTTAGCGAGCTTTTTTCAATGATC
34	oPA891	CATTATTATTACTAAAGTTTCGTTTACCAATTCGTCTGCTCA AGAAAATAAATTAAATAC
35	oPA892	CTTGAGCAGACGAATTGGTAAACGAAACTTTAGTAATAAT AATG
36	oPA904	AGCGTAATCTGGAACATCGTATGGGTAAGCGTAATCTGGA ACATCGTATGGGTAAGCGTAATCTGGAACATCGTATGGGT ACTGGAAATCCTTTGGGATC
37	oPA905	TACCCATACGATGTTCCAGATTACGCTTACCCATACGATGT TCCAGATTACGCTTACCCATACGATGTTCCAGATTACGCTT AGATTATTTCTAACTTGG
38	oPA985	GAAGGTAGAGGTAACAGTATCAAGACTGCCGTTTTG
39	oPA986	GTCTTGATACTGTTACCTCTACCTTC
40	oPA987	CACCAAGCTTTCGAGTTTATCATTATCAATAC
41	oPA1014	GTAAACTATTGTATTACTTTTTCTCGAAACTAAGTTCTT
42	oPA1015	GTAATACAATAGTTTACAAAATTTTTTTC
43	oPA1016	CACCGTCGACGGGATCATCAATTAACGGTAG

44	oPA1024	TTAGAAACACTTGTGGTGAACGATAG
45	oPA1025	CTACTGGAAATCCTTTGGGATCAACC
46	oPA839	CATAGGATCCGTTTTAAGAGCTTGGTGAGC
47	oPA840	CACCGGATCCTCGAGTTCAAGAGAAAAAAAAG
48	oPA1021	CAATGTCGACGATCCGCTGCACGGTCC
49	oPA1022	CACCGGATCCACGATCGCAATCTGAATCTTG

2.17 Ultra-competent bacterial cell preparation

Escherichia coli DH5α from -80°C stock was streaked on LB plates and incubated overnight at 37°C. Individual colony was seeded into 25 ml of LB broth and incubated at 37 °C at 220 rpm for 7 h. It was then subcultured into 50 ml of LB broth with O.D$_{600}$ ~ 0.025 and incubated at 18°C in shaking incubator (220 rpm) until the cells reach mid log phase O.D$_{600}$ ~ 0.5. The culture was chilled on ice for 10 min and spun at 6500xg for 10 min at 4°C. The pellet was washed with 16 ml of Inoue buffer (55 mM MnCl$_2$, 15 mM CaCl$_2$, 250 mM KCl, and 10 mM PIPES pH-6.7) at 6500xg for 10 min at 4°C. The pellet was gently re-suspended in 4 ml of Inoue buffer followed by addition of 300 μl of DMSO after 15 minutes incubation on ice. 200 μl of cell suspension was aliquoted into in pre-chilled 1.5 ml microfuge tubes and flash frozen in liquid nitrogen before permanently stored in -80°C.

2.18 Site directed mutagenesis

Stratagene multi site quick-change mutagenesis kit© was used to insert mutation at the desired site in the plasmid DNA. Briefly, 100 ng of the desired plasmid was mixed with 10 pmol of mutant oligonucleotide and PCR reagents as mentioned by the manufacturer. The PCR reaction was amplified for 30 cycles using Eppendorf thermal cycler©. The template DNA present in the sample was removed by 1μl Dpn I enzyme (10 U/μl), followed by transformation into ultracompetent *E. coli* DH5α cells.

2.19 Instant screening of recombinant clones

The bacterial transformants were patched on LB agar containing appropriate antibiotics and incubated for 14 hours (h) at 37°C. Small amount of colony was re-suspended into 50μl of crack lysis buffer (10% W/V sucrose, 100 mM NaOH, 60 mM KCl, 5mM EDTA, 0.25 % SDS, and 0.01 % of bromophenol blue) and incubated at 37°C for 7 minutes, followed by incubation on ice for 5 minutes. The resultant mixture was spun at 13000 xg for 20 minutes and 15 μl of supernatant was electrophoresed on 0.85 % agarose gel.

2.20 Bacterial colony PCR

A single average sized bacterial colony was resuspended in 20 μl of ddH$_2$O and lysed at 95°C for 5 minutes, followed by centrifugation at 13000 xg for 2 minutes. 3 μl of supernatant was used as a template in 10 μl final PCR reaction mix using appropriate oligonucleotide. The PCR reaction was carried for 25 cycles with appropriate annealing temperature using Eppendorf thermal cycler©.

2.21 DNA sequencing

Big dye terminator v3.1 cycle sequencing kit was purchased from Invitrogen and sequencing reaction was set up as per the following table.

S.No	Components	Volume (µl)
1	Readymade reaction mix	0.5
2	Dilution buffer	1.75
3	Plasmid DNA (100 ng/µl)	2
4	Oligonucleotide (1 pmol/µl)	2
5	Milli Q	3.75
	Total	10

The reaction mixture was set up on PCR with the following reaction conditions for 25 cycles.

Temperature (°C)	Time
95	10 Sec
50	5 Sec
60	4 min

Following the PCR reaction, the products were cleaned as follows. 10 µl of PCR product was transferred into 0.5 ml microfuge tube and added with 12 µl of master mix I (10 µl Milli Q, and 2 µl 125 mM EDTA, pH 8) and 52 µl of master mix II (50 µl of 100 % ethanol, and 2 µl of 3 M Sodium acetate, pH 4.6). The resultant mixture was incubated at RT for 15 minutes and centrifuged at 13000xg for 20 minutes at RT. The pellet was washed with 250 µl of 75% ethanol and air dried for 5 minutes. The pellet is dissolved in 10 µl of Hi-Di formamide and denatured in

95°C for 5 minutes before snap chilled on ice for 5 minutes. These purified DNA fragments were subjected to capillary electrophoresis in 3130 XL genetic analyzer (Applied Biosystems).

2.22 Isolation of Genomic DNA from yeast

Desired yeast strain was cultured overnight in 4 ml of YPD medium and harvested by centrifugation at 6500xg for 5 min. The pellet was resuspended in 300 μl of lysis buffer (2% Triton X-100, 1% SDS, 100 mM NaCl, 10 mM Tris-Cl pH 8.0, 1 mM EDTA) and frozen at -80°C for 5 minutes followed by thawing in 95°C for 1 minutes. The above freeze thaw cycle was repeated thrice. The resultant cell lysate was mixed with an equal volume (300 μl) of Phenol: Chloroform: Isoamyl alcohol (25:24:1). The mixture was subjected to vortex for 2 minutes and spun at 13000xg for 5 minutes at RT. The aqueous phase was carefully transferred to fresh 1.5 ml microfuge tube and mixed with an equal volume (300 μl) of Chloroform: Isoamyl alcohol (24:1) followed by vigorous shaking for 30 sec and spun at 13000 xg for 5 minutes. To the aqueous phase, ice cold ethanol was added and incubated at RT for 5 minutes before spinning at 13000 xg for 5 minutes at RT. The DNA pellet was washed with 1 ml of 70% ethanol after spinning at 13000xg for 5 minutes at RT, and the pellet was air dried. The resultant DNA pellet was resuspended in 30 μl of 10 mM Tris-Cl, pH 7.5 and stored at -20°C.

2.23 Transformation of yeast

A single colony of yeast was seeded into 4 ml of broth containing essential nutrients and incubated at 30°C at 220 rpm overnight. It was then subcultured into 25 ml of broth with $O.D_{600}$ - 0.15 and allowed to grow up to $O.D_{600}$-0.7. The cells were harvested at 4700 xg for 5 min at 20°C. The cell pellet was washed with 5 ml of 1X TE (100 mM Tris-Cl, 10 mM EDTA, pH 7.8) followed by 5 ml of 100 mM Lithium acetate pH 7.5 (in 1X TE) after spinning at 4700 xg for 5 min at 20°C.

The cells were re-suspended with 600 μl of 100 mM Lithium acetate pH 7.5 (in 1X TE) and incubated at 30°C for 20 minutes. The transformation mixtures were prepared as per the following order; 100 μg of calf thymus DNA (Sigma), 3 μg of plasmids, 75 μl of competent cells, 300 μl of 40% PEG (in 100mM Lithium acetate pH 7.5 and 1X TE). The mixtures were incubated at 30°C for 30 minutes followed by heat shock at 42°C for 20 minutes. The cells were spun at 4700xg for 4 min and the pellet was re-suspended in 200μl sterile ddH$_2$O and spread on minimal media agar containing appropriate nutrients and incubated for appropriate days at 30°C.

2.24 Isolation of plasmid from Yeast

A single isolated colony was seeded into a 4 ml of minimal broth (SCD) containing essential nutrients and incubated at 30°C at 220 rpm overnight. The cells were harvested at 5000xg for 5 min at 4°C. The cells were washed with YS1 buffer (0.9 M sorbitol, 0.1 M EDTA pH 7.5, 14 mM β-Mercaptoethanol) by centrifugation at 5000 xg for 5 min at 4°C. The pellet was resuspended in 1 ml of YS1 buffer and treated with 50 units of Lyticase (Sigma) followed by incubation at 37 °C for 2 h with intermittent shaking. Following incubation, the spheroplasts were harvested at 5000 xg for 10 min at 4°C. The resulting pellet was subjected to miniprep using Qiagen mini prep kit. 10 μl of the isolated plasmids were transformed into ultra-competent *E.coli* DH5α as per the standard protocol.

2.25 Growth assay

Yeast cells were inoculated in the SCD media containing essential nutrients and grown to mid log phase at 30°C at 220 rpm overnight. 5 μl of serially diluted cultures (with optical densities O.D$_{600}$ ~ 0.5, 0.05, 0.005, 0.0005, and 0.00005) were spotted on appropriate nutrient plates and incubated at 30°C for the stipulated time.

2.26 Acid washing of glass beads

One volume of glass bead (200-300 μm) was mixed with two volumes of 5.8 M HCl and incubated in RT for 3 h with intermittent mixing. After incubation, the beads were washed with two volumes of distilled water for 8-10 times (till the pH come to ~ 6.8)

2.27 β-galactosidase assay

Three colonies from each transformant (carrying appropriate reporter plasmids) were grown overnight at 30°C with shaking at 220 rpm in SCD medium containing required amino acids along with histidine. The cells were harvested and washed twice with SCD medium with no histidine followed by sub culture in 35 ml of SCD media with histidine (un-induced) and without histidine (induced) with initial $O.D_{600} \sim 0.15$. The cells were grown at 30°C for 2 h, followed by induction with 25 mM 3AT for 6 h (the cells that are growing in SCD minus histidine media). Both induced and un-induced cultures were harvested after 8 h of incubation. The cells were re-suspended in LacZ buffer (60 mM Na_2HPO_4, 40 mM NaH_2PO_4, 10 mM KCl, and 1 mM $MgSO_4$, pH 7.0) and lysed using acid washed glass beads (200-300 micron from Sigma) in FastPrep®-24 (MP biomedicals) for 20 sec at 4 m/s followed by 1 min incubation on ice, and repeated thrice. Cell extracts were spun down at 13000 xg for 20 min at 4°C to remove glass beads and cell debris. Clarified extract (~30 μg) was mixed with LacZ buffer (to make up to 20 μl), followed by addition of 180 μl of ONPG (4 mg/ml in lacZ buffer). After 30 min, absorbance was measured using 420 nm wavelength filter (Bio-Rad iMark plate reader). Protein estimation was performed using Bradford assay and β-galactosidase activity per min per mg of total cell extract was calculated using following formula.

$$\text{Specific activity} = \frac{O.D._{420} \times \text{Assay volume (ml)}}{\text{molar extinction coefficient of ONPG} \times \text{Time (min)} / \text{ protein used (mg)}}$$

2.28 Quantification of *HIS4* mRNA

Desired yeast transformants were harvested as per the protocol mentioned in the β-galactosidase assay (in section 2.27). The cells were lysed using acid washed glass beads and the total RNA was isolated by using TRIzol© reagent. Approximately 10 μg of total RNA was subjected to DNaseI treatment at 37°C for 30 min followed by heat inactivation at 75°C for 10 min. Re-purification of RNA was performed using RNA isolation kit (Qiagen©) and the purity was analyzed by 260/280 ratio measured by (Nano drop one C, Thermo Scientific©). Total RNA (2 μg) was reverse transcribed using oligonucleotide oPA1024 (for Actin) and oPA1025 (for *HIS4*) using SuperScript© reverse transcriptase III at 50°C for 1 hour followed by heat inactivation at 70°C for 15 min. The resultant cDNA (40 ng) was used to perform real-time PCR in total 20 μl reaction mixture using Actin (*ACT1*) (assay id; Sc04120488_s1) and *HIS4* (assay id; Sc04104318_s1) TaqMan© probe. The reaction was carried on the Applied Biosystems 7500 machine©. Each reaction was carried using three biological replicates and two technical replicates.

2.29 Immunodetection of translation initiation factors

Yeast cells were harvested lysed using acid washed glass beads (as mentioned in section 2.27) and the cell extract was clarified at 13000xg for 20 min at 4°C and quantitated by Bradford assay using a standard protocol. 15 and 30 μg of total cell extract were electrophoresed in 10% SDS-PAGE gel and electro blotted onto Polyvinylidene difluoride (PVDF) membrane followed by probing using anti-HA tag antibody (to detect HIS4p) and anti-eIF1 (to detect eIF1). Coomassie Brilliant Blue stained blot was used to normalize the quantification.

Chapter 3

Defect in the GTPase activating protein function of eIF5 causes repression of *GCN4* translation

3.1 INTRODUCTION

Eukaryotic translation initiation factor 5 (eIF5) acts as a GTPase activating protein (GAP) for eIF2γ during the selection of translation start site in the scanning 48S complex (Das *et al.* 2001). This GAP function was proposed to be carried out by eIF5^{R15} residue in the N-terminal domain (NTD) conserved across other eukaryotes (figure 3.1). The substitution mutation eIF5^{R15A} completely abolished its GAP function and found to be lethal (Das *et al.* 2001). The eIF5^{G31R} mutant was isolated as dominant suppression of initiation codon mutants (Sui$^-$) capable of using UUG as a start codon due to its premature GTPase activity (Huang *et al.* 1997). Later studies showed that it is not the premature GTPase activity but the inappropriate P_i release that causes the non-AUG codon selection (Saini *et al.* 2014). The importance of NTD of eIF5 in start codon selection was further highlighted by isolating more mutants including G31S, I32N, and G58S which also conferred Sui$^-$ phenotype (Singh *et al.* 2005). The C-terminal domain (CTD) of eIF5 plays a critical role in 48S assembly/post-assembly process and mutations in this region affected the scanning of *GCN4* mRNA causing Gcd$^-$ or Gcn$^-$ phenotype (Singh *et al.* 2005). Despite its robust role in start codon selection, no Gcd$^-$ or Gcn$^-$ phenotypes were reported in the NTD of eIF5. In this study, we found that the dominant negative hyper GTPase active eIF5^{G31R} mutant shows Gcn$^-$ phenotype due to a novel mechanism that is linked to UUG initiation codon recognition from the 5′ regulatory region of the *GCN4* transcript.

```
                              Arg finger              G31R
                                                       ↓
human     LSVN-VNRSVMD-QFYRYKMPRLIAKVEGKGNGIKTVIVNMVDVAKALNRPPTYPTK--- 55
Rattus    MSVN-VNRSVSD-QFYRYKMPRLIAKVEGKGNGIKTVIVNMVDVAKALNRPPTYPTKYFG 58
Yeast     MSIN-ICRDNHD-PFYRYKMPPIQAKVEGRGNGIKTAVLNVADISHALNRPA-------- 50
Zeamays   MALQNIGASNRDDAFYRYKMPRMITKIEGRGNGIKTNVVNMVDIAKALARPASYTTKYFG 60
Pv        MALQNIGAGNSDDAFYRYKMPRMVTKIEGRGNGIKTNVVNMVDIAKRLARPASYTTKYFG 60
          ::::: :  .  * ******* : :*:**:****** ::*:.*::: * **.
```

Figure 3.1: eIF5 has conserved arginine finger.

Multiple sequence alignment of eIF5-NTD from various organisms [human (*Homo sapiens*), Rattus (*Rattus norvegicus*), Yeast (*Saccharomyces cerevisiae*), Zea mays (*Zea mays*), and Pv (*Phaseolus vulgaris*)] has been aligned using Clustal-W program. The box indicates the putative arginine finger involved in GTPase activation of eIF2γ. The black arrow indicates the conserved Gly^{31} residue responsible for the Sui$^-$ phenotype.

3.2 RESULTS

3.2.1 Construction of reporter plasmids and yeast strain

The *HIS4* gene encodes a multifunctional enzyme that is involved in catalyzing four biochemical steps of histidine biosynthesis (Alifano *et al.* 1996). Lack or impairment of the synthesis of HIS4 protein causes the strain to become histidine auxotroph. The reporter strain involves deletion of an endogenous *HIS4* gene with the support of the plasmid borne either wild type *HIS4* gene (henceforth *HIS4^{AUG}* allele) or *HIS4* allele having a mutation in AUG start codon (AUU), and so the third UUG codon would be utilized as translation start codon (henceforth *HIS4^{UUG}* allele). A Sui‾ mutant would utilize *HIS4^{UUG}* allele and show His⁺ phenotype when plated on medium lacking histidine. To this end, we deleted the *HIS4* gene using homologous recombination approach as follows.

Plasmid construct pFA6a-KanMx6 (pA559) carrying 1.6 kb *KanMx6* gene disruption cassette, was used as a PCR template to amplify the *KanMx6* cassette using oligonucleotides flanking 40 nucleotides of 5′ and 3′ end of *HIS4* ORF (Wach *et al.* 1997). The PCR amplified product was gel purified and (approximately 3 μg) transformed into the yeast (YP823) using standard protocol (Gietz and Woods 2006). The transformants were screened based on their resistance on the modified SCD+G418 plate. The *HIS4* gene deletion was further confirmed using the oligonucleotides as shown in figure 3.2.
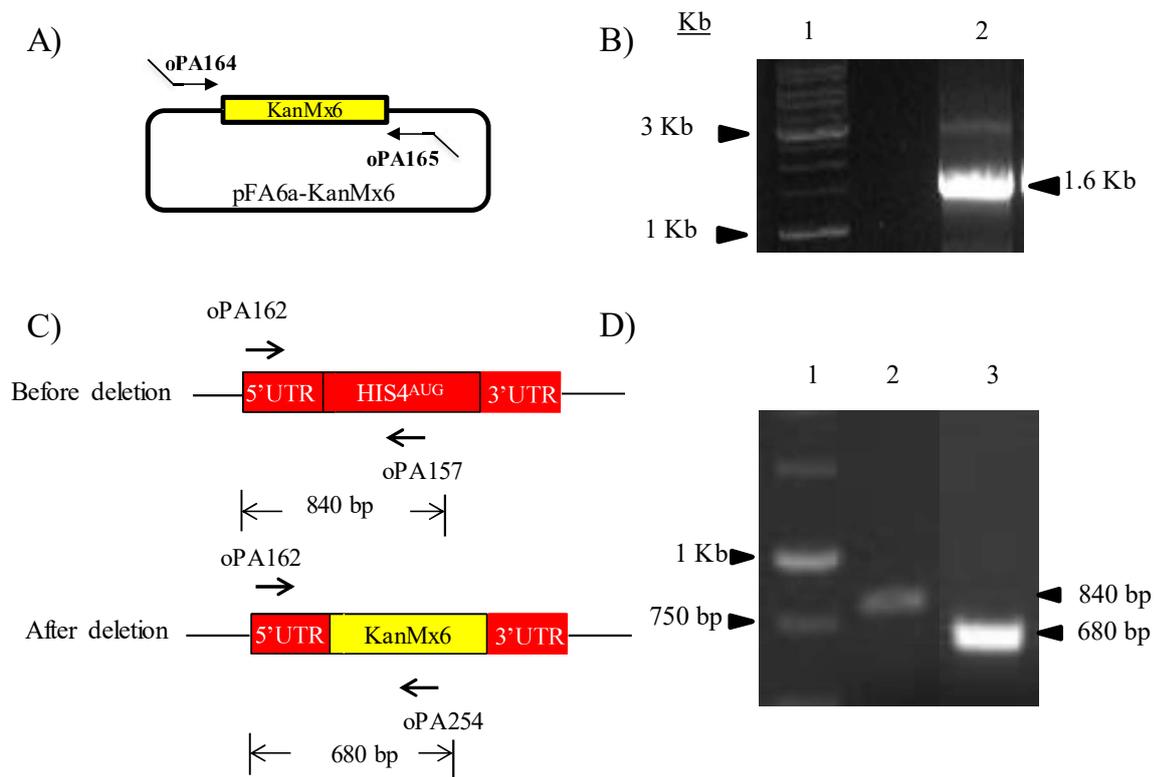
Figure 3.2: Preparation of reporter strain to study start codon selection:

A) Schematic of pUG6 plasmid carrying *KanMx6* based disruption cassette and the binding site of oligos whose 5′ overhangs carry 40 nucleotides of *HIS4* gene.

B) PCR amplification showing the *HIS4* gene disruption cassette (*LoxP-KanMx6-LoxP*). Lane 1- 1kb DNA ladder, lane 2- PCR amplicon of *LoxP-KanMx6-LoxP*.

C) Schematic showing the PCR based strategy to screen the successful disruption of *HIS4* gene by *LoxP-KanMx6-LoxP*.

D) Yeast colony PCR showing the successful deletion of *HIS4* gene. Lane 1- 1kb DNA ladder, lane 2- PCR amplification of *HIS4* gene specific amplicon before *HIS4* gene deletion from the yeast YP823 using oligos oPA156 and oPA157. lane 3- PCR amplification of *KanMx6* gene specific amplicon after *HIS4* gene deletion from the yeast YP824.

3.2.2 eIF5^{G31R} recognizes UUG as a start codon

eIF5^{G31R} is one of the strongest dominant Sui⁻ mutant known so far. Though all Sui⁻ mutants are capable of using UUG as a start codon, they have the ability to use other non-AUG codons including CUG, GUG, and UUA codons. However, eIF5^{G31R} mutant preferentially utilizes UUG initiation codon as compared to the other alternative codons (Huang *et al.* 1997). Before genetically characterizing the effect of eIF5^{G31R}, we checked the effect of this mutant on yeast growth and Sui⁻ phenotype and compared the data with previous literature study. To this end, we constructed clones carrying eIF5^{G31R} mutant with either *HIS4^{AUG}* or *HIS4^{UUG}* allele and transformed them into a yeast strain YP824 (*his4Δ*) as a sole source of the *HIS4* allele. The resultant transformants were subjected to serial dilution and spotted on both media containing and not containing histidine (figure 3.3).

After 2 days of incubation, yeast cells carrying *eIF5^{G31R}* showed slow growth (Slg⁻) compared to empty vector. In the absence of eIF5^{G31R} mutant, the yeast cells showed growth on medium lacking histidine with *HIS4^{AUG}* allele whereas no growth was observed with the *HIS4^{UUG}* allele (compare figure 3.3 row 3 and row 5 on SCD-H), confirming the authenticity of deletion for *HIS4* gene as well as the inability of wild type (WT) to recognize UUG as a start codon. As expected, the yeast carrying eIF5^{G31R} mutant along with *HIS4^{UUG}* allele could grow on the medium lacking histidine (compare figure 3.3 row 5 and row 6 on SCD-H).
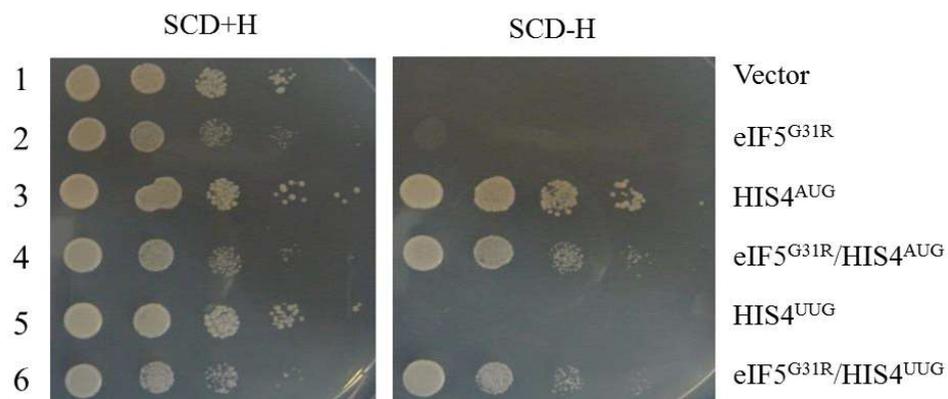
Figure 3.3. eIF5^{G31R} causes Slg⁻ and Sui⁻ phenotype. Yeast strain transformed with either vector (pA823), or *eIF5^{G31R}* (pA860), or *HIS4^{AUG}* (pA858), or *eIF5^{G31R}/HIS4^{AUG}* (pA861), or *HIS4^{UUG}* (pA859), or *eIF5^{G31R}/HIS4^{UUG}* (pA862). The resulting transformants were serially diluted and spotted on minimal medium containing (SCD+H) and not containing (SCD-H) histidine followed by incubation at 30 °C for 2 days.

3.2.3 eIF5^{G31R} causes Gcn$^-$ phenotype

Based on the literature analysis, it has been observed that many of the Sui$^-$ mutants also showed defects in the regulation of *GCN4* expression (Hinnebusch 2011). However, previous studies showed that the variant in NTD of eIF5 (eIF5^{G31S}) is a recessive Sui$^-$ and Gcn$^+$ (Singh *et al.* 2005). It is possible that G31S substitution may have a weak effect on eIF5 function that could not have affected *GCN4* expression. We hypothesized that the strong Sui$^-$ phenotype of eIF5^{G31R} mutant might affect the *GCN4* expression. In order to test this hypothesis, we first compared the Sui$^-$ phenotype of eIF5^{G31R} and eIF5^{G31S} mutant by transforming P_{HIS4}-*HIS4^{AUG}-LacZ* (p3989) or P_{HIS4}-*HIS4^{UUG}-LacZ* (p3990) reporter constructs along with empty vector (pA823), or *eIF5^{G31R}* (pA860), or *eIF5^{G31S}* (pA1034) to yeast strain YP823. The resultant β-galactosidase activity was plotted as UUG/AUG ratio to evaluate the Sui$^-$ phenotype.

As expected, eIF5^{G31R} mutant showed high UUG/AUG ratio compared to WT (figure 3.4A). However, no significant difference was observed with eIF5^{G31S} mutant suggesting that G31S substitution has a weak effect on eIF5 function and probably is a weak Sui$^-$ in dominant condition. To test whether G31R substitution causes Gcn$^-$ phenotype, we used *GCN2$^+$* yeast strain (YP823) and transformed with empty vector (pA823) or vector carrying derivatives of *TIF5* gene; eIF5^{WT} (pA870), eIF5^{G31S} (pA1034), or eIF5^{G31R} (pA860) and tested for 3AT sensitivity. While the wild type (WT) cells can overcome the histidine starvation by de-repressing *GCN4* expression and grow on 3AT media, the Gcn$^-$ mutants having a defect in the scanning of *GCN4* mRNA cannot grow on 3AT media and confer 3AT sensitivity. Consistently, the eIF5^{G31R} mutant could not grow on 3AT media in comparison to eIF5^{G31S} mutant or vector control (figure. 3.4B), suggesting that eIF5^{G31R} mutant confers Gcn$^-$ phenotype, while eIF5^{G31S} mutant remains Gcn$^+$ possibly due to the weak effect of G31S substitution. Next, we tested the levels of *GCN4* expression of these mutants

74

by using a *GCN4-LacZ* reporter (p180) construct as the Gcn⁻ mutants downregulate the *GCN4* expression. Consistent with its 3AT sensitivity, the eIF5^{G31R} mutant causes significant down regulation of *GCN4* expression, while the eIF5^{G31S} mutant showed no significant difference in *GCN4* level in comparison to the vector control (figure 3.4C). This indeed confirms that eIF5^{G31R} mutant is a Gcn⁻ mutant.

3.2.4 eIF5^{G31R} causes reinitiation defect

The Gcn⁻ phenotype can be caused by three possible mechanisms. They are 1) leaky scanning, 2) slow scanning, and 3) reinitiation defect (Hinnebusch 2011). In order to decipher the molecular mechanism behind Gcn⁻ phenotype shown by the eIF5^{G31R} mutant, we used modified derivatives of *GCN4-LacZ* (p180) reporter constructs as depicted in figure 3.5. The construct pM226 has point and frameshift mutations that elongate uORF1 and overlapped 130 nucleotides out of frame with *GCN4* main ORF(Grant *et al.* 1994).

Ribosomes that initiate translation at elongated uORF1 were unable to translate *GCN4* main ORF. The increased expression of *GCN4* ORF under these conditions could be due to leaky scanning of the elongated uORF1. The construct, pM199 has point mutations that remove uORF2-4 while keeping uORF1 intact and is used to measure re-initiation defects post uORF1 translation. Yeast strain (YP823) was transformed with either single copy empty vector (pA823) or eIF5^{G31R} mutant (pA860) along with pM199 or pM226 constructs and the resultant β-galactosidase activity is summarized in a tabular form (figure 3.5). In the case of eIF5^{G31R} mutant, the *GCN4* expression was not significantly altered for pM226 construct suggesting that the Gcn⁻ phenotype was not caused due to leaky scanning of elongated uORF1. However, the *GCN4* expression was significantly reduced in pM199 construct, suggesting that the eIF5^{G31R}
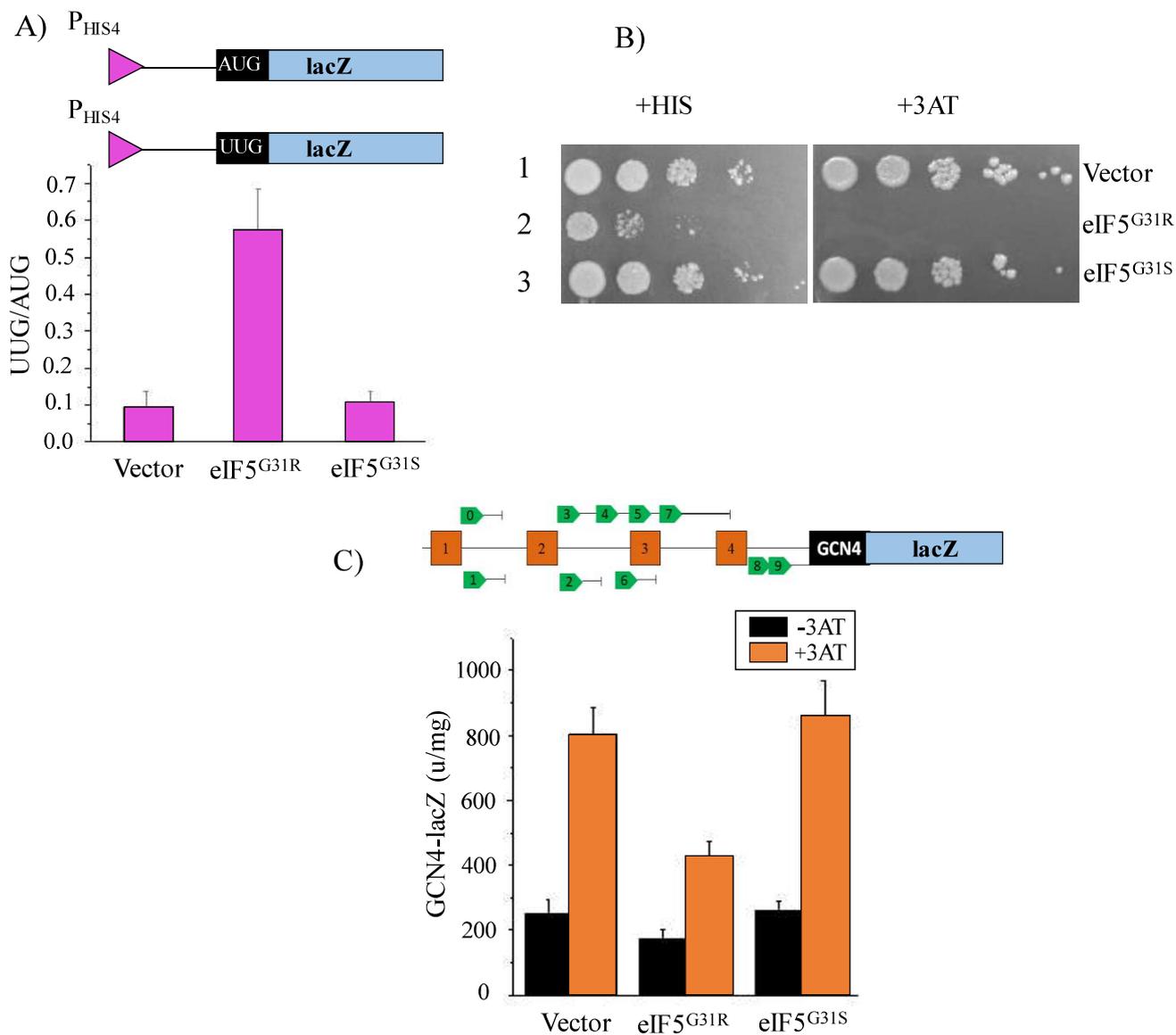
Figure 3.4: eIF5^G31R shows Sui¯ and Gcn¯ phenotype.

A) Analysis of *HIS4-LacZ* expression. Yeast strain (YP823) carrying either *HIS4^{AUG}-lacZ* (p3989) or *HIS4^{UUG}-lacZ* (p3990) reporter is transformed with either vector (pA823) or *eIF5^{G31R}* (pA860) or *eIF5^{G31S}* (pA1034) plasmids and grown up to an O.D$_{600}$ ~ 0.8 in SCD media followed by β-galactosidase assay as mentioned earlier. The resultant values were plotted as UUG/AUG ratio to assess the Sui¯ phenotype conferred by eIF5 variants.

B) Colonies from the panel (A) were serially diluted and spotted on minimal media (SCD) and minimal media devoid of histidine and supplemented with 25 mM 3-Amino-1,2,4-triazole (SCD+3AT) and incubated at 30°C for 2 (SCD) or 3 (SCD+3AT) days.

(C) Analysis of *GCN4-LacZ* expression. Yeast strain (YP823) carrying *GCN4-lacZ* reporter (p180) was transformed with either vector (pA823) or *eIF5^{G31R}* (pA860) or *eIF5^{G31S}* (pA1034) plasmids and grown up to an O.D.$_{600}$ ~ 0.8 in SCD (white bars; uninduced) or in SCD supplemented with 25 mM 3AT (grey shaded bars; induced). The whole-cell extracts were prepared, and β-galactosidase activity was calculated as described in section 2.25.

		Vector		eIF5^{G31R}	
		- 3AT	+ 3AT	- 3AT	+ 3AT
pM226		97±10	211 ±50	110±9 (100%)	215 ±26 (100%)
pM199		1943 ±102	2604 ±161	1289 ±113 (66%)	2025 ±109 (77%)
pM231		529 ±47	575 ±16	441±57 (83%)	533 ±52 (92%)
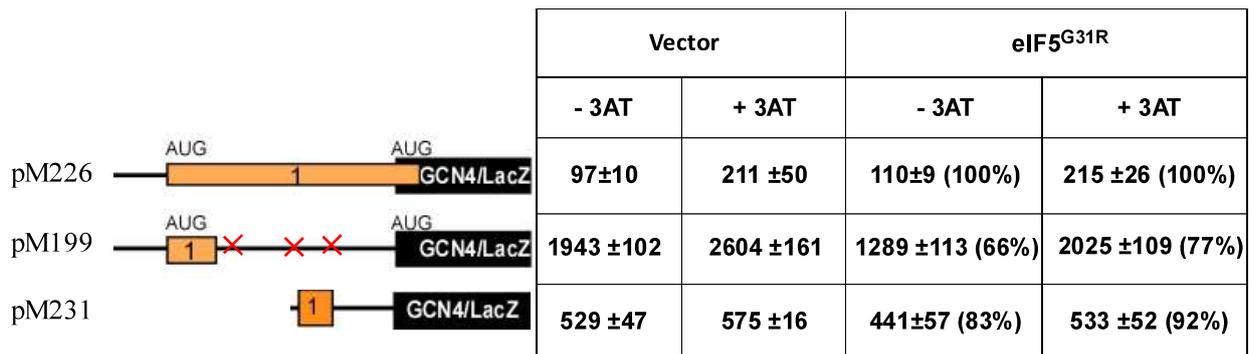
Figure 3.5: eIF5^{G31R} causes reinitiation defect: Derivative of *GCN4-lacZ* reporter (p180) having uORF1 elongated and overlapped 130 nucleotides out of frame with *GCN4* main ORF (pM226) or consist of only uORF1 with the distance between uORF1 and main *GCN4* as 140 nt (pM199) or 50 nt (pM231) (as depicted in the schematic) was co-transformed with either empty vector (pA823) or *eIF5^{G31R}* (pA860). The resulting transformants were subjected to β-galactosidase assay. The *GCN4-LacZ* values were represented in the tabular form along with the standard deviations. Percentage changes with respected to the WT (100%) were shown in the parenthesis.

mutant has translation re-initiation defect, possibly due to the premature release of 40S ribosome before translating *GCN4* main ORF. This result also rules out the slow scanning defect as the slow scanning mutant should have a high *GCN4* expression similar to the WT in pM199 construct. Previously isolated Gcn⁻ mutants that are possessing reinitiation defect tend to show the exacerbation of reinitiation defect when the 5′ UTR length is reduced, as the ribosome reinitiation frequency decreases when the distance between two ORFs are decreased. To perform this analysis, we used a construct pM231, whose inter ORF length is reduced from 140 nt 50 nt. However, the reinitiation defect associated with eIF5^{G31R} was partially rescued when the distance between uORF1 and main *GCN4* ORF was reduced (figure 3.5 compare construct 2 and 3). This result suggested that the nucleotide sequences present between uORF1 and main *GCN4* ORF might possibly affect the reinitiation event in the eIF5^{G31R} mutant.

3.2.5 Reinitiation defect caused by upUUGs of *GCN4* mRNA

To understand the above contrasting behavior of eIF5^{G31R} from rest of the reinitiation defective Gcn⁻ mutants, we carefully examined the 5′ UTR of *GCN4* transcript and found the presence of 10 UUG codons (henceforth upUUG) between uORF1 and main *GCN4* ORF, which we call upUUG-ORFs. In order to test the role of these upUUG-ORFs in the disruption of *GCN4* expression, we used the following modified derivatives of *GCN4-LacZ* (p180) reporter constructs. The construct p227 has point mutations in the AUG codon which removes short uORF1-4 (uORF-less) and is used to test Cap-dependent *GCN4* expression devoid of any translation regulations contributed by the uORF1-4. The construct pA901 is modified by point mutations that removes uORF1-4 and upUUG-ORF1-10 (uORF-less & upUUG-less) and used to measure the contributions of UUG codons in *GCN4* expression. Yeast strain (YP823) was transformed with either single copy empty vector (pA823) or *eIF5^{G31R}* (pA860) mutant along

A)

Vector		eIF5^{G31R}	
- 3AT	+ 3AT	- 3AT	+ 3AT
252 ±11	922 ±50	172 ±46(68 %)	476 ±46 (51 %)

B)

Vector		eIF5^{G31R}	
- 3AT	+ 3AT	- 3AT	+ 3AT
3945 ±241	3495 ±119	2682 ±178(68 %)	2617 ±82 (74 %)

C)

Vector		eIF5^{G31R}	
- 3AT	+ 3AT	- 3AT	+ 3AT
3004 ±228	3120 ±184	2835 ±384(94%)	2926 ±290(94%)
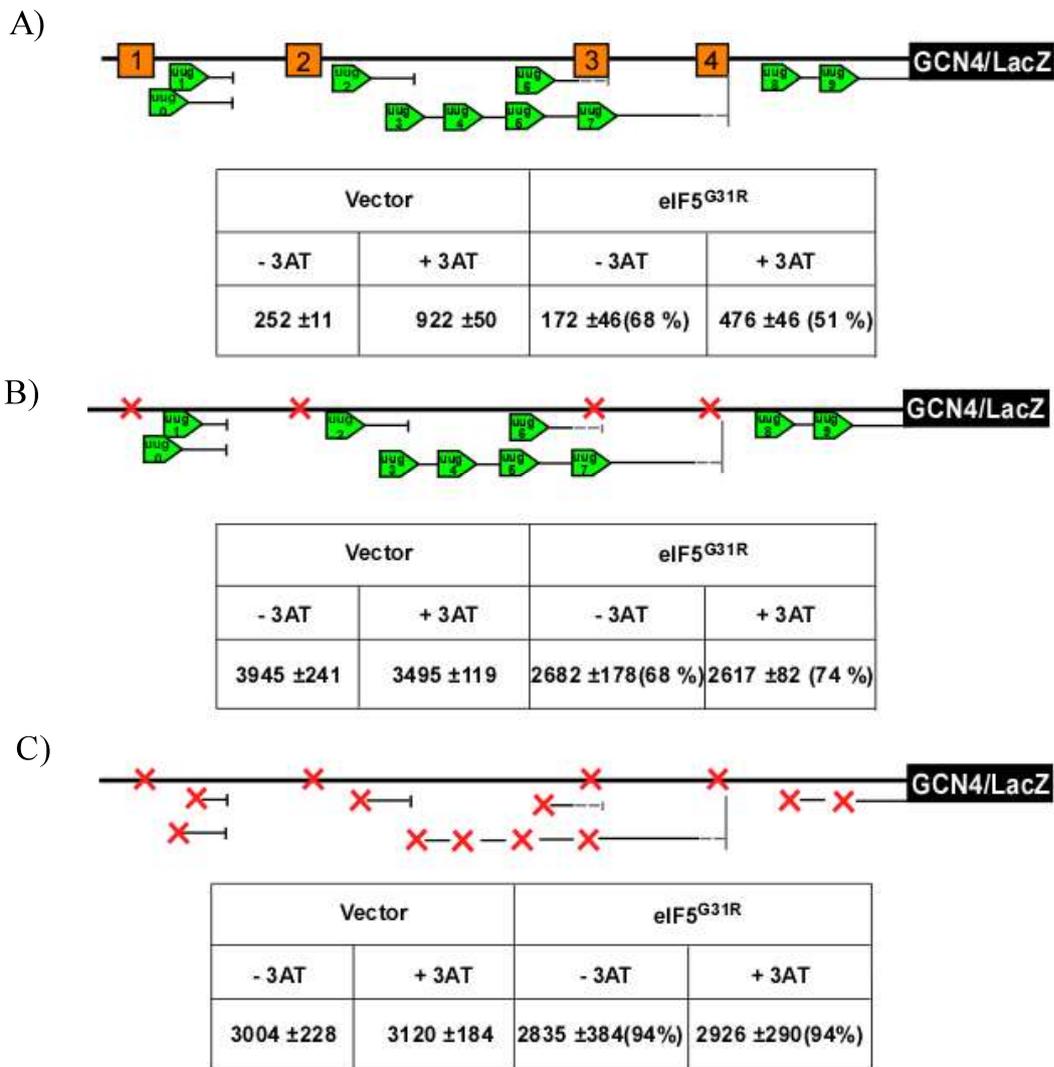
Figure 3.6: eIF5^{G31R} recognizes upUUG of *GCN4* mRNA: (A)(B)(C) Derivatives of yeast strain YP823 carrying either vector (pA823) or *eIF5^{G31R}* (pA860) plasmid were transformed with *GCN4-LacZ* (p180), or uORF less *GCN4-LacZ* (p227) or uORF less & upUUG less *GCN4-LacZ* (pA901) and subjected to the *GCN4-LacZ* analysis as mentioned earlier. The *GCN4-LacZ* values were represented in the tabular form along with the standard deviations. Percentage changes with respected to the WT (100%) were shown in the parenthesis. The square boxes (1-4), mentioned in the schematic represents the AUG based upstream open reading frames (uORF), horizontal pentagon boxes with line (UUG 1-10) show upstream UUG codons containing reading frames terminating at various length. The cross represents the mutations in either AUG codons to form ORFless constructs or mutations in UUG codons to form ORF less & UUG less construct.

with either p180, pM227 or pA901 *GCN4-LacZ* constructs and the β-galactosidase activities were normalized to 100% for WT and compared with the eIF5^{G31R} mutant and represented in the table below each schematic (figure 3.6).

Under repressed (-3AT) condition, the removal of uORF1-4 did not significantly improve the *GCN4* expression in comparison to the vector control (68%; compare figure 3.6A and B) indicating premature dissociation of 40S ribosome before reaching *GCN4* main ORF. However, after additional elimination of upUUG-ORF1-10 along with uORF1-4 as in the case of pA901 construct, the *GCN4* expression for eIF5^{G31R} was significantly increased as compared to vector control (94%; compare figure 3.6B and C). These data suggest that eIF5^{G31R} mutant causes premature dissociation of 40S ribosome possibly due to the utilization of upUUG-ORF from the 5′ UTR region of the *GCN4* transcript leading to the repression of *GCN4* expression.

3.3 DISCUSSION

Isolation of Gcn⁻ or Gcd⁻ mutations at the eIF5-CTD predominantly implicated its role in the integrity and scanning function of the 48S complex. The Sui⁻ mutants at the eIF5-NTD did not show any of these defects, possibly due to the weak effect of these mutations on eIF5 function (Singh *et al.* 2005). It is also likely that the eIF5-NTD does not directly participate in maintaining the integrity and scanning function of 48S complex and the G31R substitution may have only exacerbated the regulatory function of GAP region in comparison to the weaker G31S substitution. Thus, the G31R mutation shows strong dominant Sui⁻ phenotype as compared with the G31S mutation. It is likely that the Gcn⁻ phenotype observed for the eIF5^{G31R} in this study is not due to the leaky scanning defects of the uORF1 rather premature release of 40S ribosome post uORF1 translation. It has been reported earlier that non-AUG codons upstream of uORF1 were
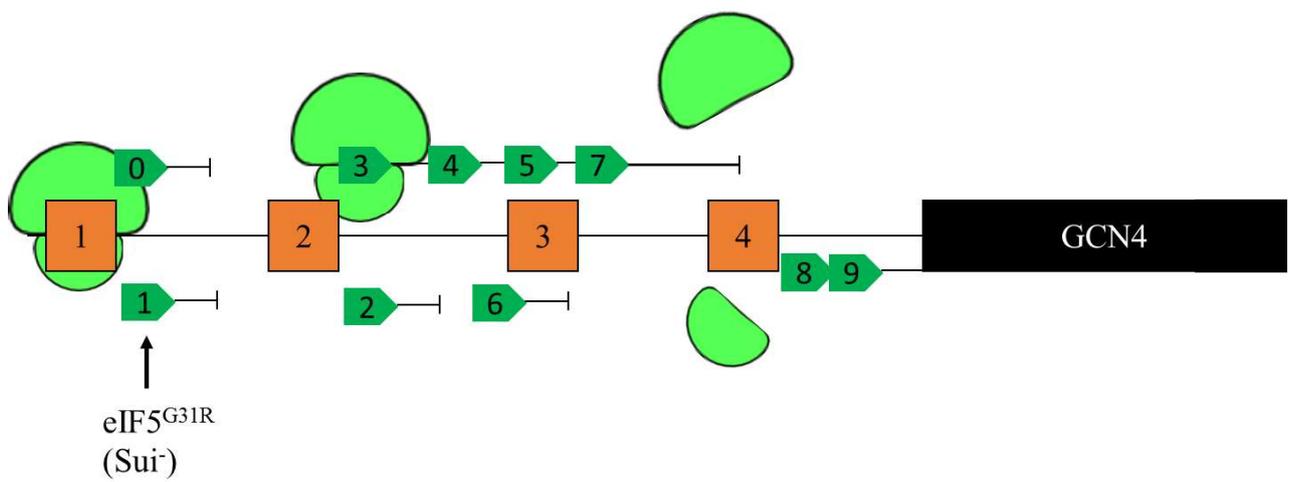
Figure 3.7 Model depicting the mechanism of Gcn⁻ phenotype exhibited by eIF5^{G31R} mutant

Schematic representation of *GCN4* construct. The open square boxes (1-4) shows upstream open reading frames (uORFs), horizontal pentagon boxes with line (UUG 1-10) show upstream UUG codons based reading frames terminating at various length. The eIF5^{G31R} mutant utilizes upUUG codons and terminates translation before reaching *GCN4* main ORF.

translated but played a minor role in the regulation of *GCN4* expression (Zhang and Hinnebusch 2011). However, the ten UUG codons in the 5′ UTR region of the *GCN4* transcript between uORF1 and the main *GCN4* ORF constituting upUUG-ORFs might have an influence on *GCN4* regulation in the eIF5^{G31R} mutant. Consistently, the removal of uORF1-4 and upUUG-ORFs 1-10 improved the *GCN4* expression level significantly (figure 3.6), suggesting the use of upUUG-ORFs by the eIF5^{G31R} mutant could possibly cause 40S ribosome dissociation upon their translation (figure 3.7). This would represent a novel mechanism of the Gcn⁻ phenotype caused by the utilization of UUG codons from the 5′ UTR region of the *GCN4* transcript in comparison to the other reported mechanisms of Gcn⁻ phenotype that involves leaky scanning, slow scanning and premature dissociation of the 40S ribosome (Cuchalová *et al.* 2010). It is very intriguing to compare the Gcn⁻ phenotypes of *prt1-1* mutant, which has a hyper-accurate AUG codon recognition ability in contrast to the poor AUG codon recognition and better UUG codon recognition ability of the eIF5^{G31R} mutant (Nielsen *et al.* 2004; Martin-Marcos *et al.* 2014; Saini *et al.* 2014). Thus, our data suggest that strong Sui⁻ phenotype of the eIF5^{G31R} mutation is responsible for the Gcn⁻ phenotype.

It is equally important to contemplate about the varying degrees of Sui⁻ phenotype shown by different mutants. Most of the Gcd⁻ mutants such as eIF2γ^{N135D} or eIF2β^{S264Y} that also shows Sui⁻ phenotype are naturally supported by the de-repression of *GCN4* expression, as it increases the *HIS4^{UUG}* transcript level several-fold thus synthesizing HIS4p and helps to stimulate histidine biosynthesis (Castilho-Valavicius *et al.* 1990; Alone *et al.* 2008). However, the Gcn⁻ mutants that also shows Sui⁻ phenotype, need to have an extraordinarily strong ability to recognize the UUG initiation codon from the basal level *HIS4^{UUG}* transcript under repressed *GCN4* expression; this might be the reason for Gcn⁻ mutant eIF1A$^{98-101}$ not being able to suppress the His⁻ phenotype and thus believed to be a weak Sui⁻ (Fekete *et al.* 2005). In this regard, the eIF5^{G31R} mutation

represents a special category of a Sui⁻ mutant that has an extraordinarily strong ability to recognize the UUG initiation codon that downregulates *GCN4* expression, which could be a possible molecular mechanism underpinning the Gcn⁻ phenotype.

Chapter 4

Fidelity of *HIS4* start codon selection influences 3AT sensitivity in GTPase defective eIF5 mutant

4. 1 INTRODUCTION

In the previous section, we showed the eIF5^{G31R} mutant repressed *GCN4* expression (Gcn$^-$ phenotype) and showed 3AT sensitivity by recognizing upUUG initiation codon in the 5′ UTR region of the *GCN4* transcript (Antony A and Alone 2017). We have observed that the *HIS4^{UUG}* allele could rescue the 3AT sensitivity of the eIF5^{G31R} mutant. The 3AT is a competitive inhibitor of an enzyme imidazole glycerol-phosphate dehydratase (henceforth HIS3p) encoded by the *HIS3* gene that blocks the histidine biosynthesis pathway and is used extensively to induce histidine starvation to study regulation of translation initiation controlled by the four upstream short open reading frames (uORFs 1-4) present at the 5′ regulatory region of *GCN4* mRNA (Hilton *et al.* 1965; Hinnebusch 1988, 2005). The *HIS4* gene encodes a multifunctional enzyme histidinol dehydrogenase/phosphoribosyl-AMP cyclohydrolase/phosphoribosyl-ATP pyrophosphatase (henceforth HIS4p) that catalyzes four biochemical steps both upstream and downstream of HIS3p in the histidine biosynthesis pathway, however, its role in 3AT mediated inhibition is unknown (Alifano *et al.* 1996). In this section, we have investigated the molecular mechanism underpinning the rescue of 3AT sensitivity of the eIF5^{G31R} mutant.

4.2 RESULTS

4.2.1 The *HIS4^{UUG}* allele rescues 3AT sensitivity of eIF5^{G31R} mutant

The dominant negative GTPase defective eIF5^{G31R} mutation has remarkable ability to initiate at the UUG codon and shows strong Sui$^-$ phenotype (Huang *et al.* 1997). Consistently, the YP824 (*his4Δ*) yeast strain carrying eIF5^{G31R} mutation supplemented with plasmid borne wild type *HIS4* (henceforth *HIS4^{AUG}* allele) or *HIS4-303* (henceforth *HIS4^{UUG}* allele) construct could grow on medium lacking histidine (figure 4.1 SCD-H plate compare rows 3 and 4). We previously found

that the eIF5^{G31R} (supplemented with $HIS4^{AUG}$) allele causes Gcn^{-} phenotype by utilizing upUUG codons from the 5′ UTR region of the $GCN4$ transcript and showed sensitivity to 3AT induced histidine starvation (figure 4.1 SCD-H+3AT plate compare rows 1 and 3) (Antony A and Alone 2017). Interestingly, this 3AT sensitivity was rescued when eIF5^{G31R} mutant was supplemented with $HIS4^{UUG}$ allele (figure 4.1 SCD-H+3AT plate compare rows 3 and 4). It is intriguing to note here that the $HIS4^{UUG}$ allele is rescuing the 3AT sensitivity of eIF5^{G31R} mutant that is ostensibly not a direct target of 3AT inhibition. It might be possible that the eIF5^{G31R} mutant has better ability to initiate at UUG codon than AUG codon of $HIS4$ allele under 3AT starvation condition and the higher $HIS4^{UUG}$ expression might be playing a critical role in alleviating 3AT sensitivity. In order to understand the molecular mechanism underpinning the 3AT resistance, we tested the levels of $HIS4^{AUG}$ and $HIS4^{UUG}$ alleles expression. To perform this quantitation, we fused 6HA-tag at the C-terminal of both $HIS4^{AUG}$ and $HIS4^{UUG}$ alleles. The resultants $HIS4$ alleles were transformed into YP824 strain either carrying eIF5^{G31R} mutant or empty vector. The Western blot analysis was performed on the whole cell extract prepared from these transformants treated with or without 3AT and probed using anti-HA antibody (figure. 4.2). As the $HIS4$ transcription is regulated by $GCN4$ de-repression under 3AT starvation condition, it is imperative to quantitate the levels of $HIS4$ transcript. The quantification of $HIS4$ mRNA level was performed by RT-qPCR using $HIS4$ specific TaqMan probe. For better comparison, the HIS4-protein (HIS4p) is normalized to mRNA level to calculate the translation efficiency and summarized in a table below the figure.
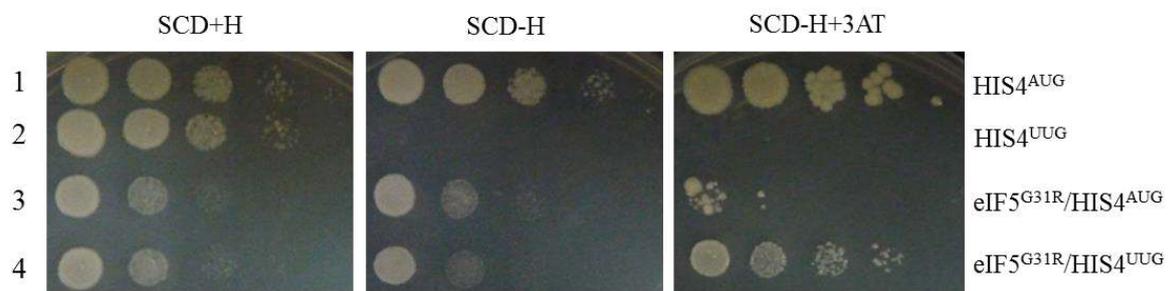
Figure 4.1: 3AT sensitivity of eIF5^{G31R} is rescued by *HIS4^{UUG}* allele: Derivative of yeast strain YP824 (*his4Δ*) carrying either *HIS4^{AUG}* (pA858), or *HIS4^{UUG}* (pA859), or *eIF5^{G31R}/HIS4^{AUG}* (pA861), or *eIF5^{G31R}/HIS4^{UUG}* (pA862) were spotted on minimal media containing (SCD+H) or not containing (SCD-H) histidine, or supplemented with 25 mM 3AT and incubated at 30°C for 36 h (SCD+H and SCD-H) and 66 h (SCD-H+3AT).

As expected, while WT cells able to recognize and translate $HIS4^{AUG}$ allele (100%) efficiently, $HIS4^{UUG}$ allele (15%) was not translated. Interestingly, eIF5^{G31R} caused a defect in the expression of $HIS4^{AUG}$ (70%), but efficiently translated $HIS4^{UUG}$ allele (62%). Notably, the UUG codon recognition efficiency of eIF5^{G31R} is further elevated under 3AT induced amino acid starvation condition up to 92%. This data primarily suggests the better utilization of UUG start codon especially under starvation.

In order to confirm the eIF5^{G31R} mutant has better ability to utilize UUG start codon from $HIS4^{UUG}$ transcript without the influence of $GCN4$ de-repression under 3AT starvation condition, we used P_{HIS4}:$HIS4^{AUG}$-$LacZ$ (p3989) and P_{HIS4}:$HIS4^{UUG}$-$LacZ$ (p3990) reporter constructs having native $HIS4$ promoter or P_{GAPDH}:$HIS4^{AUG}$-$LacZ$ (pA1056) and P_{GAPDH}:$HIS4^{UUG}$-$LacZ$ (pA1057) reporter, where the native promoter was replaced with $GAPDH$ promoter and the resultant β-galactosidase activity was measured in the presence (+) or absence (-) of 3AT for the eIF5^{G31R} mutant (figure 4.3A [P_{HIS4}] and 4.3B [P_{GAPDH}]. In the WT background, the expression from P_{HIS4}:$HIS4^{AUG}$-$LacZ$ reporter was significantly higher in 3AT treated cell than the untreated cells, consistent with the de-repression of $GCN4$ and its target genes (left panel). However, the expression from P_{GAPDH}:$HIS4^{AUG}$-$LacZ$ reporter showed no significant change in the presence or absence of 3AT treatment (right panel), suggesting that the expression from $GAPDH$ promoter was independent of $GCN4$ de-repression. Interestingly, there was approximately two-fold down-regulation of P_{GAPDH}:$HIS4^{AUG}$-$LacZ$ reporter expression in the presence of eIF5^{G31R} mutant, consistence with our earlier observation in Western blot. However, the eIF5^{G31R} mutant has

Western Blot

HIS4^{AUG}	HIS4^{UUG}	HIS4^{AUG} eIF5^{G31R}	HIS4^{UUG} eIF5^{G31R}	HIS4^{AUG}	HIS4^{UUG}	HIS4^{AUG} eIF5^{G31R}	HIS4^{UUG} eIF5^{G31R}	Allele
−	−	−	−	+	+	+	+	3AT
100	5 ±2	40±6	13 ±3	300±16	23 ±2	130 ±4	96 ±4	Protein amount (%)
100	33 ±1	54 ±12	21 ±7	320±15	171 ±18	195 ±14	109 ±6	mRNA amount (%)
100	15	74	62	94	13	66	88	Translation efficiency (%)
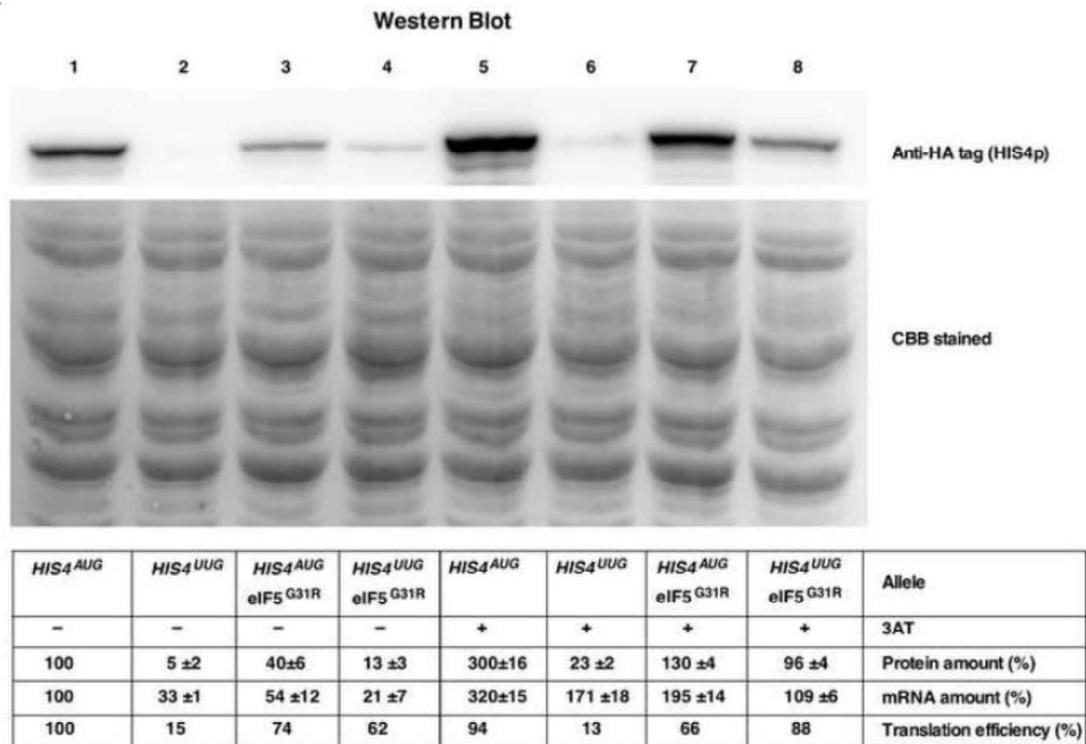
Figure 4.2: eIF5^{G31R} highly efficient in the translation of UUG mRNA. Quantification of *HIS4* alleles using Western blot and real time RT-qPCR. Yeast strain YP824 carrying single copy (s.c) *HIS4^{AUG}*-6xHAtag (pA974), *HIS4^{UUG}*-6xHAtag (pA978), *eIF5^{G31R}/ HIS4^{AUG}*-6xHAtag (pA975) and *eIF5^{G31R}/ HIS4^{UUG}*-6xHAtag (pA979) were cultured overnight in SCD medium. The culture was harvested and washed twice with SCD minus histidine medium followed by subculture in two sets of SCD minus histidine medium. One set was induced with 25 mM 3AT for 6 h (+3AT; induced) while the other set was allowed to grow for 6 h (-3AT; un-induced) in the presence of histidine before harvesting. The cells were lysed and whole cell extracts were prepared and quantified using Bradford method. Whole cell extracts (30 µg) were subjected to immunoblot analysis using anti-HA tag antibody (upper panel) and normalized to that of whole cell extract proteins stained by Coomassie Brilliant Blue (lower panel). Real time RT-qPCR was performed on cDNA prepared from *HIS4* alleles using TaqMan assay and normalized to Actin cDNA. The table summarizes the amount of mRNA or HIS4 protein transcribed or translated from *HIS4* alleles under -3AT and +3AT conditions after normalization with wild type. The translation efficiency (amount of protein produced per transcript) of *HIS4* mRNA is calculated using following formula. [Translation efficiency=Amount of protein/Amount of mRNA].

significantly higher level of P_{GAPDH}:$HIS4^{UUG}$-$LacZ$ reporter expression in 3AT treated cells than the untreated cells, confirming that utilization of UUG start codon was upregulated in the eIF5^{G31R} mutant under 3AT starvation condition. Our data suggest the eIF5^{G31R} mutant has better UUG start codon recognition ability from the $HIS4^{UUG}$ allele under the 3AT starvation condition, however, the amount of HIS4p expression was considerably below than the expression from the $HIS4^{AUG}$ allele under similar condition, suggesting additional factors might also be contributing to 3AT resistant other than $HIS4$ expression.

In this regard, it is important to check the levels of $GCN4$ expression in eIF5^{G31R} mutant, as lower HIS4p expression from $HIS4^{UUG}$ allele under 3AT starvation might have triggered additional $GCN4$ de-repression to overcome the histidine starvation. We tested the levels of $GCN4$ expression by transforming $GCN4$-$LacZ$ reporter (p180) into the yeast strain carrying eIF5^{G31R} mutant in presence of either $HIS4^{AUG}$ or $HIS4^{UUG}$ allele. In presence of $HIS4^{AUG}$ allele, the 3AT treatment caused 3-fold higher de-repression of $GCN4$ reporter, however, the $HIS4^{UUG}$ allele de-repressed the $GCN4$ reporter expression by 9-fold (figure 4.4; row 1 and 2). These results are consistent with the fact that in the absence of eIF5^{G31R}, the seldom translation initiation from $HIS4^{UUG}$ allele resulted in extremely lower protein expression (figure 4.2; protein, lane 2 and 6) causing exacerbation of histidine starvation leading to additional de-repression of $GCN4$. The eIF5^{G31R} mutant showed significant down-regulation of $GCN4$ reporter expression in the presence of $HIS4^{AUG}$ allele consistent with its 3AT sensitivity, however, in the presence of $HIS4^{UUG}$ allele, $GCN4$ reporter expression was moderately high consistent with its resistance to 3AT (figure 4.4; row 3 and 4 and also, figure 4.1; row 3 and 4). Together, these results suggest that in presence of eIF5^{G31R} mutant a below threshold level of expression from $HIS4^{UUG}$ allele is regulating $GCN4$ de-repression to alleviate 3AT induced starvation.
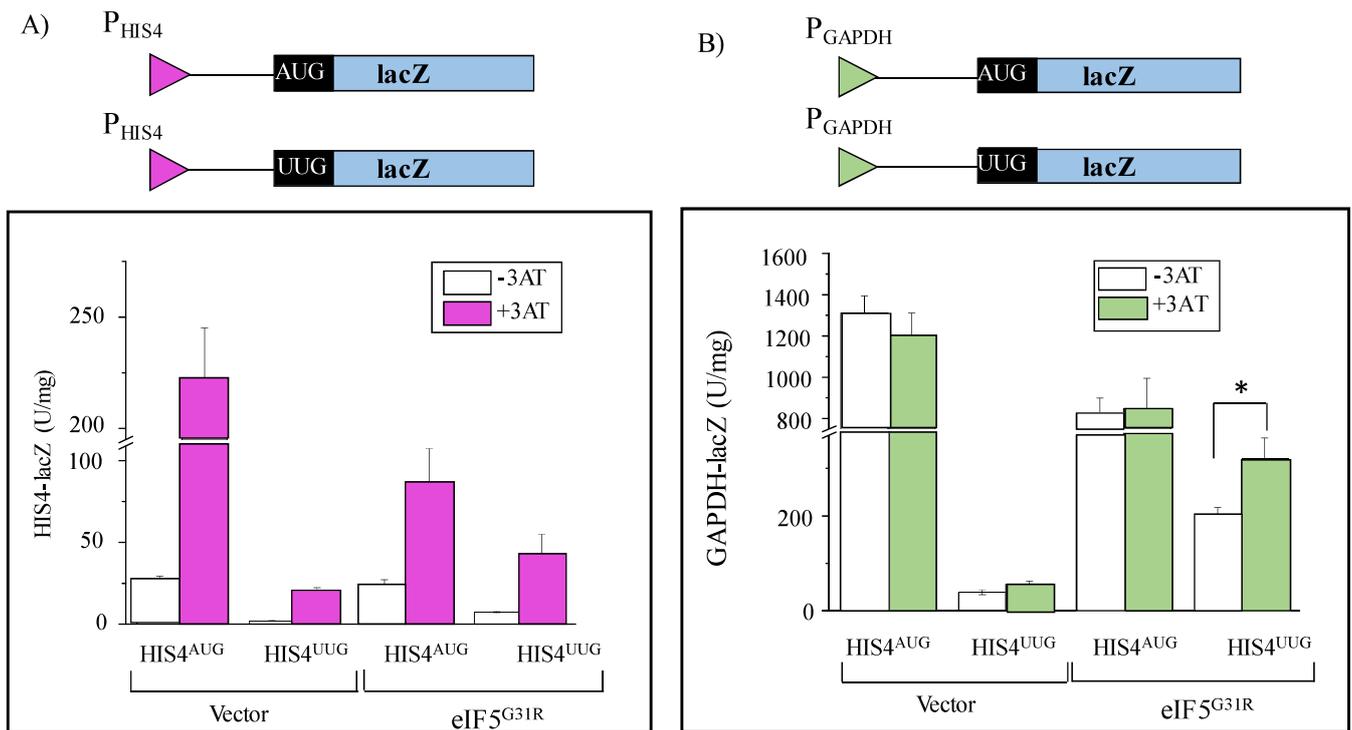
Figure 4.3: Starvation causes more UUG codon recognition in eIF5^{G31R} mutant

HIS4-LacZ reporter expression using native *HIS4* or *GAPDH* promoter.

A) Yeast strain YP823 carrying either P_{HIS4}:*HIS4*^{AUG}-*LacZ* (p3989), or P_{HIS4}:*HIS4*^{UUG}-*LacZ* (p3990), constructs were transformed with either empty vector (pA823) or *eIF5*^{G31R} (pA860). Three colonies from each transformant were grown overnight in SCD medium and treated as mentioned in figure 4.2. The whole cell extract prepared from these cells were subjected to the β-galactosidase activity (nmol of O-nitrophenyl-β-D- galactopyranoside cleaved per min per mg) analysis. The white bars represent un-induced (-3AT) while the shaded bars represent induced (+3AT) samples.

B) Yeast strain YP823 carrying either P_{GAPDH}:*HIS4*^{AUG}-*lacZ* (pA1056) or P_{GAPDH}:*HIS4*^{UUG}-*lacZ* (p1057) constructs were transformed with either empty vector (pA823) or *eIF5*^{G31R} mutant (pA860). The resulting transformants were subjected to the β-galactosidase activity as mentioned in the panel (A).

GCN4-LacZ expression

		- 3AT	+ 3AT
1	*HIS4*^{AUG} (s.c)	227 ±10	758 ±30 (100%)
2	*HIS4*^{UUG} (s.c)	240 ±15	2217 ±57 (292%)
3	eIF5 ^{G31R}/ *HIS4*^{AUG} (s.c)	203 ±18	508 ±26 (67%)
4	eIF5 ^{G31R}/ *HIS4*^{UUG} (s.c)	212 ±21	651 ±34 (85%)

β-Gal activity (U/mg)
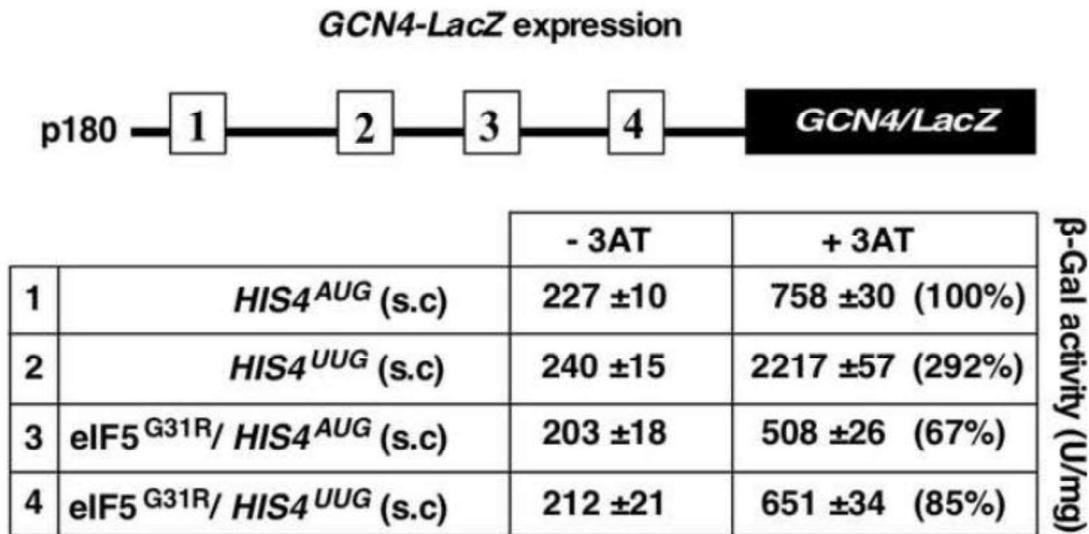
Figure 4.4: HIS4^{UUG} allele causes additional de-repression of *GCN4* expression in eIF5^{G31R} mutant.

Analysis of *GCN4-LacZ* expression. Derivative of yeast strain YP824 (*his4Δ*) carrying *GCN4-lacZ* (p180) construct [uORF1-4 open square boxes] is transformed with either *HIS4*^{AUG} (pA858), or *HIS4*^{UUG} (pA859), or *eIF5*^{G31R}/*HIS4*^{AUG} (pA861), or *eIF5*^{G31R}/*HIS4*^{UUG} (pA862) and the β-galactosidase activity was measured as per figure 4.3, in the absence (-3AT; un-induced) or presence of 3AT (+3AT; induced). The table indicates the β-galactosidase activity normalized to WT (100 %) and the error represents an average deviation.

4.2.2 eIF1 overexpression suppresses UUG codon recognition of *HIS4*^{UUG} allele, regulates *GCN4* expression and rescues 3AT sensitivity of eIF5^{G31R} mutant

It is evident from our data that the eIF5^{G31R} mutant (carrying *HIS4*^{AUG}) mediated 3AT sensitivity and its rescue of 3AT sensitivity by *HIS4*^{UUG} allele is thereof is related to the UUG codon recognition from the 5′ UTR of *GCN4* and *HIS4*^{UUG} transcript respectively. It is possible that this effect could be reversed by eIF1 over-expression. eIF1 has an important gate-keeper function at the P-site of the 40S ribosome that monitors the codon:anti-codon interaction and maintains the fidelity of start codon selection. The increased utilization of the UUG codon caused

by the premature release of eIF1 from the P-site is suppressed by overexpression of eIF1 (Martin-Marcos *et al.* 2014). Consequently, the overexpression of eIF1 should increase the stringency of AUG codon utilization while concomitantly weakening UUG codon recognition by the eIF5^{G31R} mutant. In order to test this, we overexpressed eIF1 and checked the growth in the presence or absence of eIF5^{G31R} mutant containing either *HIS4^{AUG}* or *HIS4^{UUG}* allele by spotting on SCD, SCD-H or SCD-H+3AT medium. The overexpression of eIF1 caused slow growth in the strain that was expressing the eIF5^{G31R} mutant along with the *HIS4^{UUG}* allele in SCD-H plate and confers 3AT sensitivity, consistence with the suppression of UUG start codon recognition by eIF1 overexpression (figure. 4.5A; compare, rows 4 and 8). Conversely, the growth defect associated with the *HIS4^{AUG}* allele in the eIF5^{G31R} mutant was also partially suppressed by the eIF1 overexpression and it rescued 3AT sensitivity (figure. 4.5A; compare, rows 2 and 6). Next, we tested the levels of *GCN4* expression from these cells by transforming *GCN4-LacZ* reporter construct (p180). The eIF5^{G31R} mutant showed significant down regulation of *GCN4* expression (62%) in the presence of *HIS4^{AUG}* allele, however in the presence of the *HIS4^{UUG}* allele there was additional de-repression of *GCN4* expression (82%) consistent with its resistance to 3AT (figure. 4.5B; and also, figure. 4.5A; compare rows 2 and 4). The overexpression of eIF1 showed an overall reduction in the *GCN4* expression, this observation is consistent with the earlier reports that the overexpression of eIF1 reduces the level of *GCN4* expression possibly by stringent AUG codon recognition of uORFs (Cheung *et al.* 2007; Luna *et al.* 2013). Interestingly, in the presence of eIF5^{G31R} mutant and *HIS4^{AUG}* allele, the overexpression of eIF1 causes significant up-regulation of *GCN4* level (62% vs 71%), consistent with its 3AT resistance (figure. 4.5A; compare, row 2 and 6). It is possible that the overexpression of eIF1 could stringently recognize AUG start codon from *HIS4^{AUG}* transcript and improve its expression, in addition to the suppression of the upUUG

codon recognition from 5′ UTR of *GCN4* transcript causing additional de-repression of *GCN4* expression. However, the overexpression of eIF1 caused no significant change in the *GCN4* expression levels in the presence of eIF5^{G31R} mutant and *HIS4^{UUG}* allele (82% vs 84%). This suggests that despite having higher *GCN4* levels, the overexpression of eIF1 might have suppressed UUG start codon recognition from *HIS4^{UUG}* allele resulting in less expression of HIS4p and sensitivity to 3AT (figure 4.5B; and also, figure 4.5A; compare row 4 and 8). These results suggest that the *HIS4* expression level influences sensitivity to 3AT inhibition. To confirm, whether the overexpression of eIF1 suppresses upUUG codon recognition from 5′ UTR of *GCN4* transcript and de-repress *GCN4* expression, we transformed in these cells a derivative of *GCN4-LacZ* reporter construct (p227) that have point mutation in AUG codons to remove short uORF1-4 (uORF-less) and used to test utilization of upUUG-ORF1-10 codon present at the 5′ UTR of *GCN4* transcript. The normalized β-galactosidase activity indicated that in comparison to empty vector control the overexpression of eIF1 caused significant up-regulation of *GCN4* expression, suggesting that overexpression of eIF1 indeed repressed the recognition of upUUG codons by the eIF5^{G31R} mutant (figure 4.5C). This also suggests that despite having moderately higher *GCN4* level, the overexpression of eIF1 might have suppressed UUG start codon recognition from *HIS4^{UUG}* allele resulting in 3AT sensitivity (figure 4.5B; and also, figure 4.5A; row 4 and 8). These results suggest that the translational control of *HIS4* expression status influence the sensitivity to 3AT inhibition. To confirm this, we checked the level of *HIS4* expression from *HIS4^{AUG}* and *HIS4^{UUG}* allele in presence or absence of high copy eIF1. The Western blot analysis suggested that in presence of eIF5^{G31R} mutant the overexpression of eIF1 resulted in improved expression from *HIS4^{AUG}* allele, whereas, it has exacerbated expression from *HIS4^{UUG}* allele (figure 4.5D; lane 2, 4, 6 and 8).

A

	LEU2 (h.c)	TRP1 (s.c)
1	E.V	$HIS4^{AUG}$
2	E.V	eIF5^{G31R}/$HIS4^{AUG}$
3	E.V	$HIS4^{UUG}$
4	E.V	eIF5^{G31R}/$HIS4^{UUG}$
5	eIF1	$HIS4^{AUG}$
6	eIF1	eIF5^{G31R}/$HIS4^{AUG}$
7	eIF1	$HIS4^{UUG}$
8	eIF1	eIF5^{G31R}/$HIS4^{UUG}$
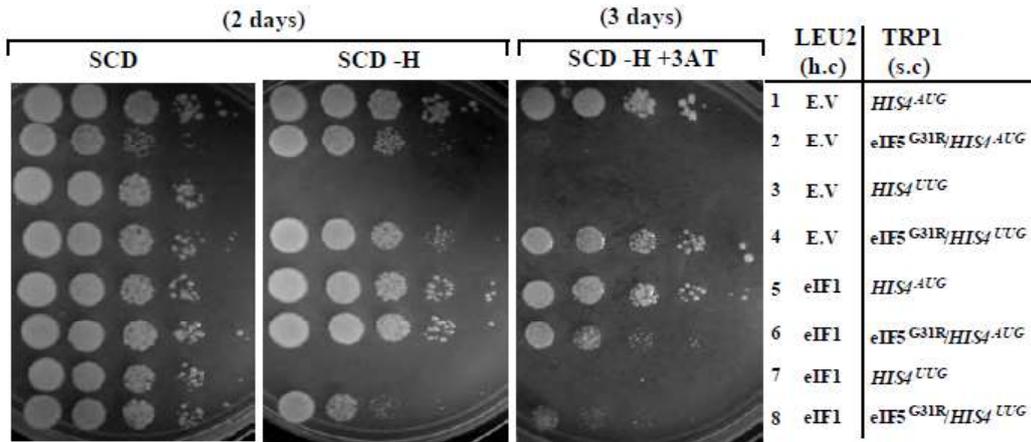
B)
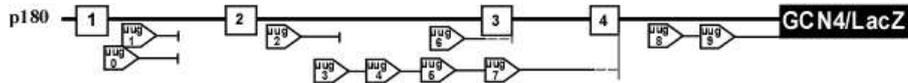
	-3AT	+3AT
$HIS4^{AUG}$(s.c)/ E.V (h.c)	220±15	739±64 (100%)
eIF5^{G31R}/ $HIS4^{AUG}$(s.c)/ E.V (h.c)	200±18	461±37 (62%)
eIF5^{G31R}/ $HIS4^{UUG}$(s.c)/ E.V (h.c)	214±59	608±57 (82%)
$HIS4^{AUG}$(s.c)/ eIF1 (h.c)	186±22	594±60 (100%)
eIF5^{G31R}/ $HIS4^{AUG}$(s.c)/ eIF1 (h.c)	122±9	421±12 (71%)
eIF5^{G31R}/ $HIS4^{UUG}$(s.c)/ eIF1 (h.c)	134±20	497±68 (84%)

C)
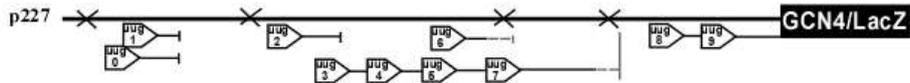
$HIS4^{AUG}$ (s.c)/ E.V (h.c)		eIF5^{G31R}/ $HIS4^{AUG}$ (s.c)/ E.V (h.c)	
- 3AT	+ 3AT	- 3AT	+ 3AT
3605±343 100%	3250±45 100%	2020±390 56%	1763±197 54%
$HIS4^{AUG}$ (s.c)/ eIF1 (h.c)		eIF5^{G31R}/ $HIS4^{AUG}$ (s.c)/ eIF1 (h.c)	
- 3AT	+ 3AT	- 3AT	+ 3AT
2042±198 100%	1870±203 100%	1734±121 85%	1615±114 86%

D)

Western Blot

	HIS4^AUG eIF5^G31R		HIS4^AUG eIF5^G31R		HIS4^UUG eIF5^G31R		HIS4^UUG eIF5^G31R		Allele
3AT	−	−	+	+	−	−	+	+	
eIF1 (h.c)	−	+	−	+	−	+	−	+	
HIS4 Protein amount (%)	100	238 ±29	660 ±50	850 ±64	100	76 ±12	602 ±29	436 ±69	

Figure 4.5: eIF1 overexpression suppresses UUG codon recognition by eIF5^{G31R} mutant and its 3AT sensitivity.

A) Yeast strain YP824 carrying either high copy (h.c) empty vector (E.V) (pA417) or h.c eIF1 (pA810) were transformed with *HIS4^{AUG}* (pA858) or *HIS4^{UUG}* (pA859), or *eIF5^{G31R}/HIS4^{AUG}* (pA861), or *eIF5^{G31R}/HIS4^{UUG}* (pA862) plasmids. The resulting transformants were serially diluted and spotted on medium containing histidine (SCD) or devoid of (SCD-H) histidine or medium containing 25 mM 3-Amino-1, 2, 4-triazole (SCD-H+3AT) and incubated at 30ºC for indicated period.

(B) Analysis of *GCN4-LacZ* expression. Colonies from the panel (A) were transformed with *GCN4-lacZ* (p180) construct and allowed to grow for 6 h in the presence of either histidine (-3AT; un-induced) or 3AT (+3AT; induced). The whole-cell extracts were prepared, and β-galactosidase activity was measured from three independent experiments using three individual colonies.

(C) Analysis of *GCN4-LacZ* expression. Colonies from the panel (A) carrying *HIS4^{AUG}* (pA858) or *eIF5^{G31R}/ HIS4^{AUG}* (pA861) plasmids, was transformed with *uORFless GCN4-LacZ* plasmid

(p227). The resulting transformants were subjected to β-galactosidase assay as described in panel (B). The table indicates the β-galactopyranoside activity normalized to WT (100 %) and the error represent an average deviation.

D) Western blot analysis. *HIS4* allele expression in the presence or absence of high copy eIF1 was performed as per figure 4.2. The # and * represent the groups that are significantly different (P < 0.01) using T-test.

4.2.3 The 3AT sensitivity of eIF5^{G31R} mutant can be rescued by overexpression of *HIS3* but not by overexpression of *HIS4^{AUG}* or *HIS4^{UUG}* alleles

Translation initiation using UUG as a start codon seldom occurs in yeast strain (*his4Δ*) harbouring *HIS4^{UUG}* allele resulting in His$^-$ phenotype. However, eIF5^{G31R} recognizes UUG codon from *HIS4^{UUG}* allele resulting in lower level of HIS4p expression and causing His$^+$ phenotype (figure 4.5 A row 3 and row 4). Our results suggest that the rescue of 3AT sensitivity of eIF5^{G31R} mutant could be due to critically under-expression from *HIS4^{UUG}* allele causing additional de-repression of *GCN4* expression (figure 4.4). In order to confirm the rescue of 3AT sensitivity is related to *HIS4* expression level, we used yeast strain YP824 (*his4Δ*) and expressed *HIS4^{AUG}* or *HIS4^{UUG}* allele from single copy (s.c), low copy (l.c) or high copy (h.c) vectors in presence or absence of eIF5^{G31R} mutation. The yeast strain showed 3AT sensitivity when supplemented with *HIS4^{UUG}* allele in single or low copy vector (figure 4.6A, row 5 and 6), consistent with extremely low HIS4p expression levels causing blockage of histidine biosynthesis pathway. Intriguingly, high copy expression of *HIS4^{UUG}* allele caused 3AT resistance (figure 4.6A, row 7) suggesting that HIS4p expression might be critically low, however, sufficient enough to stimulate histidine biosynthesis pathway to overcome 3AT induced starvation. In presence of eIF5^{G31R} mutant, the *HIS4^{AUG}* alleles expressed from single, low or high copy vectors showed 3AT sensitivity (figure 4.6A, row 9, 10 and 11), whereas expression from *HIS4^{UUG}* alleles from single or low copy vectors showed 3AT resistance (figure 4.6A, row 12 and 13). Interestingly, the high copy overexpression of *HIS4^{UUG}* alleles caused 3AT sensitivity (figure 4.6A, row 14). Together, these results suggest that eIF5^{G31R} mutant caused 3AT sensitivity when *HIS4* expression was above certain critical threshold as in the case of single, low or high copy expression from *HIS4^{AUG}* alleles and also high copy expression from *HIS4^{UUG}* alleles. Whereas the 3AT resistance was observed when *HIS4^{UUG}*

alleles was expressed from single and low copy vector, possibly due to critically low threshold of *HIS4* expression resulting in additional de-repression of *GCN4* expression (figure 4.4).

The enzyme Imidazole glycerol-phosphate dehydratase (HIS3p) encoded by *HIS3* gene is a direct target of 3AT inhibition causing histidine starvation and 3AT sensitivity. High copy overexpression of *HIS3* gene would result in synthesis of more molecules of HIS3p that can better compete with its substrate to overcome inhibition by 3AT. To test this, we transformed yeast strain carrying eIF5^{G31R} mutant with high copy vector harbouring *HIS3* gene. The overexpression of *HIS3* gene rescued 3AT sensitivity of eIF5^{G31R} mutant (figure 4.6B).

4.2.4 *HIS4^{UUG}* allele increases *HIS3* expression level in eIF5^{G31R} mutant

Our results suggest that *HIS4^{UUG}* allele rescues 3AT sensitivity of eIF5^{G31R} mutant by additionally de-repressing of *GCN4* expression (figure 4.4). The GCN4p upregulates expression of its target genes including *HIS3* and *HIS4* genes to overcome histidine starvation. Thus, it is possible that *HIS4^{UUG}* allele up-regulates the expression of *HIS3* gene in eIF5^{G31R} mutant under 3AT starvation condition. In order to test this, we transformed *HIS3-LacZ* reporter construct (pA1062) into a yeast strain carrying either *HIS4^{AUG}* or *HIS4^{UUG}* allele in presence of eIF5^{G31R} mutant and checked β-galactosidase activity. Similar to *GCN4* expression pattern observed in the figure 4.4, the *HIS4^{UUG}* allele up-regulated *HIS3-LacZ* reporter expression for the eIF5^{G31R} mutant under 3AT starvation condition (figure 4.7).

A)
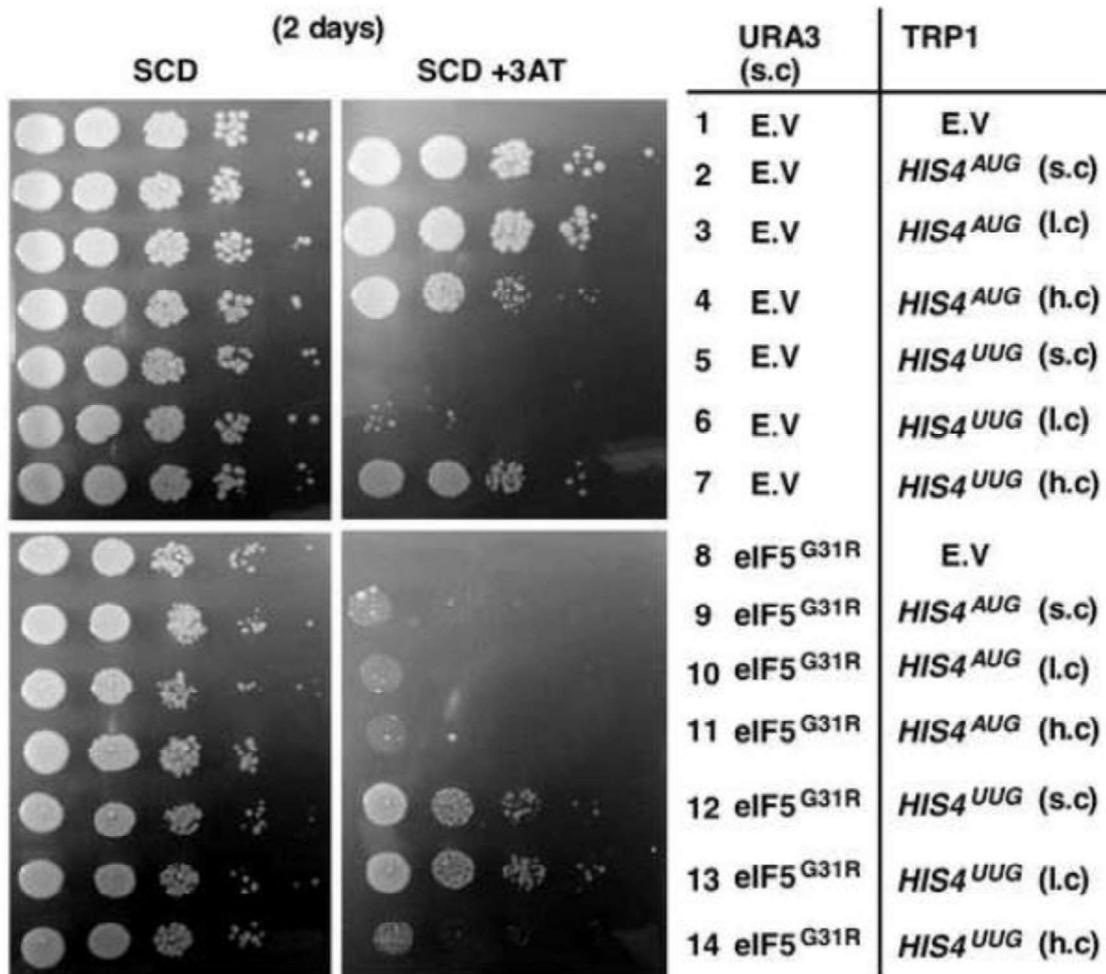
B)
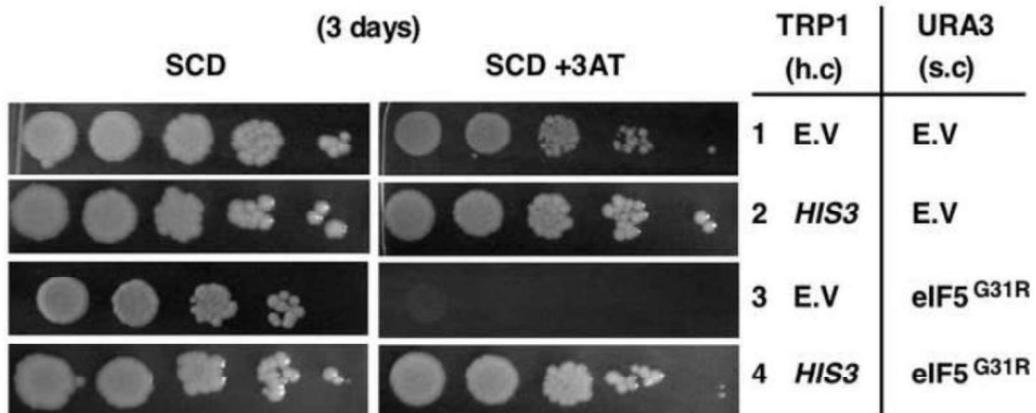
Figure 4.6: Overexpression of the *HIS3* but not *HIS4* gene rescues 3AT induced starvation.

A) Growth analysis. YP824 strain carrying either single copy (s.c) E.V (pA309) or s.c eIF5^{G31R} (pA703) were transformed with (s.c) E.V (pA823), or (s.c) *HIS4^{AUG}* (pA858), or (l.c) *HIS4^{AUG}* (pA616), or (h.c) *HIS4^{AUG}* (pA780), or (s.c) *HIS4^{UUG}* (pA859), or (l.c) *HIS4^{UUG}* (pA792), or (h.c) *HIS4^{UUG}* (pA781). The resulting transformants were serially diluted and spotted as per figure 4.1.

(B) Growth rate analysis. YP823 strain carrying either single copy (s.c) E.V (pA309) or s.c eIF5^{G31R} (pA703) were transformed with (h.c) E.V (pB1377), or (h.c) *HIS3* (pA905) vectors. The resulting transformants were serially diluted and spotted as per figure 4.1.
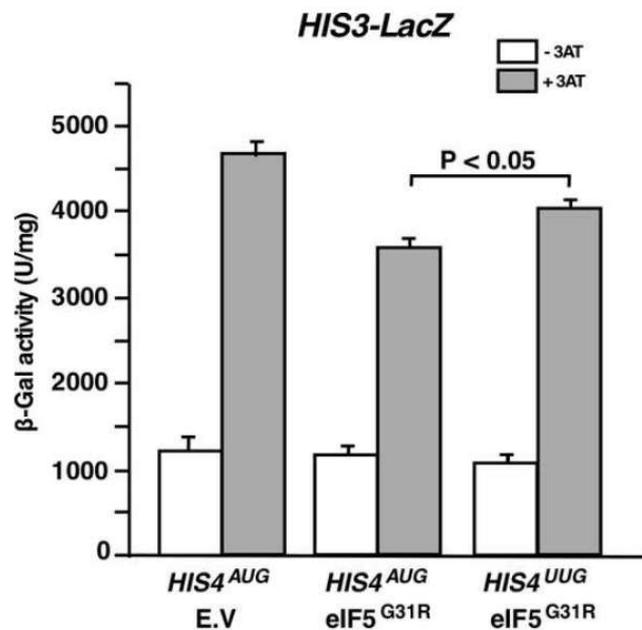
Figure 4.7. Analysis of *HIS3* expression level.

Yeast strain YP824 carrying *HIS3-LacZ* reporter construct (pA1062) and also carrying either single copy (s.c) E.V (pA309) or (s.c) eIF5^{G31R} (pA703) vector were transformed with either (s.c) *HIS4^{AUG}* (pA858), eIF5^{G31R}/*HIS4^{AUG}* (pA861) or (s.c) eIF5^{G31R}/*HIS4^{UUG}* (pA862) alleles. The resulting transformants were subjected to β-galactosidase activity as per figure 4.3, in absence (-) or presence (+) of 3AT. The error bar represents an average deviation. The P value was calculated using paired T test.

4.3. DISCUSSION

Biological systems are dynamic in nature, which provides a flexible mechanism to tackle adverse effects of some inhibitory compounds and understanding these mechanisms provides us an opportunity to comprehend the fundamentals of the living system. In *Saccharomyces cerevisiae*, the 3AT is a widely-used HIS3p inhibitor to induce histidine starvation to study translation regulation of *GCN4* expression (Hinnebusch 1988; Albrecht *et al.* 1998). The yeast cells respond by phosphorylating eIF2α subunit and de-repressing *GCN4* expression regulated by its upstream four open reading frames (uORFs 1-4) (Dever 1997). However, the GTPase defective eIF5^{G31R} mutant recognizes upUUG initiation codon from the 5′ UTR region of the *GCN4* transcript and repress *GCN4* expression (Gcn$^-$ phenotype) and shows 3AT sensitivity (Antony A and Alone 2017).

Our data suggests *HIS4* allele is playing a critical role in rescue of 3AT sensitivity of eIF5^{G31R} mutant. It is intriguing to understand the dynamism of this process as 3AT is known to competitively inhibit HIS3p and not HIS4p, thus the rescue of 3AT sensitivity of eIF5^{G31R} mutant by *HIS4^{UUG}* allele suggests that yeast has an inbuilt redundant process to overcome 3AT inhibition. Basal expression of genes involved in histidine biosynthesis pathway is essential to maintain sufficient pool of histidine inside the cell. Deletion of *HIS4* gene in a yeast strain and replacement with *HIS4^{UUG}* allele could interrupt this pathway as UUG initiation codon is seldom utilized by translation initiation machinery leading to poor expression of HIS4p (figure 4.1, row 2 and figure 4.2, lane 2) thus causing His$^-$ phenotype and also showing 3AT sensitivity. Despite having 9-fold higher de-repression of *GCN4* expression in these cells, the level of HIS4p expression might be extremely low to catalyze biochemical steps in histidine pathway to overcome 3AT induced starvation (figure 4.2, lane 6, and figure 4.4). The eIF5^{G31R} mutant caused more than 2-fold

reduction in HIS4p protein expression and showed only up to 67% *GCN4* de-repression in presence of *HIS4^{AUG}* allele. It is possible that the level of HIS4p is sufficiently high to show growth on medium lacking histidine (His$^+$ phenotype); however, the level of *GCN4* expression might not be sufficient enough to overcome 3AT starvation (figure 4.1, row 3; figure 4.2, lanes 3 and 7; figure 4.4). Whereas, the eIF5^{G31R} mutant initiates translation from UUG codon of *HIS4^{UUG}* allele which may be sufficient enough to show growth on medium lacking histidine (His$^+$ phenotype). However, under 3AT starvation condition the amount of HIS4p might be below critical threshold thus causing additional de-repression of *GCN4* expression (85%) to overcome 3AT starvation (figure 4.1, row 4; figure 4.2, lanes 4 and 8; figure 4.4). This allows the transcriptional upregulation of genes (specially *HIS3* gene) that are involved in histidine biosynthesis to overcome 3AT sensitivity (figure 4.7, figure 4.8A). Alternatively, the yeast cells might be using *HIS4^{UUG}* allele to its advantage to compete with eIF5^{G31R} mutant factor to translate *HIS4^{UUG}* allele while relatively freeing-up *GCN4* transcript to translate with wild type eIF5 factor thus, causing de-repression of *GCN4* expression. If this was the case then over-expression of *HIS4^{UUG}* allele from high copy vector should have caused 3AT resistant (figure 4.6A, row 14), thus ruling out this alternate mechanism.

The overexpression of eIF1 causes stringent AUG codon utilization due to shift in the equilibrium of 48S complex towards Open/P$_{OUT}$ conformation giving a better chance to scan for the AUG codon while discouraging Closed/P$_{IN}$ conformation at the UUG codon (Cheung *et al.* 2007; Luna *et al.* 2013). The higher concentration of eIF1 prevents the recognition of UUG start codon from *HIS4^{UUG}* allele causing low expression of HIS4p, however, it also stringently recognizes AUG start codon and improves expression from *HIS4^{AUG}* allele (figure 4.5D and 4.8A). This could be the reason for partial suppression of the 3AT sensitivity of eIF5^{G31R} mutant in

presence of the $HIS4^{AUG}$ allele while exacerbating the 3AT sensitivity in presence of the $HIS4^{UUG}$ allele, consistent with suppression of Sui⁻ phenotype by overexpression of eIF1.

In eIF5^{G31R} mutant, the expression of $GCN4$ is playing a critical role in causing 3AT sensitivity and its rescue thereof in presence of $HIS4^{UUG}$ allele. However, despite moderately increasing $GCN4$ expression levels, the repression of HIS4p expression from $HIS4^{UUG}$ allele by eIF1 overexpression causes 3AT sensitivity. This could be possible if the limitation of HIS4p slows down the second and third biochemical steps in the histidine biosynthesis pathway causing inadequate availability of substrate (D-erythro-imidazole-glycerol-phosphate) to compete with 3AT in order to bind with HIS3p resulting in 3AT sensitivity (figure 4.8B).

Thus, our study has outlined an optimal interplay between the expression levels of $GCN4$ and $HIS4$ genes that leads to rescue of 3AT sensitivity of eIF5^{G31R} mutant by $HIS4^{UUG}$ allele due to additional de-repression of $GCN4$ expression. It also highlighted the importance of $HIS4$ expression in maintaining the flux of substrate necessary to compete with 3AT.

A)

moderate

low

0

3 4 5 7

1 2 3 4 GCN4

1 2 6 8 9

eIF1 (h.c) ⊣ eIF5^{G31R} (Sui⁻)

HIS4^{AUG} *HIS4^{UUG}*

B)

3AT inhibition of histidine biosynthesis pathway

1

PRPP+ATP → HIS1 → Phosphoribosyl-ATP

(Pyrophosphatase)

HIS4   2

L-histidine

10 HIS4 ↑ (Dehydrogenase)

histidinal

(Cyclohydrolase)

Phosphoribosyl-AMP

HIS4   3

9 HIS4 ↑ (Dehydrogenase)

histidinol

Phosphoribosylformimino
AICAR-phosphate

HIS6   4

8 HIS2 ↑

L-histidinol phosphate

Phosphoribosylformimino
AICAR-P

HIS7   5   6   7 HIS5 ↑

HIS3   Imidazole acetol phosphate

D-erythro imidazole glycerol phosphate

3AT

Figure 4.8 Model depicting the mechanism of rescue of 3AT sensitivity.

A) *GCN4* dependent rescue of 3AT sensitivity by *HIS4^{UUG}* allele. Schematic representation of *GCN4* transcript showing upstream open reading frames (uORF) open square boxes 1-4, the pentagon boxes with line shows UUG codon based upstream reading frames terminating at various length (upUUG 1-10). The eIF5^{G31R} mutant utilizes upUUG 1-10 codons present in the 5′ UTR of *GCN4* transcript and terminates translation before reaching main ORF (effect 1), it also utilizes UUG codons from *HIS4^{UUG}* allele and initiates translation (effect 2), however, the below critical level of HIS4p expression causes de-repression of *GCN4* expression from low to moderate. The eIF5^{G31R} mutant down-regulates AUG codon selection from *HIS4^{AUG}* allele and repress its translation (effect 3). All the effects of eIF5^{G31R} mutant can be partially reversed by high copy (h.c) over-expression of eIF1.

B) The histidine biosynthesis pathway showing all the ten biochemical steps. *HIS4* is involved in four catalytic steps (steps 2,3,9,10). D-erythro-imidazole-glycerol-phosphate (green triangle) and 3AT (V-shape) are the substrates and competitive inhibitor of HIS3p/enzyme (step 6) respectively. 3AT out-competes the substrate to bind to the otherwise poorly expressing HIS3p (grey square), thus showing high sensitivity to 3AT induced inhibition.

Chapter 5

C1209U suppressor mutation in 18S rRNA restores start codon selection fidelity of GTPase defective eIF5 and eIF2β mutant

5.1 INTRODUCTION

The 40S subunit provides a platform on which translation initiation factors, tRNA$_i^{Met}$ and mRNA assembles to decode the genetic code and set up an open reading frame for protein translation. 18S rRNA not only provide a scaffold for ribosomal proteins and initiation factors binding but also shown to directly take part in AUG codon selection. Mutating residue A1152U (corresponding to G928 in 16S rRNA) located in helix 28 caused leaky scanning of uORF4 and uORF1 in *GCN4* and shows Gcd$^-$ phenotype (Dong *et al.* 2008). Another substitution mutation A1193U in the helix 31 of 18S rRNA caused increased leaky scanning of *GCN4* uORF1 and showed Gcn$^-$ phenotype. The A1193U mutation also suppresses the Sui$^-$ phenotype of the intrinsic GTPase defective eIF2β^{S264Y} mutant (Nemoto *et al.* 2010). It has been observed that hyper GTPase eIF5^{G31R} mutant showed strong specificity (>100 fold) to initiates at UUG start codon than the GUG or CUG codon (Huang *et al.* 1997). It may be possible the eIF5^{G31R} mutant pre-maturely changing the conformation of 48S initiation scanning complex to 'Closed/P$_{IN}$' state and exposing other residues in the P-site of 18S rRNA that can stabilize the UUG codon and CAU anti-codon interactions. A genetic suppressor screening can be employed to identify critical residues in the 18S rRNA that are involved in the recognition of UUG as a start codon in the eIF5^{G31R} mutant.

5.2 RESULTS

5.2.1 Construction of reporter yeast strain to screen suppressor of eIF5[G31R] mutant on 18S rRNA:

A yeast strain YP843 (*Mat a, ade2-1, ura3-1, trp1-1, leu2-3,112, his3-11 can1-100 rdn$\Delta\Delta$::HIS3,* pNOY130 [P$_{GAL7}$-*35SRDN^{WT}/URA3*]) was kindly gifted by Prof. Masayasu Nomura University of California-Irvine USA. This strain carries deletion for tandemly repeated 150 copies of chromosomal *35SRDN* gene (encodes for 18S, 5.8S, and 25S rRNA). In order to screen eIF5[G31R] suppressor of Sui¯ mutant (Ssu¯) in the 18S rRNA we decided to delete the chromosomal copy of *HIS4* gene using homologous recombination technique. To this end, the PCR amplified *KanMx6* disruption cassette (1.6 kb) flanked by 40 base pair of *HIS4* gene specific region was transformed into YP843 yeast strain and plated on media supplemented with G418 antibiotic (figure 5.1A). The G418 resistant colonies were picked up and *KanMx6* recombinant positive colonies were identified by PCR using *HIS4* and *KanMx6* specific primers (figure 5.1B and C). The resultant yeast strain was designated as YP844 (*Mata, ade2-1, ura3-1, trp1-1, leu2-3,112, his3-11 can1-100 rdn$\Delta\Delta$::HIS3, his4Δ::KanMx6,* pNOY130 [P$_{GAL7}$-*35SRDN^{WT}/URA3*]). Further, we confirmed the authenticity of this strain by checking the nutrient auxotrophic nature and 5-fluroorotic acid (5-FOA) selection. Complementing the yeast strain with 35S *RDN* (Henceforth called as *18SRDN^{WT}* to represent the fact, where only the 18S rRNA portion of *35SRDN* was mutated in this study) in either *LEU2*, or *URA3*, or *TRP1* behaved as per expectation by showing growth on appropriate plates. The strain YP844 carries *18SRDN^{WT}* in URA3 based plasmid as a solo source of *18SRDN^{WT}*. Counter selecting this plasmid in this strain using 5-FOA showed the lethality which confirms the authenticity of the strain (figure 5.2A).
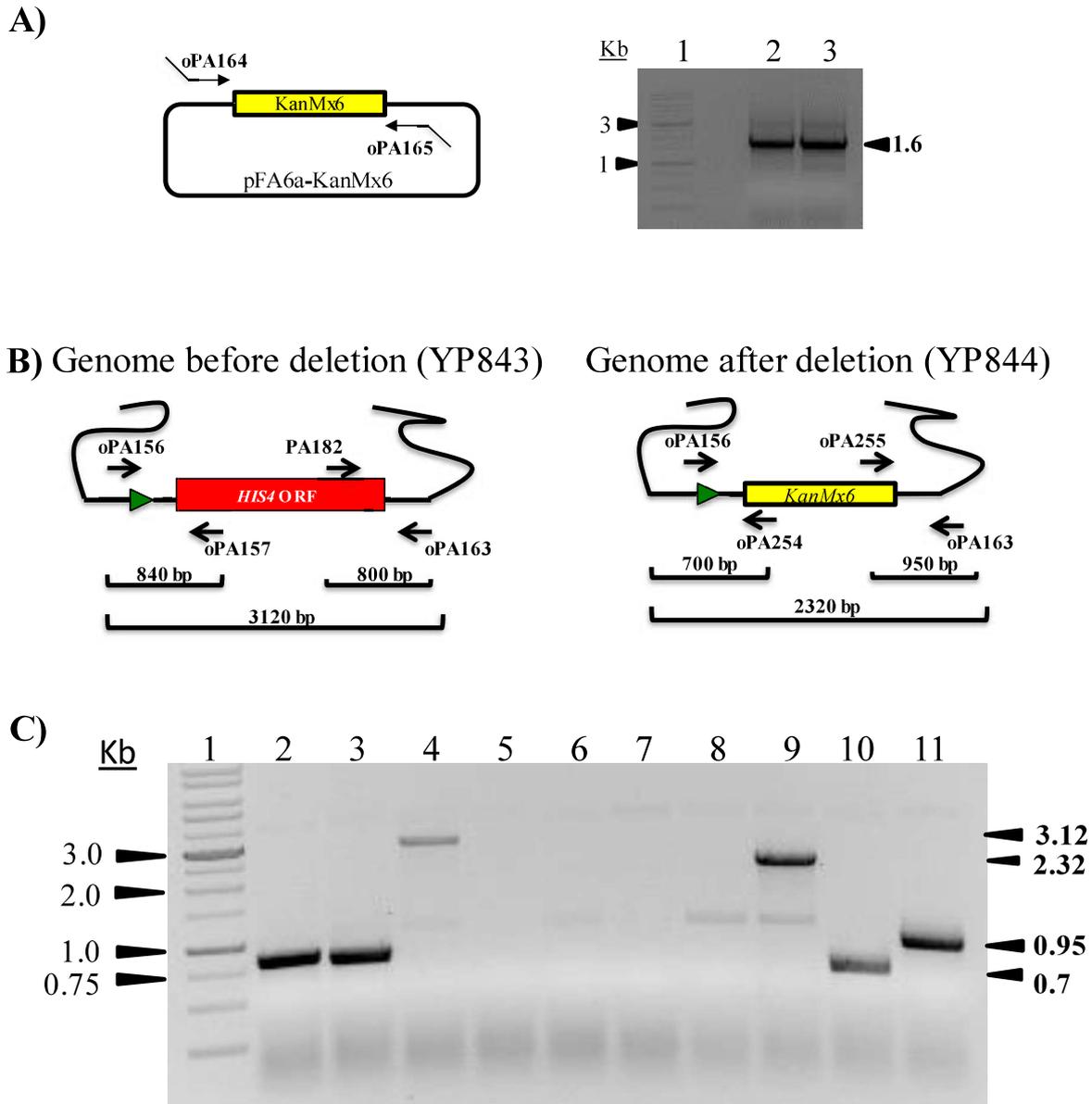
Figure 5.1. Deletion of *HIS4* gene for suppressor of Sui⁻ screening.

A) Left panel schematic showing pFA6a-*KanMx6* (pA559) plasmid carrying *KanMx6* disruption cassette along with primers carrying *HIS4* gene specific flanking regions. Right panel showing 1.6 Kb PCR amplicon in lane 2 and 3 indicated by black arrow resolved on 0.8% agarose gel. Lane 1 showing DNA ladder with 1 and 3 Kb DNA marker indicated with a black arrow. The *KanMx6*

based disruption cassette (1.6 Kb) from the panel (A) is transformed into to yeast strain (YP843) and successful recombinants were screened on a plate containing G418 antibiotic.

B) Schematic representation and analysis of *HIS4* gene deletion. The panel shows a schematic representation of *HIS4* gene from yeast strains before (left) and after deletion (right) with appropriate primer binding sites as indicated.

C) Confirmation of *HIS4* gene deletion by PCR. 0.8% agarose gel showing PCR amplified product using various primers. Oligonucleotides oPA156 binds to the *HIS4* promoter region while oligo oPA157 binds to 5′ proximal region of *HIS4* ORF (B, left panel), it gives specific 840 bp amplification of *HIS4* gene (lane 1). The oligo oPA182 binds to the 3′ proximal region of *HIS4* ORF while oligo oPA163 binds to the chromosomal region downstream of *HIS4* gene and give specific amplification of 800 bp (lane 2). Using oligos oPA156/ oPA163 a complete amplification of intact *HIS4* gene (3120 bp) can be obtained (lane 4). The insertion of *KanMx6* cassette and deletion of *HIS4* gene can be confirmed by using oligonucleotide flanking to the *HIS4* chromosomal region (oPA156 and oPA163) and *KanMx6* gene (oPA254 and oPA255) (Panel B, right). Oligonucleotide oPA156/oPA254 gives 700 bp amplification (lane 10) while oligos oPA255/oPA163 gives 950 bp PCR amplification (lane 11). Oligo nucleotides oPA156/oPA163 gives complete amplification of *KanMx6* cassette along with the *HIS4* chromosomal flanking region (lane 9). The oligonucleotide oPA156/oPA254 and oPA255/oPA163 combination cannot give PCR amplification reaction before replacement of *HIS4* gene by *KanMax6* cassette, lane 5 and lane 6 respectively. The oligonucleotide oPA156/oPA157 and oPA182/oPA163 combination cannot give PCR amplification reaction after replacement of *HIS4* gene by *KanMax6* cassette, lane 7 and lane 8 respectively.

A) Replica plating analysis with a selectable auxotrophic marker.

	Plasmids		
	PolI_RDN (*TRP1*)	*GAL7_RDN* (*URA3*)	
	+	−	YP843 (WT)
	−	+	
	−	+	YP844 (ΔHIS4)
	−	+	
	−	+	

Plate 1: YP+Gal
Plate 2: SCGal+Leu+Trp+His
Plate 3: SCGal+Leu+Trp-His
Plate 4: SCGal+Leu+Trp+His+G418
Plate 5: SCGal+Leu+Trp Ura+His+5FOA

B)

SCD+H	SCD-H	P_{PolI}-18SRDN^{WT} (LEU2)	P_{Gal7}-18SRDN^{WT} (URA3)	TRP1
		+	+	Vector
		+	+	eIF5^{G31R}
		+	+	HIS4^{AUG}
		+	+	HIS4^{UUG}
		+	+	eIF5^{G31R}/ HIS4^{AUG}
		+	+	eIF5^{G31R}/ HIS4^{UUG}

Figure 5.2. Confirmation of yeast strain YP844 for eIF5^{G31R} mutant suppressor screening.

A) Replica plating analysis with a selectable auxotrophic marker. Yeast cells YP807 (*rdn*ΔΔ) harboring *P_{GAL7}-18SRDN^{WT}/TRP1* (pA538) [row 1], YP843 (*rdn*ΔΔ) harboring *P_{GAL7}-18SRDN^{WT}/URA3* (pA539) [row 2] and 3 different suspected *HIS4* deleted strains of YP844 (*rdn*ΔΔ, *his4*Δ) harboring *P_{GAL7}-18SRDN^{WT}/URA3* (pA539) were patched on YPGal plate. After 2 days of incubation at 30°C, it was replica plated on SCGal+Leu+Trp+His (plate 2), SCGal+Leu+Trp-His (plate 3), SCGal+Leu+Trp+His+G418 (plate 4), SCGal+Leu+Ura+Trp+His+ 5FOA (plate 5) and incubated at 30°C for 3 days.

B) Confirmation of yeast strain for Sui⁻ suppressors (Ssu⁻) screening. The yeast strain YP844 was transformed with *P_{POLI}-18SRDN^{WT}/LEU2* (pA687) RDN plasmid along with different combinations of *HIS4* alleles or *eIF5^{G31R}* and spotted (as mentioned in material and methods) on SCD+H and SCD-H plate and incubated at 30°C for 3 days.

5.2.2 Confirmation of *HIS4* reporter plasmids and strain

To confirm the Sui$^-$ phenotype of eIF5^{G31R} mutant in the reporter strain (YP844) carrying P$_{GAL7}$-*18SRDN^{WT}/LEU2* (pA687), we transformed both *HIS4^{AUG}* and *HIS4^{UUG}* alleles in the combination with eIF5^{G31R} mutant as indicated in figure 5.2B. Yeast cells expressing eIF5^{G31R} mutant showed slow growth compared to wild type (WT) cells (figure 5.2 compare row 1,3,4 and 2,5,6 in SCD+H plate). Yeast strain carrying plasmid borne *HIS4^{AUG}* allele complemented the histidine auxotrophy and grown on medium lacking histidine while *HIS4^{UUG}* allele could not support growth (figure 5.2B compare row 3 and 4). However, yeast cells carrying eIF5^{G31R} mutant complements the histidine auxotrophy when supplemented with either *HIS4^{AUG}* or *HIS4^{UUG}* allele (figure 5.2B compare row 5 and 6). The test confirms the yeast strain and the plasmid constructs are fit for screening the 18S rRNA suppressors against eIF5^{G31R} mutant.

5.2.3 Strategy to screen suppressor of eIF5^{G31R} mutant in 18S rRNA

A schematic representation of suppressor screening is shown in the figure 5.3A. Briefly, yeast strain YP844 (*rdn*ΔΔ, *his4*Δ) carrying P$_{GAL7}$-*18SRDN^{WT}/URA3* (pA539) can grow on medium containing galactose and histidine. In presence *18SRDN^{WT}*, the *eIF5^{G31R}* mutation enables recognition of UUG codon from *HIS4^{UUG}* allele. Random mutations will be incorporated into 18S rDNA region of *35SRDN* gene by error prone polymerase approach and cloned under native *POLI* promoter based plasmid (P$_{POLI}$-*18SRDN^{WT}/LEU2*) [pA687]. The resultant pool of 18S*RDN* mutant libraries will be transformed into yeast cell expressing *eIF5^{G31R}*/*HIS4*^{UUG} allele. The resultant transformants will be patched on media containing galactose and histidine (SCGal+H) followed by replica plating on galactose (SCGal) or dextrose (SCD) media supplemented with (+H) or without histidine (-H). If the random mutants of *18SRDN* (*18SRDN**) affect UUG codon

recognition of eIF5^{G31R} mutant, the expression of $HIS4^{UUG}$ allele will be suppressed and lead to histidine auxotrophy (His⁻). This strategy also enables to categorize the dominant and recessive nature of suppressor mutants by replica plating them on galactose or glucose as sole carbon source. In the presence of galactose as a sole carbon source (figure 5.4 A left) cells uptake galactose and induce expression of genes related galactose metabolism including P$_{GAL7}$-$18RDN^{WT}$. Since the mutant $18SRDN*$ (pA687*) (* represents random mutations) is cloned under constitutive $POLI$ promoter, it expresses all conditions independent of carbon sources. Thus, analyzing the effect of UUG codon suppression phenotype (His⁻) by replica plating on media containing (SCGal+H) or not containing (SCGal-H) histidine, mimics dominant Ssu⁻ screening. While analyzing the same effect on media containing glucose as carbon source (SCD+H and SCD-H) in which all galactose metabolism related promoters are turned-off (including P_{GAL7}-$18SRDN^{WT}/URA3$) the mutant $18SRDN*$ only will express which mimics a condition for recessive suppressor screening (figure 5.4 A and B). The positive suspected Ssu⁻ colonies will then be picked up from the master replica plate and will be subjected to plasmid isolation followed by DNA sequencing to map the mutation as mentioned in material and methods.

The random mutant libraries were generated using error prone PCR as follows; initially, we generated an intermediate plasmid by replacing the 2 kb of $18SRDN^{WT}$ with a stuffer fragment (750 bp) to generate pYEp351-stuffer plasmid. Later, the $18SRDN^{WT}$ fragment (2 kb) is PCR amplified by error prone polymerase (Stratagene; Genemorph random mutagenesis kit) that lacks proof reading activity using oligonucleotides oPA135 and oPA142 (figure 5.3 C left panel) and cloned into pYEp351-stuffer plasmid by replacing the 750 bp stuffer DNA fragment to generate random pool of mutant 18S rRNA ($18SRDN*$) plasmids (figure 5.3 C right panel).

A)

Error prone PCR

Mutagenesis

P_{GAL7} — 18S^{WT} — URA3

P_{POLI} — 18S* — LEU2

eIF5^{G31R} — HIS4^{UUG} — TRP1

Yeast transformation

SCGal +H

SCGal/D+H

SCGal/D-H

plasmid rescue

DNA sequencing

B)

Nde I — oPA135 — 18S^{WT} — DraIII — LEU2

oPA142

P_{POLI}

pYEp351-P_{POLI}-RDN

Nde I — stuffer — Dra III
0.75 kb

NdeI/DraIII   Ligation

18S^{WT}
2.0 kb

Nde I — stuffer — Dra III — LEU2

pPOLI

pYEp351-stuffer (pA688)

NdeI/DraIII

stuffer

18SrRNA cassette amplified by mutagenizing PCR

Nde I — Dra III — Leu2

pPOLI

pYEp351

Ligation of randomly mutated 18S* with vector

Leu2   Leu2   Leu2

pYEp351-P_{POLI}-18S*

C)

Kb   1   2

2.0
1.5

2.0

Kb   1   2   3   4   5

2.0
1.5
0.75

2.0

0.75

115

Figure 5.3. Strategy for screening suppressor of Sui¯ phenotype (Ssu¯) and creating random mutant libraries.

A and B) Schematic representation of strategy to screen suppressor of Sui¯ and generating mutant *18SRDN** pool (please see details in section 5.2.3).

C) Left panel showing 2.0 Kb of *18SRDN** fragment amplified and resolved on 0.8% agarose gel lane 2, and lane 1-DNA marker with molecular weight indicated by black arrow. Right panel, showing restriction digestion analysis of recombinant clones on 0.8% agarose gel. Lane 1, DNA marker; lane 2 undigested mutant 18S* plasmid; lane 3, NdeI and DraIII digested plasmid showing the release of 2.0 Kb *18SRDN* fragment; lane 4, undigested plasmid containing 750 bp stuffer fragment; lane 5, NdeI and DraIII digested plasmid showing the release of 750 bp of stuffer fragment.

5.2.4 Suppressor of Sui¯ (Ssu¯) screening for the eIF5^{G31R} mutant.

We used error prone PCR to generate *18SRDN** random mutant library and transformed into yeast expressing *eIF5^{G31R}/HIS4^{UUG}* construct. Upon screening of approximately 10,000 colonies, we obtained many suspected Ssu¯ mutants labelled with numbers prefixed by YR (yeast *RDN* suppressor) as indicated in figure 5.4C. We could successfully isolate P$_{POLI}$-*18SRDN** (pA687*) plasmids from four of these suspected Ssu¯ mutants (YR3, YR4, YR7, and YR9) and subjected to DNA sequencing to map the mutation on both secondary and tertiary structure of 18S rRNA (figure 5.5).

The suppressor mutation A737G was located in the central region and observed in both YR3 T280G, A737G (figure 5.5A and 5.5E, red color), and YR4 A148G, A737G (figure 5.5B and 5.5E, purple color) suppressor. The residue T280G was located in helix 10 of the right foot while A148G was located in the helix 8 of right foot region of 5′ domain and disturb the A-minor interaction with A86 residue. Unexpectedly, the suppressor YR7 carries a total of 7 mutations (figure 5.5C). Among them, two were present in 5′ domain; G281A which disturbed the helix 10 and A412G was located in helix 14 which forms the part of inter subunit surface. The remaining five mutations were exclusively present in the 3′ major domain; T1250G, T1303C, ΔA1344, G1412A, and G1428C. The YR9 suppressor carried six mutations (figure 5.5D). Among them, ΔG153 was on helix 8, A256G, and A548T are present in the 5′ domain. Residues A236G and A760G were present in ES3 and ES6 respectively. The C1209U mutation was present in the 3′ major domain and disturbed the local stem-loop structure. Predicting possible suppressor mechanism from these multi-mutants was challenging, we reasoned that it would be easier to interpret the effect of a single mutation on suppressor activity. By using site directed

A)

+Gal/-Glu

P_{GAL1} — WT-RDN

P_{POLI} — *RDN

-Gal/+Glu

P_{GAL1} — WT-RDN

P_{POLI} — *RDN

1. Vector
2. eIF5^{G31R}
3. HIS4^{AUG}
4. eIF5^{G31R}/HIS4^{AUG}
5. HIS4^{UUG}
6. eIF5^{G31R}/HIS4^{UUG}

B)

SCGal+H   SCGal-H   SCGlu+H   SCGlu-H

118

C)

| SCGal+H	SCGal-H	SCD+H	SCD-H	
				eIF5^{G31R}/HIS4^{AUG}
				HIS4^{UUG}
				eIF5^{G31R}/HIS4^{UUG}
				YR1
				YR2
				YR3
				YR4
				YR7
				YR8
				YR9
				YR10
				YR13
				YR14
				YR15
				YR16
				YR17
				YR18
				YR19
				YR20
				YR43
				YR44
				YR45
				YR46
				YR54
				YR55
				YR56
				YR57
				YR58
				YR59
				YR60
				YR61

Figure 5.4 Screening of Ssu⁻ phenotype for eIF5^{G31R} mutant

A) Schematic represent the conditional expression system of *18SRDN* used in the screening. Yeast strain YP844 carries *18SRDN^{WT}* (pA539) under galactose inducible promoter (GAL7) whose expression is turned off in dextrose media. However, the random mutations carrying 18S* (pA687*) is cloned under constitutive *POLI* promoter whose expression is independent of carbon source.

B) Growth analysis of Ssu⁻ screening by replica plating. Yeast strain YP844 carrying P$_{GAL7}$-*18SRDN^{WT}* (pA539) along with P$_{POLI}$-*18SRDN^{WT}* (pA687) was transformed with 6 different combination of reporter plasmids [empty vector (pA823), or *eIF5^{G31R}* (pA860), or *HIS4^{AUG}* (pA858), or *eIF5^{G31R}/HIS4^{AUG}* (pA861), or *HIS4^{UUG}* (pA859), or *eIF5^{G31R}/HIS4^{UUG}* (pA862)] indicated as numbering on master replica plate (SCGal+H). The remaining colonies carry P$_{GAL7}$-*18SRDN^{WT}* (pA539) along with P$_{POLI}$-*18SRDN** (pA687*) in the presence of *eIF5^{G31R}/HIS4^{UUG}* (pA862). The white arrow indicates one suspected dominant suppressor of Sui⁻ (Ssu⁻) for eIF5^{G31R} as the colony did not grow on medium lacking histidine containing galactose as well as dextrose probably by suppressing UUG codon based expression from *HIS4^{UUG}* allele which was supported by eIF5^{G31R}.

C) Growth analysis of suspected Ssu⁻ mutants. Derivatives of yeast strain (YP844) carrying P$_{GAL7}$-*18SRDN^{WT}* (pA539) and P$_{POLI}$-*18SRDN^{WT}* (pA687) was transformed with *eIF5^{G31R}/HIS4^{AUG}* (pA861) or *HIS4^{UUG}* (pA859) or *eIF5^{G31R}/HIS4^{UUG}* (pA862) (row 1-3) and spotted along with suspected Ssu⁻ mutants (carrying P$_{GAL7}$-18S^{WT} (pA539), P$_{POLI}$-*18SRDN** (pA687*), *eIF5^{G31R}/HIS4^{UUG}* (pA862) indicated in YR based numbering on indicated plates for 3 days at 30°C.

mutagenesis we introduced single mutation C1209U as observed in YR9 suppressor (figure 5.6). This residue was present in the "head region" in the vicinity to the 'P' site and close to the eIF1A binding site. Since these sites are important in AUG codon recognition the mutation at C1209U may provide insight into the mechanism of UUG codon recognition in eIF5^{G31R} Sui$^-$ mutant. Since each of these suspected Ssu$^-$ mutants including *18SRDN^{C1209U}* possess both *18SRDN^{WT}* (P$_{GAL7}$-*18SRDN^{WT}/URA3*) and *18SRDN** (P$_{POLI}$-*18SRDN*/LEU2*) plasmids, we subjected these cells to 5-FOA to counter select URA3 based *18SRDN^{WT}* to assess the recessive phenotype of the suppressor mutants (figure 5.7). Strikingly, suspected suppressor mutant YR3, YR4, YR7 and YR9 which suppress the growth on medium lacking histidine could not grow on 5-FOA plate (figure 5.7). The lethality of these mutants on 5-FOA plate suggest that the mutant ribosomes may have a defect in general translation apart from its Ssu$^-$ phenotype.

A) **Suppressor YR3**

eIF1A

A737G

T280G

B) **Suppressor YR4**

Met-tRNA$_i$

eIF2 g

A737G

A148G

C) **Suppressor YR7**

ΔA1344

G1412A

T1250G

G1428C

T1303C

A412G

G281A

D) **Suppressor YR9**

C1209U

G548U

A760G

ΔG153

A256G

A236G
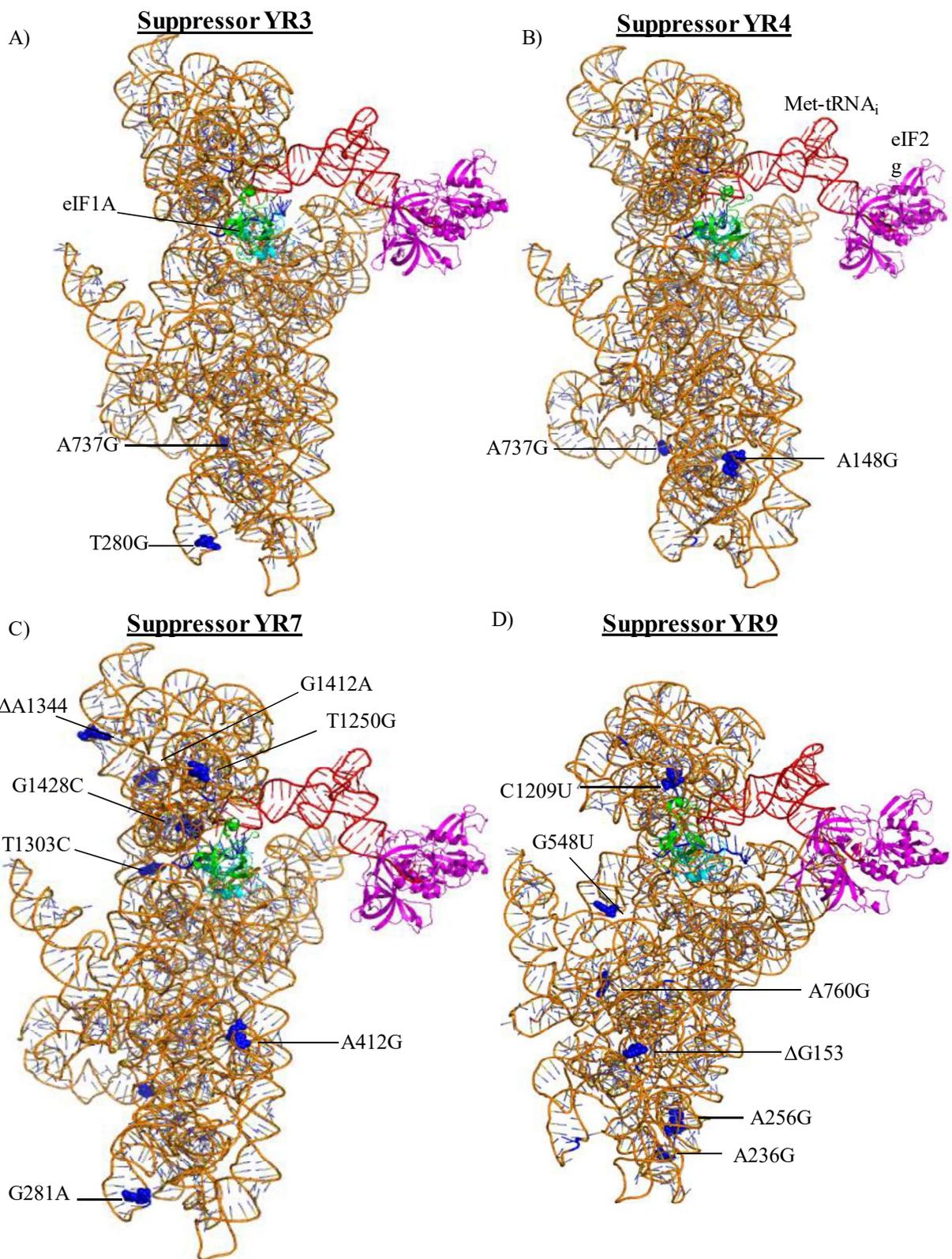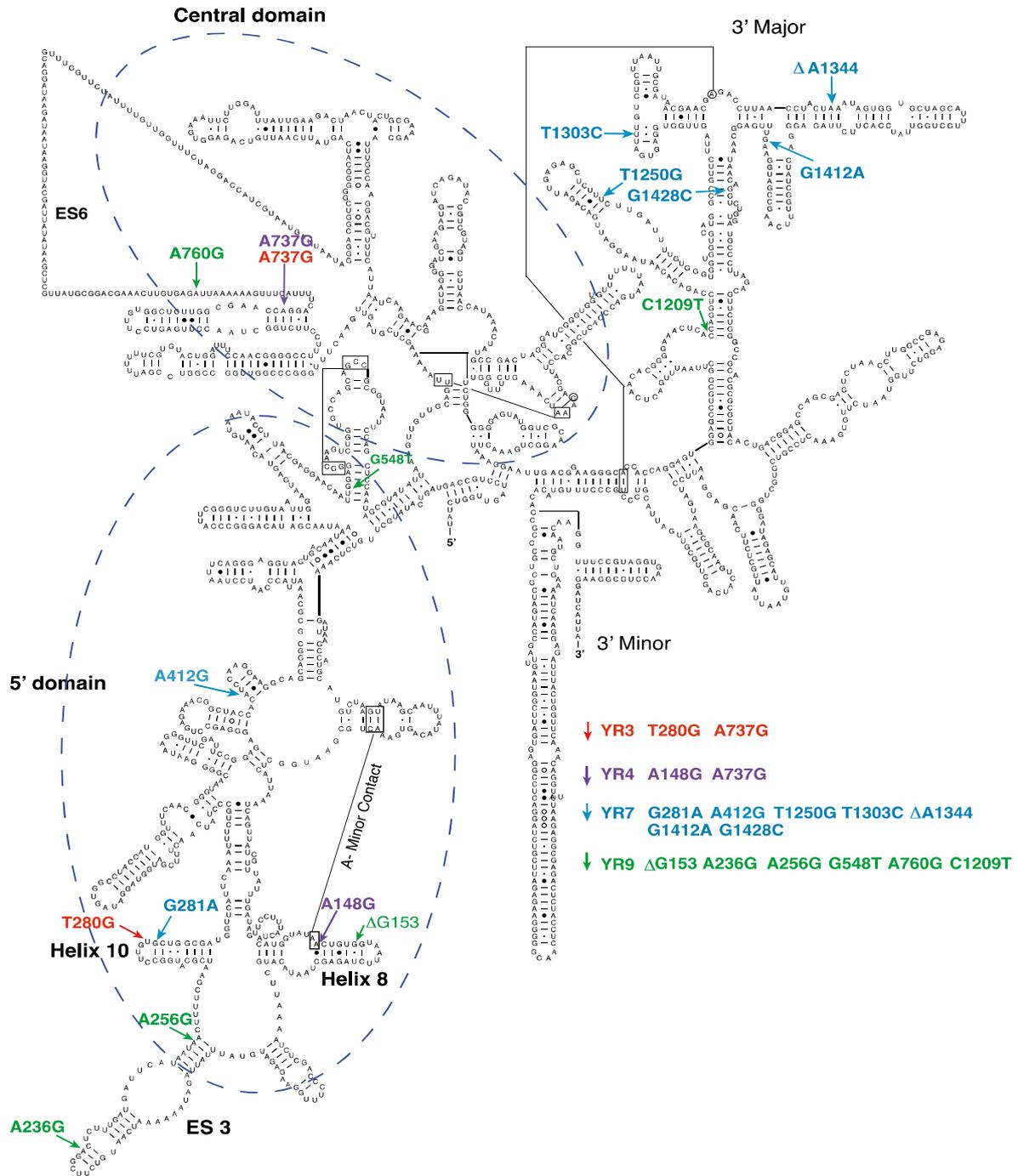
Figure 5.5 Location of suppressor mutations on 18S rRNA.

Crystal structure of 40S ribosome (PDB:3U5B) showing 18S rRNA (orange), modeled with eIF1A (green), eIF1 (cyan), mRNA (light blue) Met-tRNA$_i$ (red) and eIF2γ (magenta).

A) Suppressor YR3 identified mutations at T280G, and A737G.

B) Suppressor YR4 identified mutations at A148G, and A737G.

C) Suppressor YR7 identified mutations at G281A, A412G, T1250G, T1303C, ΔA1344, G1412A and G1428C,

D) Suppressor YR9 identified mutations at ΔG153, A236G, A256G, G548U, T672C, A760G, C1209U.

E) Yeast 18S rRNA secondary structure showing suppressor mutations. The secondary structure is divided into 5′ domain, central domain, 3′ major and 3′ minor regions. Mutations identified in different suppressors as per (A), are colored as red, YR3; purple, YR4; cyan, YR7 and green YR9 respectively.

A)
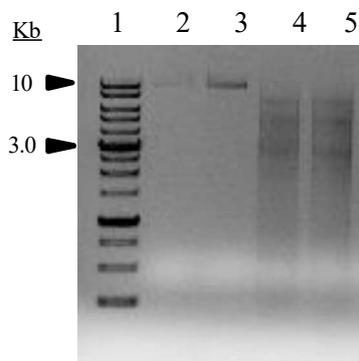
B)
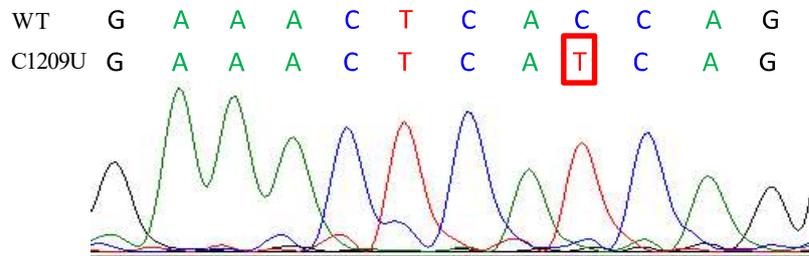
Figure 5.6 Generation of *18SRDN*^{C1209U} mutation.

A) *18SRDN*^{C1209U} mutation was engineered on *RDN* cassette by site directed mutagenesis. Agarose gel (0.8 %) analysis. Lane 1, DNA marker; lane 2, 10 ng of template DNA (pA687); lane 3, 100 ng of template DNA (pA687); lane 4, mutagenized PCR reaction mix; lane 5, mutagenized PCR reaction mix after Dpn I digestion.

B) DNA sequencing electropherogram showing the successful point mutation at 1209 position (red open square) in the mutant DNA compared with WT sequence above.
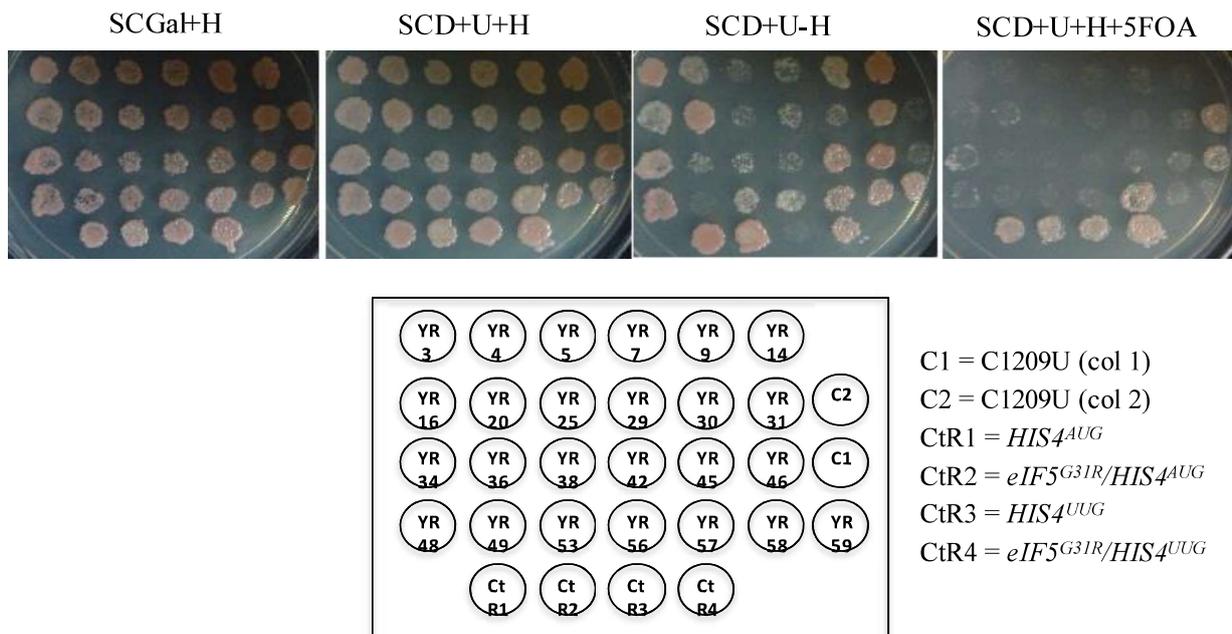
Figure 5.7 Analysis of recessive lethality of Ssu⁻ mutants.

Yeast suppressor colonies (YR#) from figure 5.4 were patched on SCGal+H plate. After 2 days of incubation at 30°C, it was replica plated on SCD+U+H, SCD+U-H, SCD+Ura+His+5FOA, and incubated at 30°C for 3 days. The bottom panel shows the location of each suppressor colony (YR#). CtR1, CtR2, CtR3 and CtR4 represent control colonies having *HIS4^AUG* (pA858), *eIF5^G31R/HIS4^AUG* (pA861), *HIS4^UUG* (pA859), and *eIF5^G31R/HIS4^UUG* (pA862) plasmid combination respectively. C1 and C2 represent different colonies of *18SRDN^C1209U* mutant.

125

5.2.5 *18SRDN*^{C1209U} **suppresses UUG codon recognition of eIF5**^{G31R} **mutant.**

Yeast cell carrying *18SRDN*^{C1209U} was transformed with eIF5^{G31R} mutant plasmid in the presence of either *HIS4*^{AUG} or *HIS4*^{UUG} construct and the serial dilutions were spotted on medium lacking histidine (figure 5.8A). Interestingly, while the eIF5^{G31R} mutant supports UUG codon recognition of *HIS4*^{UUG} allele in the presence of *18SRDN*^{WT} and showed His$^+$ phenotype, the *18SRDN*^{C1209U} mutant suppresses UUG codon recognition and conferred His$^-$ phenotype (figure 5.8A compare row 4 and row 6). To further validate this result, we quantified the UUG codon suppression by transforming P_{HIS4}-*HIS4*^{AUG}-*lacZ* (p3989) or P_{HIS4}-*HIS4*^{UUG}-*lacZ* (p3990) to cells carrying either *18SRDN*^{WT} or *18SRDN*^{C1209U} mutant in the presence of either empty vector or *eIF5*^{G31R} and performed β-galactosidase assay (figure 5.8B). This revealed that eIF5^{G31R} mutant has pronounced ability to increase the UUG/AUG ratio by approximately 5-fold, which was suppressed by *18SRDN*^{C1209U} mutant.
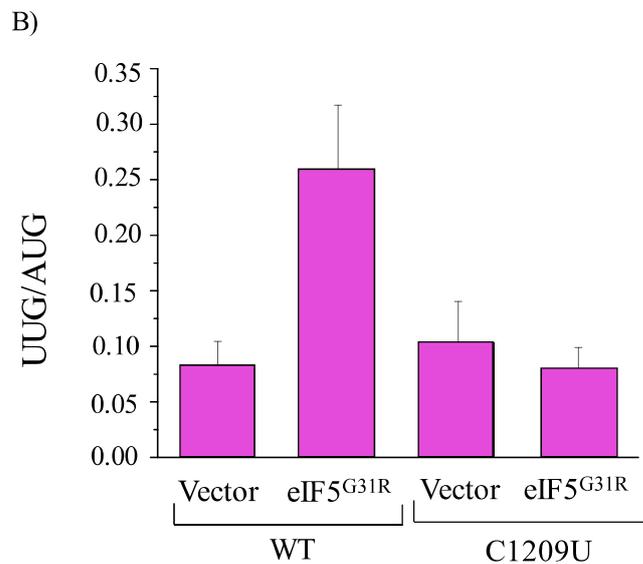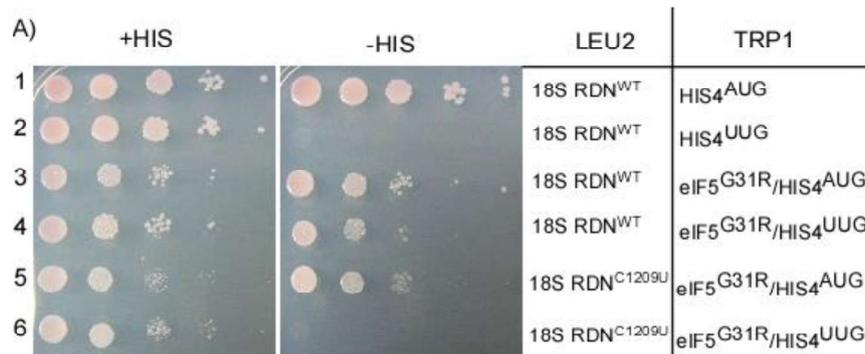
Figure 5.8 Growth analysis of *18SRDN^{C1029U}* Ssu⁻ mutant.

A) Derivatives of yeast strain YP844 (*rdn∆∆, his4∆*) carrying either *18SRDN^{WT}* (pA687) along with of 1) *HIS4^{AUG}* (pA858), 2) *HIS4^{UUG}* (pA859), 3) *eIF5^{G31R}/HIS4^{UUG}* (pA861), 4) *eIF5^{G31R}/HIS4^{UUG}* (pA862), or *18SRDN^{C1209U}* (pA761) carrying 5) *eIF5^{G31R}/HIS4^{AUG}* (pA861), 6) *eIF5^{G31R}/HIS4^{UUG}* (pA862) were spotted on SCD+H or SCD-H and incubated at 30°C for 3 days.

B) Derivative yeast strain YP844 carrying either *18RDN^{WT}* (pA687) or *18SRDN^{C1209U}* (pA761) along with either P_{HIS4}-*HIS4^{AUG}*-*lacZ* (p3989) or P_{HIS4}-*HIS4^{UUG}*-*lacZ* (p3990) was transformed with either empty vector (pA823) or *eIF5^{G31R}* (pA860) and grown in minimal media containing essential nutrients and harvested at O.D$_{600}$ ~ 0.8. The harvested cells were subjected to β-galactosidase assay and the resultant values were plotted as UUG/AUG ratio. The asterisk (**) indicates the significance of difference between the two populations with the P value < 0.001.

5.2.6 $18SRDN^{C1209U}$ rescues Gcn⁻ phenotype of eIF5^{G31R} mutant.

As mentioned in the previous chapters, eIF5^{G31R} causes Gcn⁻ phenotype by repressing the *GCN4* expression due to the utilization of upUUGs present in the 5′ UTR of *GCN4* mRNA and showed 3AT sensitivity. This is caused by its ability to utilize UUG as start codon and resulted in premature fall off from the mRNA before it reaches main *GCN4* mRNA (reinitiation defect). If the isolated 18S rRNA suppressor is capable of suppressing the recognition of UUG codon by eIF5^{G31R}, then the Gcn⁻ phenotype associated with eIF5^{G31R} should also be rescued by this Ssu⁻ mutant ($18SRDN^{C1209U}$).

To test this possibility, we transformed either *HIS4^{AUG}*, *HIS4^{UUG}* allele or *eIF5^{G31R}/HIS4^{AUG}* to the yeast carrying $18SRDN^{C1209U}$ suppressor mutant and we tested the growth sensitivity on 3AT plate. As expected, eIF5^{G31R} mutant cells showed 3AT sensitivity. However, the cells expressing $18SRDN^{C1209U}$ mutant rescued this 3AT sensitivity (figure 5.9A compare rows 3 and 6). This is further validated by analyzing the *GCN4* expression. To this end, we transformed uORFless *GCN4-lacZ* reporter plasmid (p180) to the suppressor mutant along with eIF5^{G31R} mutant and quantified the expression of β-galactosidase (figure 5.9B). In the presence of eIF5^{G31R} mutant, the expression of *GCN4* was 53% in comparison to the WT. However, the $18SRDN^{C1209U}$ mutant de-repressed *GCN4* expression level to 86%. This is possible by the fact that *GCN4* expression in eIF5^{G31R} mutant is repressed by the utilization of upUUGs in the 5′ UTR, which is suppressed by the C1209U of 18S rRNA. This is evidenced by the quantification of *GCN4-lacZ* construct (p227) which carries mutations in uORF1 to 4 but retaining 10 upUUGs in the 5′ UTR. As expected, eIF5^{G31R} mutant utilized the upUUGs and decreased the expression down to 54%, which is rescued by $18SRDN^{C1209U}$ suppressor mutant (89%) (figure 5.9C).
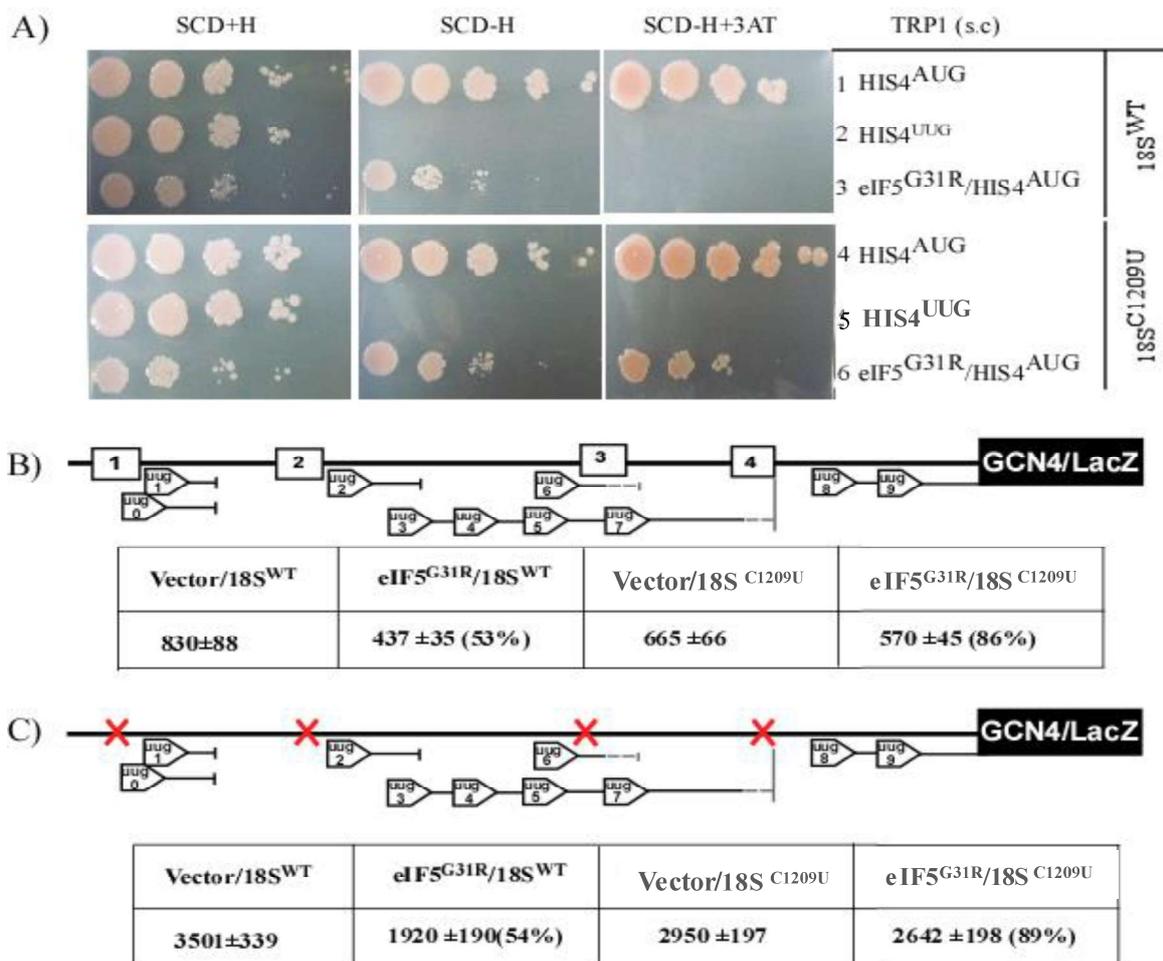
Figure 5.9 *18SRDN^{C1209U}* **rescues Gcn⁻ phenotype of eIF5^{G31R} mutant.**

A) Derivative of yeast strain YP844 carrying either *18SRDN^{WT}* (pA687) or *18SRDN^{C1209U}* (pA761) was transformed with either *HIS4^{AUG}* (pA858), or *HIS4^{UUG}* (pA859), or *eIF5^{G31R}/HIS4^{AUG}* (pA861). The resulting transformants were spotted on minimal media containing (SCD+H) or not containing (SCD-H) histidine or supplemented with 3AT (SCD-H+3AT) and incubated at 30°C for 2 (SCD+H and SCD-H) or 3 (SCD-H+3AT) days.

B and C) Derivatives of yeast strain YP844 carrying either *18SRDN^{WT}* (pA687) or *18SRDN^{C1209U}* (pA761) along with either *HIS4^{AUG}* (pA858) or *eIF5^{G31R}/HIS4^{AUG}* (pA861) was transformed with plasmid p180 for (A) or plasmid p227 for (B). The resulting transformants were grown up to $O.D_{600}$ ~ 0.6 and subjected to 3AT treatment for 6 h before harvesting. The β-galactosidase assay was performed and the resultant values were tabulated and the percentage of variation in eIF5^{G31R} mutant relative WT cells is mentioned in parenthesis.

5.2.7 *18SRDN^{C1209U}* **mutant suppresses Sui⁻ and Gcd⁻ phenotype of eIF2β^{S264Y} mutant.**

The in-vitro GTPase assay suggests that the eIF2β^{S264Y} mutation causes intrinsic GTPase activity in the absence of GTPase activating protein eIF5 (Huang *et al.* 1997). It has been proposed that the intrinsic GTPase activity may be causing Sui⁻ and Gcd⁻ phenotype in the eIF2β^{S264Y} mutant. The A1193U substitution mutation in the helix 31 of 18S rRNA caused increasing leaky scanning of *GCN4* uORF1 and showed Gcn⁻ phenotype and also suppresses the Sui⁻ phenotype of eIF2β^{S264Y} mutant (Nemoto *et al.* 2010). The *18SRDN^{C1209U}* suppressor mutation is located in the helix 32 region. It may be possible that this mutation may suppress Sui⁻ and Gcd⁻ phenotype of the eIF2β^{S264Y} mutant. In order to check this, the yeast strain (YP851) carrying either *18SRDN^{WT}* or *18SRDN^{C1209U}* construct was transformed with a plasmid carrying *HIS4^{AUG}*, or *HIS4^{UUG}*, or *eIF2β^{S264Y}/HIS4^{AUG}* or *eIF2β^{S264Y}/HIS4^{UUG}* construct and spotted on SCD +H and SCD −H plates. In the *18SRDN^{WT}* background, the eIF2β^{S264Y} mutant utilizes UUG codon from *HIS4^{UUG}* allele and showed His⁺ phenotype, however, the *18SRDN^{C1209U}* mutation suppressed the UUG codon recognition from *HIS4^{UUG}* allele and showed His⁻ phenotype (figure 5.10A, compare row 4 and 8). The suppression of UUG codon recognition was check by quantitating UUG/AUG ratio using *HIS4^{AUG}-lacZ* and *HIS4^{UUG}-lacZ* reporter construct. The eIF2β^{S264Y} mutant has higher UUG/AUG ratio in the presence of *18SRDN^{WT}* background, however, the UUG/AUG ratio was significantly reduced in the presence of *18SRDN^{C1209U}* suppressor mutation (figure 5.10B). The intrinsic GTPase activity of eIF2β^{S264Y} mutant causes defective TC complex formation and showed Gcd⁻ phenotype (Williams *et al.* 1989). In order to check whether the *18SRDN^{C1209U}* mutant suppresses the Gcd⁻ phenotype of eIF2β^{S264Y} mutant, a construct *GCN4-LacZ* (p180) was transformed into yeast strain YP851 (*gcn2Δ, his4Δ*) in the presence of either *18SRDN^{WT}* or *18SRDN^{C1209U}* suppressor mutation. The eIF2β^{S264Y} mutant showed a considerable de-repression of *GCN4*
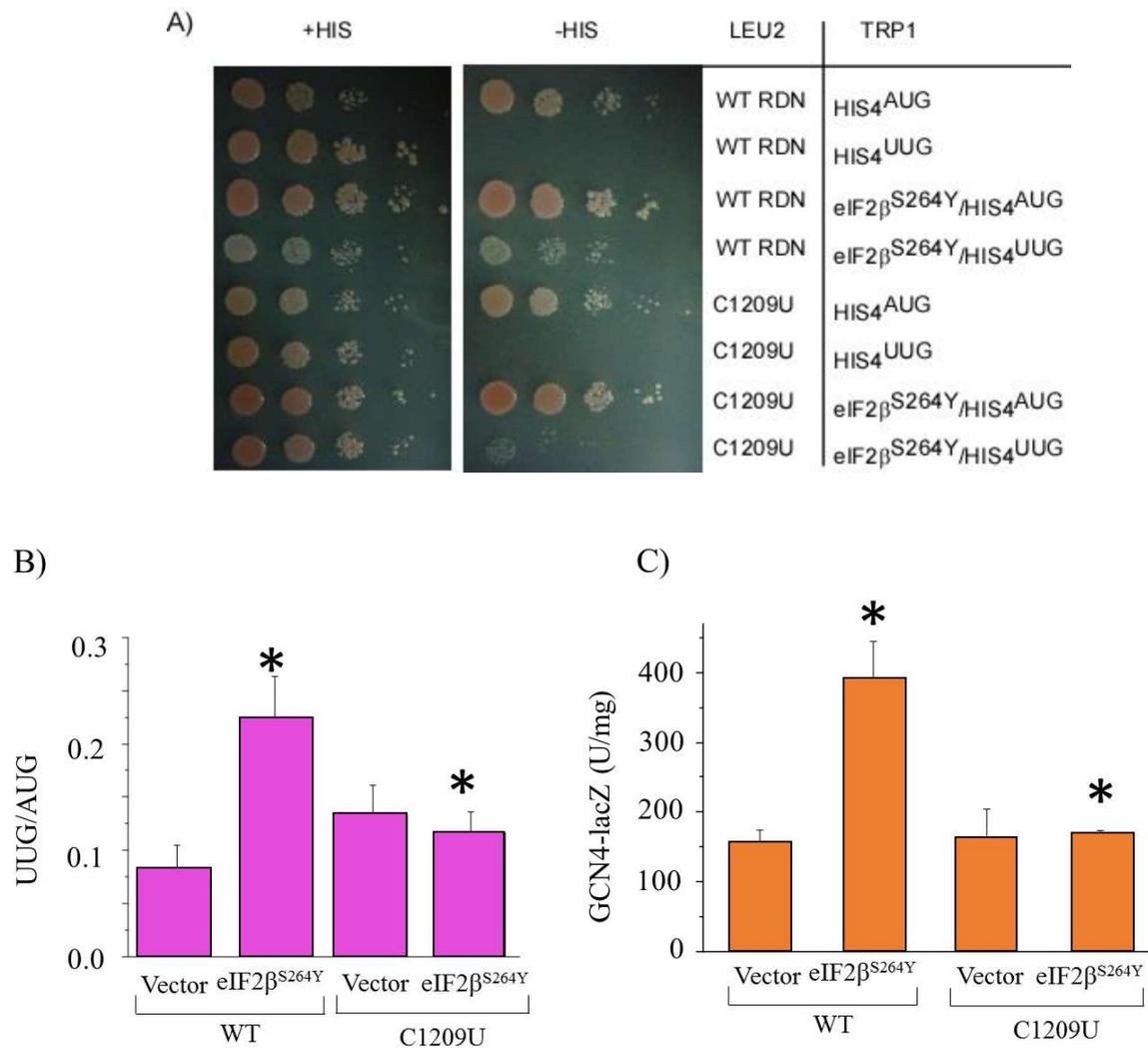
Figure 5.10 *18SRDN^{C1209U}* **mutant suppresses Sui⁻ and Gcd⁻ phenotype of eIF2β^{S264Y} mutant.**

(A) Growth analysis of *18SRDN^{C1209U}* Ssu⁻ mutant. Derivatives of yeast strain YP851 (*rdnΔΔ, his4Δ*) carrying either *18SRDN^{C1209U}* mutant or the *18SRDN^{WT}* were transformed with alleles of either *HIS4^{AUG}* (pA858), *HIS4^{UUG}* (pA859), or *eIF2β^{S264Y}/HIS4^{AUG}* (pA952) or *eIF2β^{S264Y}/HIS4^{UUG}* (pA953) and spotted media SCD+H or SCD-H and incubated at 30ºC for 3 days.

B) Analysis of *P_{HIS4}-HIS4-LacZ* expression. Derivatives of yeast strain YP843 (*rdnΔΔ*) was transformed with either *P_{HIS4}-HIS4^{AUG}-lacZ* (p3989) or *P_{HIS4}-HIS4^{UUG}-lacZ* (p3990). The whole cell extract prepared from these cells were subjected to β-galactosidase activity (nmol of O-nitrophenyl-β-D-galactopyranoside cleaved per min per mg) analysis. The UUG/AUG (A) ratio of

the *HIS4-LacZ* expression is plotted. The asterisk (*) indicates the significance of difference between the two populations with the P value < 0.05. The data is from three independent experiments and the error bars represent an average deviation.

C) Analysis of *GCN4-LacZ* expression. Yeast strain YP851 (*gcn2Δ,his4Δ*) is transformed with *GCN4-lacZ* reporter (p180) and grown up to an O.D$_{600}$ ~ 0.6 in SCD media. The cells were treated with 25 mM of 3AT and incubated further for 6 hours. The whole-cell extracts were prepared, and β-galactosidase activity (nmol of O-nitrophenyl-β-D-galactopyranoside cleaved per min per mg) was measured and plotted. The asterisk (*) indicates the significance of the difference between the two populations with the P value < 0.05. These data are from three independent experiments using three individual colonies and the error bars represent an average deviation.

expression in the absence of eIF2α phosphorylation consistent with its Gcd⁻ phenotype, however, the *18SRDN^C1209U* mutant had a significantly suppressed it's *GCN4* expression consistent with the suppression of Gcd⁻ phenotype (figure 5.10 C).

5.3 DISCUSSION

We have successfully isolated a Suppressor of Sui⁻ (Ssu⁻) mutation C1209U in the *18SRDN* region that effectively suppresses the UUG initiation codon recognition by the eIF5^G31R mutant. The C1209 is a conserved residue present in the helix 32 of the 3′ major domain (head region) and base pairs with residue G1454. The residue A1184 also has base interaction with C1209:G1454 base pair (http://apollo.chemistry.gatech.edu/RiboVision/). It is possible that the C1209U conversion may have interfered with this hydrogen bond triad and disturbed the local stem-loop structure in the head region. Previous reports of well characterized critical 18S rRNA mutations A1193U and A1152U affecting translation initiation were isolated by random mutagenesis (Dong *et al.* 2008; Nemoto *et al.* 2010). The A1193U mutation observed in the loop region of helix 31, affects PIC formation and has a defect in AUG start codon recognition. It therefore shows Gcn⁻ phenotype due to leaky scanning at 34ºC and rescues Sui⁻ phenotype of eIF2β^S264Y mutant at 30ºC (Nemoto *et al.* 2010). The A1152U mutation observed in helix 28 on the other hand, has a defect in the rate of TC loading and leaky scanning which results in Gcd⁻ phenotype. These mutations are considerably near to the P-site of the 40S ribosome that could affect the start codon selection. However, the C1209U suppressor mutation is significantly away from the GTPase center of TC and also from the P-site and could not have directly affected the start codon selection by altering hyper GTPase activity of eIF5^G31R mutant. Recent insights into the biochemistry of eIF5^G31R mutant and its suppressors suggest that hyper UUG start codon recognition is due to the premature "Closed/P_IN" conformation by decreasing the K_{off} for the TC while increasing dissociation of eIF1

at the UUG codon, and conversely increasing the K_{off} for TC at the AUG codon. This disfavors AUG base pairing while favoring UUG base pairing in the "Closed/P_{IN}" conformation (Nanda *et al.* 2013; Martin-Marcos *et al.* 2014; Saini *et al.* 2014). However, the overexpression of eIF1 or other mutants that shift the equilibrium towards "Open/P_{OUT}" conformation disfavors UUG codon recognition and increases the chance of AUG codon recognition (Valasek *et al.* 2004a; Martin-Marcos *et al.* 2014). The head region of the 40S ribosome is shown to undergo considerable head rotation (~7Å) from "Open to Closed" conformation in order to have codon:anticodon engagement (Llácer *et al.* 2015). It is possible that the C1209U mutation may have perturbed the premature head rotation in "Closed/P_{IN}" conformation for the of eIF5^{G31R} and eIF2β^{S264Y} mutant and thereby prevented UUG start codon recognition of the *HIS4^{UUG}* transcript, thus have suppressed the Sui⁻ phenotype, while holding the conformation in "Open" state might have favoured TC binding in proper orientation causing suppression of Gcd⁻ phenotype. In a similar way, the Gcn⁻ phenotype and 3AT sensitivity were partially suppressed by preventing upUUG codon recognition from the *GCN4* transcript. In this sense, the C1209U suppressor mutant is mimicking the conditions shown by the overexpression of the eIF1 subunit.

Chapter 6
SUMMARY

Summary

- eIF5 plays important role in the AUG start codon selection by providing GTPase activating protein (GAP) function through its Arg^{15} residue while interacting with eIF2γ to hydrolyze GTP molecule.

- The eIF5 protein is functionally divided into three different regions; N-terminal domain (NTD) that provide GAP function, middle domain which is involved in GDI activity and C-terminal domain (CTD) that is involved in 48S assembly/post assembly processes and mutations in this region causes both Gcd^{-} and Gcn^{-} phenotype in a temperature sensitive manner.

- The eIF5-NTD is only implicated in GAP function and none of the mutations in this region are known to be associated with Gcn^{-} or Gcd^{-} phenotype, suggesting a pre-dominantly regulatory function to this region.

- The $eIF5^{G31R}$ mutant in the NTD was isolated as a strong Sui^{-} mutant that is capable of recognizing UUG codon as translation initiation site.

- The $eIF5^{G31R}$ mutant repressed *GCN4* expression and show Gcn^{-} phenotype and sensitivity to 3AT inhibition.

- The Gcn^{-} phenotype of $eIF5^{G31R}$ mutant was due to utilization of upUUG1-10 codons present at the 5′ UTR region of the *GCN4* transcript.

- The $eIF5^{G31R}$ mutant's sensitivity to 3AT inhibition can be rescued in the presence of $HIS4^{UUG}$ allele.

- The eIF5^{G31R} mutant caused 2.6-fold less expression of HIS4p from the $HIS4^{AUG}$ allele, suggesting that the ability to initiate at AUG start codon was significantly affected.

- The 3AT treatment caused 2.4-fold and 3.7-fold less protein expression from the $HIS4^{AUG}$ and $HIS4^{UUG}$ alleles respectively in eIF5^{G31R} mutant.

- The eIF5^{G31R} mutant had better UUG start codon recognition ability from the $HIS4^{UUG}$ allele under the 3AT starvation condition.

- The $HIS4^{UUG}$ allele signals more starvation in the presence of eIF5^{G31R} mutant and triggers additional de repression of $GCN4$ expression to cause resistance to 3AT.

- Overexpression of eIF1 caused upregulation of $HIS4$ and $GCN4$ expression in the eIF5^{G31R} mutant and rescued 3AT sensitivity.

- Despite having higher $GCN4$ expression levels, the overexpression of eIF1 caused repression of $HIS4^{UUG}$ allele expression in eIF5^{G31R} mutant causing sensitivity to 3AT.

- Overexpression of $HIS4^{AUG}$ allele does not rescues 3AT sensitivity of eIF5^{G31R} mutant.

- Overexpression of $HIS3$ suppresses 3AT sensitivity of eIF5^{G31R} mutant.

- Genetic suppressor screen was setup to isolate mutation in the 18S rRNA that can suppress Sui$^-$ phenotype (Ssu$^-$) of the eIF5^{G31R} mutant.

- The mutation $18SRDN^{C1209U}$ was isolated in the helix 32 of 18S rRNA that showed Ssu$^-$ phenotype for eIF5^{G31R} mutant.

- The *18SRDN^{C1209U}* mutation suppressed the Gcn⁻ phenotype of eIF5^{G31R} mutant by blocking the utilization of upUUGs of *GCN4* transcript.

- The *18SRDN^{C1209U}* mutation suppressed the Sui⁻ and Gcd⁻ phenotype of intrinsic GTPase defective eIF2β^{S264Y} mutant.

- It is proposed that the *18SRDN^{C1209U}* mutation may have perturbed the premature head rotation in "P$_{IN}$/Closed" conformation for the of eIF5^{G31R} and eIF2β^{S264Y} mutant and thereby prevented UUG start codon recognition of the *HIS4^{UUG}* transcript.

- The *18SRDN^{C1209U}* mutation might have held the 48S conformation in "Open" state that could have favored TC binding in proper orientation causing suppression of Gcd⁻ phenotype in eIF2β^{S264Y} mutant.

REFERENCES

Acker M.G., Shin B.-S.S., Nanda J.S., Saini A.K., Dever T.E. and Lorsch J.R. 2009 Kinetic analysis of late steps of eukaryotic translation initiation. *J Mol Biol* **385**, 491–506.

Acker M.G., Shin B.S., Dever T.E. and Lorsch J.R. 2006 Interaction between eukaryotic initiation factors 1A and 5B is required for efficient ribosomal subunit joining. *J Biol Chem* **281**, 8469–8475.

Albrecht G., Mösch H., Reusser U., Gerhard H., Chem J.B., Albrecht G., et al. 1998 Monitoring the Gcn4 Protein-mediated Response in the Yeast *Saccharomyces cerevisiae*. *J Biol Chem* **273**, 12696-12702

Alifano P., Fani R., Liò P., Lazcano A., Bazzicalupo M., Carlomagno M.S., et al. 1996 Histidine biosynthetic pathway and genes: structure, regulation, and evolution. *Microbiol. Rev.* **60**, 44–69.

Alone P. V, Cao C. and Dever T.E. 2008 Translation initiation factor 2gamma mutant alters start codon selection independent of Met-tRNA binding. *Mol Cell Biol* **28**, 6877–6888.

Alone P. V and Dever T.E. 2006 Direct binding of translation initiation factor eIF2gamma-G domain to its GTPase-activating and GDP-GTP exchange factors eIF5 and eIF2B epsilon. *J Biol Chem* **281**, 12636–12644.

Antony A C. and Alone P. V. 2017 Defect in the GTPase activating protein (GAP) function of eIF5 causes repression of *GCN4* translation. *Biochem. Biophys. Res. Commun.* **486**, 1110–1115.

Asano K. 2014 Why is start codon selection so precise in eukaryotes? **2**, e28387.

Asano K., Clayton J., Shalev A. and Hinnebusch A.G. 2000 A multifactor complex of eukaryotic

initiation factors eIF1, eIF2, eIF3, eIF5, and initiator tRNAMet is an important translation initiation intermediate in vivo. *Genes Dev* **14**, 2534–2546.

Asano K., Krishnamoorthy T., Phan L., Pavitt G.D. and Hinnebusch A.G. 1999 Conserved bipartite motifs in yeast eIF5 and eIF2Bepsilon, GTPase-activating and GDP-GTP exchange factors in translation initiation, mediate binding to their common substrate eIF2. *EMBO J* **18**, 1673–1688.

Asano K., Phan L., Valasek L., Schoenfeld L.W., Shalev A., Clayton J., et al. 2001a A multifactor complex of eIF1, eIF2, eIF3, eIF5, and tRNA(i)Met promotes initiation complex assembly and couples GTP hydrolysis to AUG recognition. *Cold Spring Harb Symp Quant Biol* **66**, 403–415.

Asano K., Shalev A., Phan L., Nielsen K., Clayton J., Valasek L., et al. 2001b Multiple roles for the C-terminal domain of eIF5 in translation initiation complex assembly and GTPase activation. *EMBO J* **20**, 2326–2337.

Aström SU1, von Pawel-Rammingen U B.A. 1993 The yeast initiator tRNAMet can act as an elongator tRNA(Met) in vivo. *J Mol Biol* **233**, 43–58.

Aström SU1 B.A. 1994 Rit1, a tRNA backbone-modifying enzyme that mediates initiator and elongator tRNA discrimination. *Cell* **79**, 535–46.

Bandyopadhyay A. and Maitra U. 1999 Cloning and characterization of the p42 subunit of mammalian translation initiation factor 3 (eIF3): demonstration that eIF3 interacts with eIF5 in mammalian cells. *Nucleic Acids Res* **27**, 1331–1337.

Castilho-Valavicius B., Yoon H. and Donahue T.F. 1990 Genetic characterization of the

Saccharomyces cerevisiae translational initiation suppressors *sui1*, *sui2* and *SUI3* and their effects on HIS4 expression. *Genetics* **124**, 483–495.

Cheung Y.-N.N., Maag D., Mitchell S.F., Fekete C.A., Algire M.A., Takacs J.E., et al. 2007 Dissociation of eIF1 from the 40S ribosomal subunit is a key step in start codon selection in vivo. *Genes Dev* **21**, 1217–1230.

Chiu W.-L., Wagner S., Herrmannova A., Burela L., Zhang F., Saini A.K., et al. 2010 The C-Terminal Region of Eukaryotic Translation Initiation Factor 3a (eIF3a) Promotes mRNA Recruitment, Scanning, and, Together with eIF3j and the eIF3b RNA Recognition Motif, Selection of AUG Start Codons. *Mol. Cell. Biol.* **30**, 4415–4434.

Cigan A.M., Feng L. and Donahue T.F. 1988a tRNAi(met) functions in directing the scanning ribosome to the start site of translation. *Science* **242**, 93–97.

Cigan a M., Pabich E.K. and Donahue T.F. 1988b Mutational analysis of the *HIS4* translational initiator region in *Saccharomyces cerevisiae*. *Mol. Cell. Biol.* **8**, 2964–2975.

Cuchalová L., Kouba T., Herrmannová A., Dányi I., Chiu W.L. and Valásek L. 2010 The RNA recognition motif of eukaryotic translation initiation factor 3g (eIF3g) is required for resumption of scanning of posttermination ribosomes for reinitiation on *GCN4* and together with eIF3i stimulates linear scanning. *Mol. Cell. Biol.* **30**, 4671–86.

Cuesta R., Hinnebusch A.G. and Tamame M. 1998 Identification of *GCD14* and *GCD15*, novel genes required for translational repression of *GCN4* mRNA in *Saccharomyces cerevisiae*. *Genetics* **148**, 1007–1020.

Das S., Ghosh R. and Maitra U. 2001 Eukaryotic translation initiation factor 5 functions as a

GTPase-activating protein. *J Biol Chem* **276**, 6720–6726.

Dever T.E. 1997 Using *GCN4* as a reporter of eIF2 alpha phosphorylation and translational regulation in yeast. **11**, 403–417.

Dever T.E., Feng L., Wek R.C., Cigan A.M., Donahue T.F. and Hinnebusch A.G. 1992 Phosphorylation of initiation factor 2 alpha by protein kinase GCN2 mediates gene-specific translational control of *GCN4* in yeast. *Cell* **68**, 585–596.

Dever T.E., Kinzy T.G. and Pavitt G.D. 2016 Mechanism and regulation of protein synthesis in *Saccharomyces cerevisiae*. *Genetics* **203**, 65–107.

Dever T.E., Yang W., Aström S., Byström A.S. and Hinnebusch A.G. 1995 Modulation of tRNA(i)(Met), eIF-2, and eIF-2B expression shows that *GCN4* translation is inversely coupled to the level of eIF-2.GTP.Met-tRNA(i)(Met) ternary complexes. *Mol Cell Biol* **15**, 6351–6363.

Dhaliwal S. and Hoffman D.W. 2003 The crystal structure of the N-terminal region of the alpha subunit of translation initiation factor 2 (eIF2α) from *Saccharomyces cerevisiae* provides a view of the loop containing serine 51, the target of the eIF2α-specific kinases. *J. Mol. Biol.* **334**, 187–195.

Dominguez D., Altmann M., Benz J., Baumann U. and Trachsel H. 1999 Interaction of translation initiation factor eIF4G with eIF4A in the yeast *Saccharomyces cerevisiae*. *J. Biol. Chem.* **274**, 26720–26726.

Donahue T.F. and Cigan A.M. 1988 Genetic selection for mutations that reduce or abolish ribosomal recognition of the *HIS4* translational initiator region. *Mol Cell Biol* **8**, 2955–

2963.

Donahue T.F., Cigan A.M., Pabich E.K. and Valavicius B.C. 1988 Mutations at a Zn(II) finger motif in the yeast eIF-2 beta gene alter ribosomal start-site selection during the scanning process. *Cell* **54**, 621–632.

Dong J., Munoz A., Kolitz S.E., Saini A.K., Chiu W.L., Rahman H., et al. 2014 Conserved residues in yeast initiator tRNA calibrate initiation accuracy by regulating preinitiation complex stability at the start codon. *Genes Dev.* **28**, 502–20.

Dong J., Nanda J.S., Rahman H., Pruitt M.R., Shin B.-S., Wong C.M., et al. 2008 Genetic identification of yeast 18S rRNA residues required for efficient recruitment of initiator tRNAMet and AUG selection. *Genes Dev.* **22**, 2242–2255.

Dubitzky W., Wolkenhauer O., Cho K.-H. and Yokota H. 2013 *Encyclopedia of Systems Biology*.

Erickson F.L. and Hannig E.M. 1996 Ligand interactions with eukaryotic translation initiation factor 2: role of the g-subunit. *EMBO J* **15**, 6311–6320.

Erickson F.L., Nika J., Rippel S. and Hannig E.M. 2001 Minimum requirements for the function of eukaryotic translation initiation factor 2. *Genetics* **158**, 123–132.

Fekete C.A., Mitchell S.F., Cherkasova V.A., Applefield D., Algire M.A., Maag D., et al. 2007 N- and C-terminal residues of eIF1A have opposing effects on the fidelity of start codon selection. *EMBO J* **26**, 1602–1614.

Fekete C. a, Applefield D.J., Blakely S.A., Shirokikh N., Pestova T., Lorsch J.R., et al. 2005 The eIF1A C-terminal domain promotes initiation complex assembly, scanning and AUG

selection in vivo. *EMBO J* **24**, 3588–3601.

Fernández I.S., Bai X.-C., Hussain T., Kelley A.C., Lorsch J.R., Ramakrishnan V., et al. 2013 Molecular architecture of a eukaryotic translational initiation complex. *Science* **342**, 1240585.

Foiani M., Cigan A.M., Paddon C.J., Harashima S. and Hinnebusch A.G. 1991 *GCD2*, a translational repressor of the G*CN4* gene, has a general function in the initiation of protein synthesis in *Saccharomyces cerevisiae*. *Mol Cell Biol* **11**, 3203–3216.

Fringer J.M., Acker M.G., Fekete C.A., Lorsch J.R. and Dever T.E. 2007 Coupled release of eukaryotic translation initiation factors 5B and 1A from 80S ribosomes following subunit joining. *Mol Cell Biol* **27**, 2384–2397.

Gietz R.D. and Woods R.A. 2006 Yeast transformation by the LiAc/SS Carrier DNA/PEG method. *Methods Mol. Biol.* **313**, 107–20.

Grant C.M., Miller P.F. and Hinnebusch A.G. 1994 Requirements for intercistronic distance and level of eukaryotic initiation factor 2 activity in reinitiation on *GCN4* mRNA vary with the downstream cistron. *Mol Cell Biol* **14**, 2616–2628.

Gueldener U., Heinisch J., Koehler G.J., Voss D. and Hegemann J.H. 2002 A second set of loxP marker cassettes for Cre-mediated multiple gene knockouts in budding yeast. *Nucleic Acids Res.* **30**, e23.

Hall B.E., Bar-Sagi D. and Nassar N. 2002 The structural basis for the transition from Ras-GTP to Ras-GDP. *Proc. Natl. Acad. Sci. U. S. A.* **99**, 12138–12142.

Harashima S. and Hinnebusch A.G. 1986 Multiple GCD genes required for repression of *GCN4*,

a transcriptional activator of amino acid biosynthetic genes in *Saccharomyces cerevisiae*. *Mol Cell Biol* **6**, 3990–3998.

Hilton J.L., Kearney P.C. and Ames B.N. 1965 Mode of action of the herbicide, 3-amino-1,2,4-triazole (amitrole): inhibition of an enzyme of histidine biosynthesis. *Arch. Biochem. Biophys.* **112**, 544–7.

Hinnebusch A.G. 1988 Mechanisms of gene regulation in the general control of amino acid biosynthesis in *Saccharomyces cerevisiae*. *Microbiol. Rev.* **52**, 248–73.

Hinnebusch A.G. 2011 Molecular mechanism of scanning and start codon selection in eukaryotes. *Microbiol. Mol. Biol. Rev.* **75**, 434–67.

Hinnebusch A.G. 2014 The scanning mechanism of eukaryotic translation Initiation. *Annu. Rev. Biochem.* **83**, 779–812.

Hinnebusch A.G. 2005 Translational regulation of *GCN4* and the general amino acid control of yeast. *Annu Rev Microbiol* **59**, 407–450.

Hinnebusch A.G. and Lorsch J.R. 2012 The mechanism of eukaryotic translation initiation: New insights and challenges. *Cold Spring Harb. Perspect. Biol.* **4**, 1–25.

Hinnebusch A.G. and Natarajan K. 2002 Gcn4p, a master regulator of gene expression, is controlled at multiple levels by diverse signals of starvation and stress. *Eukaryot Cell* **1**, 22–32.

Huang H.K., Yoon H., Hannig E.M. and Donahue T.F. 1997 GTP hydrolysis controls stringent selection of the AUG start codon during translation initiation in *Saccharomyces cerevisiae*. *Genes Dev* **11**, 2396–2413.

Hussain T., Llácer J.L., Fernández I.S., Munoz A., Martin-Marcos P., Savva C.G., et al. 2014 Structural changes enable start codon recognition by the eukaryotic translation initiation complex. *Cell* **159**, 597–607.

Ivanov I.P., Loughran G., Sachs M.S. and Atkins J.F. 2010 Initiation context modulates autoregulation of eukaryotic translation initiation factor 1 (eIF1). *Proc. Natl. Acad. Sci. U. S. A.* **107**, 18056–18060.

Jackson R.J., Hellen C.U.T. and Pestova T. V 2010 The mechanism of eukaryotic translation initiation and principles of its regulation. *Nat. Rev. Mol. Cell Biol.* **11**, 113–127.

Jennings M.D. and Pavitt G.D. 2010a eIF5 has GDI activity necessary for translational control by eIF2 phosphorylation. *Nature* **465**, 378–81.

Jennings M.D. and Pavitt G.D. 2010b eIF5 is a dual function GAP and GDI for eukaryotic translational control. *Small GTPases* **1**, 118–123.

Jennings M.D., Zhou Y., Mohammad-Qureshi S.S., Bennett D. and Pavitt G.D. 2013 eIF2B promotes eIF5 dissociation from eIF2•GDP to facilitate guanine nucleotide exchange for translation initiation. *Genes Dev.* **27**, 2696–2707.

Jivotovskaya A. V, Valasek L., Hinnebusch A.G. and Nielsen K.H. 2006 Eukaryotic translation initiation factor 3 (eIF3) and eIF2 can promote mRNA binding to 40S subunits independently of eIF4G in yeast. *Mol Cell Biol* **26**, 1355–1372.

Kapp L.D., Kolitz S.E. and Lorsch J.R. 2006 Yeast initiator tRNA identity elements cooperate to influence multiple steps of translation initiation. **12**, 751–764.

Kapp L.D. and Lorsch J.R. 2004 GTP-dependent recognition of the methionine moiety on

initiator tRNA by translation factor eIF2. *J Mol Biol* **335**, 923–936.

Khoshnevis S., Gunisova S., Vlckova V., Kouba T., Neumann P., Beznoskova P., et al. 2014 Structural integrity of the PCI domain of eIF3a/TIF32 is required for mRNA recruitment to the 43S pre-initiation complexes. *Nucleic Acids Res.* **42**, 4123–4139.

Klinge S., Voigts-Hoffmann F., Leibundgut M., Arpagaus S. and Ban N. 2011 Crystal Structure of the Eukaryotic 60S Ribosomal Subunit in Complex with Initiation Factor 6. *Science* **334**, 941–948.

Kouba T., Rutkai E., Karásková M. and Valášek L.S. 2012 The eIF3c/NIP1 PCI domain interacts with RNA and RACK1/ASC1 and promotes assembly of translation preinitiation complexes. *Nucleic Acids Res.* **40**, 2683–2699.

Kozak M. 1987 An analysis of 5′-noncoding sequences from 699 vertebrate messenger RNAS. *Nucleic Acids Res.* **15**, 8125–8148.

Kozak M. 1989 Circumstances and mechanisms of inhibition of translation by secondary structure in eucaryotic mRNAs. *Mol. Cell. Biol.* **9**, 5134–42.

Kozak M. 1986 Point mutations define a sequence flanking the AUG initiator codon that modulates translation by eukaryotic ribosomes. *Cell* **44**, 283–292.

Krishnamoorthy T., Pavitt G.D., Zhang F., Dever T.E. and Hinnebusch A.G. 2001 Tight binding of the phosphorylated α subunit of initiation factor 2 (eIF2α) to the regulatory subunits of guanine nucleotide exchange factor eIF2B is required for inhibition of translation initiation. *Mol Cell Biol* **21**, 5018–5030.

Kuhle B. and Ficner R. 2014 eIF5B employs a novel domain release mechanism to catalyze

ribosomal subunit joining. *EMBO J.* **33**, 1177–1191.

Laurino J.P., Thompson G.M., Pacheco E. and Castilho B.A. 1999 The beta subunit of eukaryotic translation initiation factor 2 binds mRNA through the lysine repeats and a region comprising the C2-C2 motif. *Mol. Cell. Biol.* **19**, 173–81.

Lee J.H., Pestova T. V, Shin B.S., Cao C., Choi S.K. and Dever T.E. 2002 Initiation factor eIF5B catalyzes second GTP-dependent step in eukaryotic translation initiation. *Proc Natl Acad Sci U S A* **99**, 16689–16694.

Levin D.H., Kyner D. and Acs G. 1973 Protein initiation in eukaryotes: formation and function of a ternary complex composed of a partially purified ribosomal factor, methionyl transfer RNA, and guanosine triphosphate. *Proc. Natl. Acad. Sci. U. S. A.* **70**, 41–5.

Llácer J.L., Hussain T., Marler L., Aitken C.E., Thakur A., Lorsch J.R., et al. 2015 Conformational differences between open and closed states of the eukaryotic translation initiation complex. *Mol. Cell* **59**, 399–412.

Lomakin I.B., Kolupaeva V.G., Marintchev A., Wagner G. and Pestova T. V 2003 Position of eukaryotic initiation factor eIF1 on the 40S ribosomal subunit determined by directed hydroxyl radical probing. *Genes Dev* **17**, 2786–2797.

Lomakin I.B., Shirokikh N.E., Yusupov M.M., Hellen C.U. and Pestova T. V 2006 The fidelity of translation initiation: reciprocal activities of eIF1, IF3 and YciH. *EMBO J* **25**, 196–210.

Luna R.E., Arthanari H., Hiraishi H., Akabayov B., Tang L., Cox C., et al. 2013 The interaction between eukaryotic initiation factor 1A and eIF5 retains eIF1 within scanning preinitiation complexes. *Biochemistry* **52**, 9510–9518.

149

Luna R.E., Arthanari H., Hiraishi H., Nanda J., Martin-Marcos P., Markus M. a., et al. 2012 The C-Terminal Domain of Eukaryotic Initiation Factor 5 Promotes Start Codon Recognition by Its Dynamic Interplay with eIF1 and eIF2β. *Cell Rep.* **1**, 689–702.

Maag D., Fekete C.A., Gryczynski Z. and Lorsch J.R. 2005 A conformational change in the eukaryotic translation preinitiation complex and release of eIF1 signal recognition of the start codon. *Mol Cell* **17**, 265–275.

Majumdar R. and Maitra U. 2005 Regulation of GTP hydrolysis prior to ribosomal AUG selection during eukaryotic translation initiation. *EMBO J* **24**, 3737–3746.

Martin-Marcos P., Cheung Y.-N. and Hinnebusch A.G. 2011 Functional elements in initiation factors 1, 1A, and 2β discriminate against poor AUG context and non-AUG start codons. *Mol. Cell. Biol.* **31**, 4814–31.

Martin-Marcos P., Nanda J., Luna R.E., Wagner G., Lorsch J.R. and Hinnebusch A.G. 2013 β-Hairpin loop of eukaryotic initiation factor 1 (eIF1) mediates 40 S ribosome binding to regulate initiator tRNA(Met) recruitment and accuracy of AUG selection in vivo. *J. Biol. Chem.* **288**, 27546–62.

Martin-Marcos P., Nanda J.S., Luna R.E., Zhang F., Saini A.K., Cherkasova V.A., et al. 2014 Enhanced eIF1 binding to the 40S ribosome impedes conformational rearrangements of the preinitiation complex and elevates initiation accuracy. *RNA* **20**, 150–67.

Meng H., Li C., Wang Y. and Chen G. 2014 Molecular dynamics simulation of the allosteric regulation of eIF4A protein from the open to closed state, induced by ATP and RNA substrates. *PLoS One* **9**.

Nanda J.S., Cheung Y.-N.N., Takacs J.E., Martin-Marcos P., Saini A.K., Hinnebusch A.G., et al. 2009 eIF1 controls multiple steps in start codon recognition during eukaryotic translation initiation. *J Mol Biol* **394**, 268–85.

Nanda J.S., Saini A.K., Munoz A.M., Hinnebusch A.G., Lorsch J.R., Muñoz A.M., et al. 2013 Coordinated movements of eukaryotic translation initiation factors eIF1, eIF1A, and eIF5 trigger phosphate release from eIF2 in response to start codon recognition by the ribosomal preinitiation complex. *J. Biol. Chem.* **288**, 5316–5329.

Nemoto N., Singh C.R., Udagawa T., Wang S., Thorson E., Winter Z., et al. 2010 Yeast 18 S rRNA is directly involved in the ribosomal response to stringent AUG selection during translation initiation. *J Biol Chem* **285**, 32200–32212.

Nielsen K.H., Szamecz B., Valasek L., Jivotovskaya A., Shin B.S. and Hinnebusch A.G. 2004 Functions of eIF3 downstream of 48S assembly impact AUG recognition and *GCN4* translational control. *EMBO J* **23**, 1166–1177.

Nika J., Rippel S. and Hannig E.M. 2001 Biochemical analysis of the eIF2βγ complex reveals a structural function for eIF2α in catalyzed nucleotide exchange. *J. Biol. Chem.* **276**, 1051–1056.

Obayashi E., Luna R.E., Nagata T., Martin-Marcos P., Hiraishi H., Singh C.R., et al. 2017 Molecular Landscape of the Ribosome Pre-initiation Complex during mRNA Scanning: Structural Role for eIF3c and Its Control by eIF5. *Cell Rep.* **18**, 2651–2663.

Olsen D.S., Savner E.M., Mathew A., Zhang F., Krishnamoorthy T., Phan L., et al. 2003 Domains of eIF1A that mediate binding to eIF2, eIF3 and eIF5B and promote ternary complex recruitment in vivo. *EMBO J* **22**, 193–204.

Passmore L.A., Schmeing T.M., Maag D., Applefield D.J., Acker M.G., Algire M.A., et al. 2007
The eukaryotic translation initiation factors eIF1 and eIF1A induce an open conformation of
the 40S ribosome. *Mol Cell* **26**, 41–50.

Pavitt G.D., Yang W. and Hinnebusch A.G. 1997 Homologous segments in three subunits of the
guanine nucleotide exchange factor eIF2B mediate translational regulation by
phosphorylation of eIF2. *Mol Cell Biol* **17**, 1298–1313.

von Pawel-Rammingen U., Astrom S. and Byström A.S. 1992 Mutational analysis of conserved
positions potentially important for initiator tRNA function in *Saccharomyces cerevisiae*.
Mol. Cell. Biol. **12**, 1432–1442.

Pestova T. V, Borukhov S.I. and Hellen C.U. 1998 Eukaryotic ribosomes require initiation
factors 1 and 1A to locate initiation codons. *Nature* **394**, 854–9.

Pisarev A. V, Kolupaeva V.G., Pisareva V.P., Merrick W.C., Hellen C.U. and Pestova T. V 2006
Specific functional interactions of nucleotides at key -3 and +4 positions flanking the
initiation codon with components of the mammalian 48S translation initiation complex.
Genes Dev **20**, 624–636.

Roll-Mecak A., Alone P., Cao C., Dever T.E. and Burley S.K. 2004 X-ray structure of
translation initiation factor eIF2gamma: implications for tRNA and eIF2alpha binding. *J
Biol Chem* **279**, 10634–10642.

Saini A.K., Nanda J.S., Lorsch J.R. and Hinnebusch A.G. 2010 Regulatory elements in eIF1A
control the fidelity of start codon selection by modulating tRNA(i)(Met) binding to the
ribosome. *Genes Dev* **24**, 97–110.

Saini A.K., Nanda J.S., Martin-Marcos P., Dong J., Zhang F., Bhardwaj M., et al. 2014 Eukaryotic translation initiation factor eIF5 promotes the accuracy of start codon recognition by regulating Pi release and conformational transitions of the preinitiation complex. *Nucleic Acids Res.* **42**, 9623–9640.

Schmitt E., Panvert M., Lazennec-Schurdevin C., Coureux P.-D., Perez J., Thompson A., et al. 2012 Structure of the ternary initiation complex aIF2-GDPNP-methionylated initiator tRNA. *Nat. Struct. Mol. Biol.* **19**, 450–4.

Shin B.-S., Kim J.-R., Walker S.E., Dong J., Lorsch J.R. and Dever T.E. 2011 Initiation factor eIF2γ promotes eIF2–GTP–Met-tRNA$_i^{Met}$ ternary complex binding to the 40S ribosome. *Nat. Struct. Mol. Biol.* **18**, 1227–1234.

Singh C.R., Curtis C., Yamamoto Y., Hall N.S., Kruse D.S., He H., et al. 2005 Eukaryotic translation initiation factor 5 is critical for integrity of the scanning preinitiation complex and accurate control of *GCN4* translation. *Mol. Cell. Biol.* **25**, 5480–5491.

Sussman JK, Simons EL S.R. 1996 Escherichia coli translation initiation factor 3 discriminates the initiation codon in vivo. *Mol Microbiol.* **21**, 347–60.

Szamecz B., Rutkai E., Cuchalová L., Munzarová V., Herrmannová A., Nielsen K.H., et al. 2008 eIF3a cooperates with sequences 5′ of uORF1 to promote resumption of scanning by post-termination ribosomes for reinitiation on *GCN4* mRNA. *Genes Dev.* **22**, 2414–2425.

Valasek L., Mathew A.A., Shin B.S., Nielsen K.H., Szamecz B. and Hinnebusch A.G. 2003 The yeast eIF3 subunits TIF32/a, NIP1/c, and eIF5 make critical connections with the 40S ribosome in vivo. *Genes Dev* **17**, 786–799.

Valasek L., Nielsen K.H., Zhang F., Fekete C.A. and Hinnebusch A.G. 2004a Interactions of eukaryotic translation initiation factor 3 (eIF3) subunit NIP1/c with eIF1 and eIF5 promote preinitiation complex assembly and regulate start codon selection. *Mol Cell Biol* **24**, 9437–9455.

Valasek L., Nielsen K.H., Zhang F., Fekete C.A., Hinnebusch A.G., Valášek L., et al. 2004b Interactions of eukaryotic translation initiation factor 3 (eIF3) subunit NIP1/c with eIF1 and eIF5 promote preinitiation complex assembly and regulate start codon selection. *Mol Cell Biol* **24**, 9437–9455.

Wach A., Brachat A., Alberti-Segui C., Rebischung C. and Philippsen P. 1997 Heterologous *HIS3* marker and GFP reporter modules for PCR-targeting in *Saccharomyces cerevisiae*. **13**, 1065–1075.

Wai H.H., Vu L., Oakes M. and Nomura M. 2000 Complete deletion of yeast chromosomal rDNA repeats and integration of a new rDNA repeat: use of rDNA deletion strains for functional analysis of rDNA promoter elements in vivo. *Nucleic Acids Res* **28**, 3524–3534.

Walsh D. and Mohr I. 2011 Viral subversion of the host protein synthesis machinery. *Nat. Rev. Microbiol.* **9**, 860–875.

Williams N.P., Hinnebusch A.G. and Donahue T.F. 1989 Mutations in the structural genes for eukaryotic initiation factors 2 alpha and 2 beta of *Saccharomyces cerevisiae* disrupt translational control of *GCN4* mRNA. *Proc Natl Acad Sci U S A* **86**, 7515–7519.

Woolford J.L. and Baserga S.J. 2013 Ribosome biogenesis in the yeast *Saccharomyces cerevisiae*. *Genetics* **195**, 643–681.

Yamamoto Y., Singh C.R., Marintchev A., Hall N.S., Hannig E.M., Wagner G., et al. 2005 The eukaryotic initiation factor (eIF) 5 HEAT domain mediates multifactor assembly and scanning with distinct interfaces to eIF1 , eIF2 , eIF3 , and eIF4G. 1–6.

Yang W. and Hinnebusch A.G. 1996 Identification of a regulatory subcomplex in the guanine nucleotide exchange factor eIF2B that mediates inhibition by phosphorylated eIF2. *Mol Cell Biol* **16**, 6603–6616.

Yu Y., Marintchev A., Kolupaeva V.G., Unbehaun A., Veryasova T., Lai S.C., et al. 2009 Position of eukaryotic translation initiation factor eIF1A on the 40S ribosomal subunit mapped by directed hydroxyl radical probing. *Nucleic Acids Res* **37**, 5167–5182.

Zhang F. and Hinnebusch A.G. 2011 An upstream ORF with non-AUG start codon is translated in vivo but dispensable for translational control of *GCN4* mRNA. *Nucleic Acids Res.* **39**, 3128–3140.

Zhang F., Saini A.K., Shin B.S., Nanda J. and Hinnebusch A.G. 2015 Conformational changes in the P site and mRNA entry channel evoked by AUG recognition in yeast translation preinitiation complexes. *Nucleic Acids Res.* **43**, 2293–2312.